



Integration of Remote Sensing and GIS for Infra-Structure Planning

A Thesis

**Submitted in Fulfillment of the Requirements for
the Degree of M. Sc. in Surveying Engineering**

**Department of Surveying Engineering,
Shoubra Faculty of Engineering, Benha University**

By

Eng. Hassan Mohamed Hassan

B.Sc. Surveying Engineering

Supervised by

Prof. Ali A. El Sagheer

**Professor of Surveying and Geodesy
Head of Surveying Department
Shoubra Faculty of Engineering**

Assoc. Prof. Maher M. Amen

**Assoc. Prof. of Surveying
Shoubra Faculty of Engineering**

Assoc. Prof. Khaled M. Zaky

**Assoc. Prof. of Surveying
Shoubra Faculty of Engineering**

2012

التكامل بين الاستشعار عن بعد و نظم المعلومات الجغرافية لتخطيط البنية التحتية

رسالة

مقدمة إلى كلية الهندسة بشبرا
جامعة بنها

لاستيفاء متطلبات الحصول على
درجة الماجستير في الهندسة المساحية

مقدمة من

م/ حسن محمد حسن حسين
بكالوريوس الهندسة المساحية- كلية الهندسة بشبرا
جامعة بنها

تحت إشراف

أ.د/ على أحمد الصغير
أستاذ المساحة و الجيوديسيا - رئيس قسم الهندسة المساحية
كلية الهندسة بشبرا

أ.م.د/ ماهر محمد امين
أستاذ مساعد المساحة - قسم الهندسة المساحية
كلية الهندسة بشبرا

أ.م.د/ خالد محمد ذكي
أستاذ مساعد المساحة - قسم الهندسة المساحية
كلية الهندسة بشبرا

٢٠١٢

ACKNOWLEDGEMENT

First of all, prayerful thanks for **ALLAH** who gave me everything I have.

I owe a warm and deep thanks to **Prof. Dr. Ali A. El-Sagheer**, for his encouragement, great support, fruitful direction during supervision and the final revision of the manuscripts.

I'm appreciated and grateful to **Assoc. Prof. Dr. Maher M. Amen** for his valuable and continuous interest, continuous advice, excellent follow-up and assistance during all periods of his supervision.

I fully **Assoc. Prof. Dr. Khaled M. Zaky**, valuable instructions, great support and his sincere and truly efforts in the final revision of the research.

Grateful acknowledgement and thanks are expressed to all the staff of the **Surveying Department, Shoubra Faculty of Engineering**.

Finally with all my gratitude and love I always fell the kind care, of all the members of **my family**.

ABSTRACT

The level of urbanism is an important parameter to measure the cities degree of civilization. One of the biggest challenges that facing infra-structure planners is the over population which leads to build over agriculture lands. These areas are not planned by the government which led to lack of services as transportation, water, sewage and electricity networks. The main objective of this research is to Study the integration of Remote Sensing and GIS for providing thematic maps of spatial features with up to date attributes information. This is to assist Infra-Structure Planning purposes more speedy and low costs. Another objective of this research to Study the possibility of using free products of Google Earth program as Google Earth control points as alternative source to GPS control points or even with it, Global DEM (SRTM) as alternative source to ground DEM especially for flat terrain areas and finally using satellite image extracted from Google Earth program GEO EYE satellite image in this case (Google Earth program doesn't have Satellite images with same spatial resolution for all areas) as alternative source to QUICKBIRD satellite image.

For these purposes, a specific area was selected. This test area is located in Qaluop city, covers approximately two squares Kms and located in the Nile valley zone (the main middle zone) of the plane coordinate system of Egypt. It is considered as a large urban area that contains buildings, a network of roads. It is a part of a QUICKBIRD pansharped image acquired in May 2005 by Space Imaging QUICKBIRD satellite, with 60 cm resolution. Also it is a part of GEO EYE satellite image acquired in January 2010 extracted from Google Earth program, with 50 cm resolution. It has been found that the study area has a lack of Infra-Structure services.

Both images were geometrically corrected through performing orthorectification process using the differential rectification transformation using 5, 10 and 15 GCPs and Ground DEM and DBM. The RMS of the orthorectified images were (1.008m, 0.5976m and 0.5624m for the QUICKBIRD satellite image and 0.8885m, 0.6145m and 0.5504m for GEO EYE satellite image extracted from Google Earth program) then applying vectorization for both images to produce thematic maps using on screen digitizing process and the planimetric accuracy (RMS) of these maps were checked using 5 GCPs and were found to be (1.05m for QUICKBIRD satellite image and 0.76m for GEO EYE satellite image extracted from Google Earth

program). These results were within the required map accuracy standards for a map scale 1:5.000 according to the three map accuracy standards (NMAS, NSSDA and ASPRS). Also these results were within the required map accuracy standards for a map scale 1:2.500 according to both the NMAS and NSSDA standards. Control points extracted from Google Earth program were compared with GPS control points using 20 points evenly distributed in the study area. The results show that Control points extracted from Google Earth program can't be used as alternative source to GPS control points or even with it. The Global DEM (SRTM) was compared with Ground DEM. The results show that Global DEM (SRTM) can't be used even for flat terrain areas for producing large scale maps.

GIS planning was applied for both Water and Sewage networks as first GIS spatial analysis was applied to choose the most suitable location of both the Water tank and the Pumping station then in ARC GIS environment automatic calculators were designed to find the water or sewage consumption using the population density of the study area also programs using (Microsoft Visual Basic) in ARC GIS environment were designed for finding the diameters of pipes for planning purposes. Both water and sewage networks were produced using the utility network analysis and can be controlled easily by the end user (as enabling and disabling the pipes in damage cases and control valves also water flow direction in pipes).

ملخص البحث

المقدمة:

يعتبر مستوى العمران عامل مهم في قياس تحضر المدن. احد اهم التحديات التي تواجه المخططين لعمل شبكات بنية تحتية لهذه المدن هي الزيادة السكانية التي ينتج عنها مناطق عشوائية. هذه المناطق بنيت بدون تخطيط و تفتقد لخدمات البنية التحتية مثل شبكات الطرق ومياه الشرب والصرف الصحي وشبكات الغاز والكهرباء. المرحلة الرئيسية لعمل شبكات البنية التحتية هو معرفة الوضع الحالى من مصادر البيانات المختلفة. ونظرا للتطور الكبير في تقنية الاستشعار عن بعد و خاصة صور الاقمار الصناعية التي اصبحت ذات قدرات تحليلية كبيرة يمكن من خلالها عمل خرائط ذات مقياس رسم كبير يمكن استخدامها في عمليات التخطيط مثل القمر الصناعي كويك بيرد الذى تصل قدرته التحليلية الى ٦٠ سم. و كذلك احد اسرع و اسهل الوسائل الحالية للحصول على صور الاقمار الصناعية برنامج جوجل ايرث الذى يحتوى على صور اقمار صناعية ذات قدرات تحليلية عالية تصل الان الى ٥٠ سم من القمر الصناعي (GEO EYE). تتم عملية انتاج الخرائط من هذه الصور عن طريق عملية التقويم الرأسى (Orthorectification) للصورتين لتصحيح خطأ فروق الارتفاعات عن طريق نموذج الارتفاع الرقمى (DEM) و ازالة المباني عن طريق نموذج المباني الرقمى (DBM) ثم تحويل هذه الصور الى خرائط عن طريق عملية (Vectorization). ثم عمل قاعدة بيانات حديثة لهذه الخرائط لاستخدامها بواسطة نظم المعلومات الجغرافية في اغراض تخطيط البنية التحتية خاصة شبكات المياه و الصرف الصحى.

الهدف من البحث:

الهدف الرئيسى للبحث هو دراسة التكامل بين الاستشعار عن بعد و نظم المعلومات الجغرافية لعمل خرائط ذات المعلم الواحد للمعالم المطلوبة في التخطيط وكذلك عمل قاعدة بيانات حديثة عن هذه المناطق لاستخدامها في اغراض تخطيط البنية التحتية اسرع و بتكلفة اقل. كذلك دراسة امكانية استخدام المنتجات المتاحة مجانا لبرنامج جوجل ايرث مثل نقاط التحكم بدلا من نقاط GPS او حتى معها و ايضا نموذج الارتفاعات الرقمى العالمى SRTM المتاح مجانا بدلا من نموذج الارتفاعات الرقمى المنتج من المساحة الارضية خاصة في المناطق المستوية و اخيرا امكانية استخدام صور الاقمار الصناعية المتاحة في برنامج جوجل ايرث بدلا من صور الاقمار الصناعية للقمر كويك بيرد.

محتويات الرسالة:

الباب الأول:

اختص هذا الباب بدراسة الاستشعار عن بعد حيث تضمن مقدمة عن الاستشعار عن بعد و كذلك نبذة موجزة عن

تاريخ الاستشعار عن بعد و الأنواع المختلفة من الأقمار الصناعية وكذلك الكاميرات المحمولة عليها والتطبيقات المختلفة لكل منها. و صور الأقمار الصناعية المختلفة وفي نهاية الباب تم عرض عدد من التطبيقات المختلفة للاستشعار عن بعد مع التركيز على إنتاج الخرائط و مقاييس الرسم المختلفة التي يمكن الحصول عليها من الاقمار المختلفة.

الباب الثاني:

اختص هذا الباب بدراسة عملية تقويم صور الأقمار الصناعية حيث تم عرض الاخطاء الهندسية التي تحدث عند التقاط الصور من القمر الصناعي ايضا شرح لخطوات عملية التقويم وكذلك النماذج الرياضية المختلفة لعمل التقويم. و كذلك نماذج الأرض الرقمية بداية من شرح مفهوم نماذج الأرض الرقمية ثم عرض الطرق المختلفة لإنتاج نماذج الأرض الرقمية. ايضا العوامل التي تؤثر جودة عمل نماذج الأرض الرقمية. و اخيرا شرح للطرق المختلفة لعملية تحويل الصور الى خرائط.

الباب الثالث:

اختص هذا الباب بنظم المعلومات الجغرافية بداية بشرح التعريفات المختلفة لنظم المعلومات الجغرافية و كذلك مكونات نظم المعلومات الجغرافية من عنصر بشري و الالات و حزم برامج و بيانات. العمليات المهمة التي يمكن عملها باستخدام نظم المعلومات الجغرافية و طرق تمثيل البيانات المكانية. و اخيرا شرح للطرق المختلفة لتصميم قواعد البيانات.

الباب الرابع:

يختص هذا الباب بالجانب العملي من الرسالة حيث تم استخدام البيانات المتاحة لعمل تكامل بين الاستشعار عن بعد و نظم المعلومات الجغرافية لتخطيط شبكات البنية التحتية. بداية من عمل التقويم الراسي للصور و كذلك دراسة امكانية استخدام المنتجات المتاحة مجاناً لبرنامج جوجل ايرث مثل نقاط التحكم بدلا من نقاط GPS او حتى معها و ايضا نموذج الارتفاعات الرقمية العالمي SRTM المتاح مجاناً بدلا من نموذج الارتفاعات الرقمية المنتج من المساحة الارضية خاصة في المناطق المستوية و اخيرا امكانية استخدام صور الاقمار الصناعية المتاحة في برنامج جوجل ايرث بدلا من صور الاقمار الصناعية للقمر كويك بيرد لعمل خرائط ذات المعلم الواحد للمعالم المطلوبة في التخطيط. وفي كلتا الحالتين تم استخدام نموذج الأرض الرقمية وكذلك نموذج المباني الرقمية. وقد شرحت حسابات هذه التجارب بالتفصيل مرفقة بالجداول والرسومات وكافة الملاحظات. ايضا تقييم الخرائط المنتجة من هذه الصور حسب المقاييس العالمية. اخيرا عمل تخطيط اولي لشبكات المياه و الصرف الصحي باستخدام نظم المعلومات الجغرافية من خلال عمل تحليل مكاني لايجاد افضل مكان لكل من خزان المياه و محطة رفع الصرف الصحي ثم عمل برامج لايجاد اقطار المواسير المختلفة لتسهيل عملية التخطيط و اخيرا اخراج الشبكتين في صورة شبكات مرافق تمكن المستخدم من التحكم في مسارات المياه في المواسير و كذلك فتح و غلق المحابس في حالة حدوث عطل او صيانة في احد المواسير.

الباب الخامس:

يحتوى هذا الباب على ملخص لما تم استخلاصه من نتائج ثم عرض للتوصيات المقترحة بناءً على ما تقدم من دراسات ونتائج.

استنتاجات البحث

من خلال النتائج التي تم الحصول عليها تم التوصل الى بعض الاستنتاجات الخاصة بعمل تكامل بين الاستشعار عن بعد و نظم المعلومات الجغرافية لتخطيط شبكات البنية التحتية. وهذه الاستنتاجات يمكن ايجازها فيمايلي:

1. نتائج البحث دلت على ان (RMS) معدل الخطأ كان افضل في حالة الخرائط المنتجة من صورة القمر الصناعي (GEO EYE) الماخوذة من برنامج جوجل ايرث و تساوى ٠,٧٦ متر من حالة الخرائط المنتجة من صورة القمر الصناعي كويك بيرد و تساوي ١,٠٥ متر و كلتا النتائج تدل على انه يمكن استخدام هذه الصور لانتاج خرائط بمقياس رسم ١:٥٠٠٠٠ حسب المقاييس العالمية الثلاثة و بمقياس رسم ١:٢٥٠٠ حسب اثنين من هذه المقاييس.
2. يمكن استخدام صورة القمر الصناعي (GEO EYE) الماخوذة من برنامج جوجل ايرث المتاحة في منطقة الدراسة في هذه الحالة لانتاج خرائط ذات مقياس رسم كبير.
3. لا يمكن استخدام نقاط التحكم من برنامج جوجل ايرث لانتاج خرائط ذات مقياس رسم كبير حيث انها لها ازاحات مختلفة المقدار و الاتجاهة عن مكانها الصحيح.
4. لا يمكن استخدام نموذج الارتفاعات الرقمية العالمي SRTM المتاح مجاناً في برنامج جوجل ايرث بدلا من نموذج الارتفاعات الرقمية المنتج من المساحة الارضية حتى في المناطق المستوية لانتاج خرائط ذات مقياس رسم كبير.
5. استخدام التحليل المكاني في نظم المعلومات الجغرافية سهلت وحسنت عملية ايجاد افضل مكان لكل من خزان المياه و محطة الرفع الخاصة بالصحرى.
6. تصميم المعادلات و البرامج في البرنامج سهلت عملية ايجاد اقطار المواسير في تخطيط شبكات البنية التحتية (المياه و الصرف الصحي).
7. اخراج الشبكات في صورة شبكات المرافق في برنامج ARC GIS يسهل عملية التحكم في هذه الشبكات.

توصيات البحث

طبقا للنتائج التي تم الوصول اليها فان هناك بعض التوصيات المقترحة يمكن تلخيصها فيما يلي:

١. استخدام صور الاقملر الصناعية الماخوذة من برنامج جوجل ايرث لانتاج خرائط ذات مقياس رسم مختلفة حسب القدرات التحليلية المتاحة لكل منطقة.
٢. استخدام نظم المعلومات الجغرافية قى عملية تخطيط شبكات البنية التحتية (المياه و الصرف الصحى).
٣. استخدام التحليل المكاني فى نظم المعلومات الجغرافية فى عملية ايجاد افضل مكان لكل من خزان المياه و محطة الرفع الخاصة بالصرف الصحى.
٤. استخدام المعادلات و البرامج التي صممت فى برنامج ARC GIS فى عملية ايجاد اقطار المواسير فى تخطيط شبكات البنية التحتية (المياه و الصرف الصحى).
٥. اخراج شبكات المياه والصرف الصحى فى صورة شبكات المرافق فى برنامج ARC GIS
٦. يوصى بتطبيق النظام المقترح لتخطيط شبكات البنية التحتية على مدن و قرى ذات مساحات شاسعة لدراسة مدى جداوه الاقتصادية.

CONTENTS

Subject	Page
List of Figures	I
List of Tables	IV
Abstract	VI
Introduction	1
Objectives of the Research	2
Structure of the Thesis	2
Previous Trials and Experiences	3
1. Remote Sensing Data Concepts and Characteristics	
1.1 Introduction to Remote Sensing	7
1.2 Brief History of Remote Sensing	8
1.3 Introduction to Satellite Imagery	9
1.4 Satellite Sensor Characteristics	10
1.4.1 Spatial Resolution	10
1.4.2 Spectral Resolution	11
1.4.3 Temporal Resolution	12
1.4.4 Radiometric Resolution	13
1.5 Types and Classes of Remote Sensing Data	14
1.6 High Resolution Remote Sensing Satellites	15
1.6.1 Landsat	15
1.6.2 SPOT	20
1.6.3 EgyptSat-1	24
1.6.4 IRS	25
1.6.5 ALOS	26
1.6.6 EROS	27
1.6.7 IKONOS	28
1.6.8 QUICKBIRD	30
1.6.9 WORLDVIEW -1	32
1.6.10 GeoEye-1	32
1.7 Applications of Remote Sensing	33
1.7.1 Mapping	33

1.7.2 Geology	35
1.7.3 Agriculture	35
1.7.4 Forestry	36
1.7.5 Rangeland Resource Monitoring	36
1.7.6 Water Resources	36
1.7.7 Urbanization (Land Use Land Cover Changes)	36
1.7.8 Environmental Assessment	37
2. Orthorectification of Satellite Images	
2.1 Definition of Satellite Imagery	38
2.2 Satellite Images Collection Geometric Errors	38
2.2.1. The Systematic Errors	39
2.2.2. The Random Errors	39
2.3 Digital Elevation Model (DEM)	39
2.3.1. Different DEM Data Sources	40
2.3.1.1. Aerial and Space Images	40
2.3.1.2. Existing Topographic Maps	40
2.3.1.3. Synthetic Aperture Radar Imaging (SAR)	41
2.3.1.4. Airborne Laser Scanning (LIDAR)	42
2.3.1.5. Global Positioning System (GPS)	43
2.3.1.6. Traditional Surveying Techniques	43
2.3.2 The Quality of DEM	44
2.4 Orthorectification of Satellite Imagery	44
2.4.1. The Ground Control Points (GCPs)	45
2.4.2. The Transformation Process	45
2.4.2.1. Polynomial Transformation	45
2.4.2.2. Affine Transformation	48
2.4.2.3. Projective Transformation	49
2.4.2.4. Piecewise Transformation	50
2.4.2.5. Digital Differential Rectification	51
2.4.2.6. Direct linear Transformation	52
2.4.3. The Resampling Process	53

2.4.3.1. The Nearest Neighbor Technique	53
2.4.3.2. The Bilinear Interpolation Technique	54
2.4.3.3. The Cubic Convolution Technique	55
2.4.4 Accuracy Investigation of Orthorectification Process	56
2.5 Features Vectorization	58
2.5.1. Manual Vectorization	58
2.5.2. Semi-Manual Semi-automatic Vectorization (On Screen Digitizing)	59
2.5.3. Automatic Vectorization	61
3. Geographic Information Systems (GIS)	
3.1 The Definition of Geographic Information Systems	62
3.2 Components of GIS	63
3.2.1. People	64
3.2.2. Procedures	64
3.2.3. Hardware	65
3.2.4. Software	65
3.2.5. Data	65
3.3 GIS Tasks	66
3.3.1. Input	66
3.3.2. Manipulation	66
3.3.3. Management	67
3.3.4. Query	67
3.3.5. Analysis	67
3.3.6. Visualization	69
3.4 GIS Spatial Data Representation	70
3.4.1 Raster Data Model	70
3.4.2 Vector Data Model	71
3.4.3 Raster and Vector Advantages and Disadvantages	72
3.5 GIS Database Design	73
3.5.1.Data Base Management System	74
3.5.1.1. Advantages of Using a DBMS	79
3.5.1.2. Disadvantages of Using a DBMS	80

4. Practical Applications

4.1 Study Area Description	82
4.1.1 Selecting the Suitable Satellite Imagery for the Desired Mapping Scale	82
4.1.2 Data Sources	83
4.1.3 Used Softwares	85
4.2 Methodology of Investigation	86
4.2.1 Orthorectification of the Satellite Images	86
4.2.1.1 Generation of the Digital Elevation Model	86
4.2.1.2 Checking the Vertical Accuracy of the Ground Digital Elevation Model	90
4.2.1.3 Checking the Vertical Accuracy of the Global (SRTM) Digital Elevation Model	91
4.2.1.4 Generation of the Digital Building Model	92
4.2.1.5 Checking the Vertical Accuracy of the Digital Building Model	94
4.2.1.6 Possibility of Using Google Earth Points as Control Points	95
4.2.1.7 Orthorectification of GEO EYE Satellite Image Using GPS Control Points and Ground DEM and DBM	100
4.2.1.8 Orthorectification of QUICKBIRD Satellite Image Using GPS Control Points and Ground DEM and DBM	106
4.2.3 On Screen Digitizing and Production of the Final Thematic Maps	112
4.2.4 Checking the Planimetric Accuracy of the Map Production Process	115
4.3 Building a GIS for the Study Area	118
4.3.1 Creation of the Database for the Study Area	118
4.3.2 Analysis and Planning for Study Area	119
4.3.3. Applications of GIS	121
4.3.3.1. Pre-Planning of Water Networks for the Study Area	121
4.3.3.2. Pre-Planning of the Sewage Networks for the Study Area	132

5. Conclusions and Recommendations

5.1 Conclusions.	145
5.2 Recommendations.	146

6. References

147

List of Figures

Figure	Page
(1.1) Remote Sensing System Components.	8
(1.2) Historical Development of Remote Sensing Systems.	9
(1.3) Examples of Different Spatial Resolutions.	11
(1.4) Example of Multi Spectral Resolution.	12
(1.5) Landsat 1, 2 and 3 Daily Orbit Pattern.	16
(1.6) Landsat 4 and 5 Daily Orbital Pattern.	18
(1.7) SPOT 1, 2 Twin HRV Imaging Systems.	21
(1.8) SPOT 5 Images Samples.	24
(1.9) IKONOS Sensor Principle.	29
(2.1) Structure of a Digital Multispectral Image.	38
(2.2): An Aerial Camera.	40
(2.3): Synthetic Aperture Radar Imaging Geometry.	41
(2.4): Principle of Airborne Laser Scanning.	42
(2.5): The Projective Transformation Concept.	49
(2.6): (a) A set of Random Spaced Control Points, (b) Triangulation of Control Points and (c) Piecewise Linear Resampling of Image Using the Control Points.	51
(2.7): The Resampling Process.	53
(2.8): The Nearest Neighbor Resampling Technique.	54
(2.9): The Bilinear Interpolation Resampling Technique.	55
(2.10): The Cubic Convolution Resampling Technique.	56
(2.11): RMS Error of Point.	56
(2.12) Digitizing Table.	59
(2.13) On Screen Digitizing.	61
(3.1) Modeling the Earth Surface Using GIS.	63
(3.2) Components of GIS.	66
(3.3) Proximity Analysis.	68
(3.4) Overlay Analysis.	69
(3.5) Data Visualization in GIS.	69
(3.6) Raster Data Model.	70

(3.7) Structure of Database Systems.	77
(4.1) The QUICKBIRD Satellite Image.	83
(4.2) GEO EYE Satellite Image Extracted from Google Earth Program.	84
(4.3) 1/5000 Topographic Map of the Study Area.	85
(4.4) Sample of the Elevation Points from Ground Surveying.	87
(4.5) The Ground Digital Elevation Model of the Study Area.	88
(4.6) Sample of The Elevation Points from Global (SRTM) DEM.	89
(4.7) Digital Elevation Model Derived from the Global (SRTM).	89
(4.8) Distribution of the Check Points over the Study Area.	90
(4.9) Sample of Digital Building Model of Study Area.	93
(4.10) Sample of 3D Digital Building Model of Study Area.	93
(4.11) Distribution of GCPs over the Study Area.	96
(4.12) The Shift in Easting Direction between Google Earth and GPS 20 Points.	98
(4.13) The Shift in Northing Direction between Google Earth and GPS 20 Points.	98
(4.14) Vector Length of Shift between Google Earth and GPS 20 Points.	99
(4.15) Direction of Shift of Two Points p1 and p6.	99
(4.16) Distribution of GCPs over the Study Area (5 CPs).	101
(4.17) Distribution of GCPs over the Study Area (10 CPs).	103
(4.18) Distribution of GCPs over the Study Area (10 CPs) and DBM.	105
(4.19) RMS of the GEO EYE Satellite Image Extracted from Google Earth Program.	106
(4.20) Distribution of GCPs over the Study Area (5 CPs).	107
(4.21) Distribution of GCPs over the Study Area (10 CPs).	109
(4.22) Distribution of GCPs over the Study Area (10 CPs) and DBM.	111
(4.23) RMS of the QUICKBIRD Satellite Image.	112
(4.24) On Screen Digitizing for GEO EYE Satellite Image Extracted from Google Earth Program for Streets.	113
(4.25) On Screen Digitizing for GEO EYE Satellite Image Extracted from Google Earth Program for Buildings.	113
(4.26) On Screen Digitizing for QUICKBIRD Satellite Image for Streets.	114
(4.27) On Screen Digitizing for QUICKBIRD Satellite Image for Buildings.	114

(4.28) The Results of On Screen Digitizing for Both Streets and Buildings from GEO EYE Satellite Image Extracted from Google Earth Program.	115
(4.29) Classification of Streets According to Their Widths.	120
(4.30) Classification of Ground Levels in the Study Area.	121
(4.31): (a) Classification of Distances to Buildings (b) Classification of Distances to Streets (c) Classification of Elevations.	123
(4.32): (a) The Reclassification of Distances to Buildings Class 10 with Distance 10m (b) The Reclassification of Distances to Streets Class 10 with Distance 10m (c) The Classification of Elevations Class 10 the Highest Elevations.	124
(4.33) The Overlap of the Streets with the Suitability Map and the Most Suitable Location of the Water Tank.	125
(4.34) The Suitable Location of the Water Tank.	126
(4.35) Pressure Zones of the Study Area.	128
(4.36): Distribution of the Primary Feeder Pipes Viewed in the Designed Program.	129
(4.37): Flow Chart of the Designed Program for Water Network Pre-Planning.	130
(4.38): Sample of Final Water Network.	131
(4.39): Divided Zones with Classified Levels and Arrows give Water Flow Direction on Study Area.	133
(4.40): Distribution of the Primary Sewage Pipes Viewed in the Designed Program.	134
(4.41): Flow Chart of the Designed Program for Sewage Network Pre-Planning.	135
(4.42): (a) Classification of Distances to Buildings (b) Classification of Distances to Streets (c) Classification of Elevations.	138
(4.43): (a) Reclassification of the Distances to the Buildings Class 10 with Distance 10m (b) Reclassification of the Distances to the Streets Class 10 with Distance 10m (c) Classification of the Elevations Class 10 the Lowest Elevations.	139
(4.44): Overlap of Streets with the Suitability Map Showing the Most Suitable Location of the Pumping Station.	140
(4.45): The Most Suitable Location of the Pumping Station.	141
(4.46): Sample of Final Sewage Network.	142
(4.47): Flow Chart of the Integration of Remote Sensing and GIS for Infra-Structure Planning.	143

List of Tables

Table	Page
(1.1) Example of Revisit Intervals and Equatorial Crossing Times for Several Satellites Remote Sensing Systems.	13
(1.2) Examples of Bits Number and Pixel Ranges and Gray Scale Divisions.	14
(1.3) MSS Bands and its Applications.	17
(1.4) TM Bands and its Applications.	19
(1.5) HRVIR Bands and its Resolutions.	22
(1.6) VEGETATION Bands and its Resolutions.	22
(1.7) HRG Bands and its Resolutions.	23
(1.8) The IRS-1C and IRS-ID Bands and its Resolutions.	26
(1.9) ALOS Bands and its Resolutions.	27
(1.10) IKONOS Bands and its Resolutions.	29
(1.11) Quickbird Bands and its Resolutions.	31
(1.12) GeoEye-1 Bands and its Resolutions.	33
(1.13) Examples of the Expected Results Map Scales for Different Satellites.	34
(2.1) Comparison of Various DEM Acquisition Techniques.	43
(2.2): Number of GCPs Needed for each Order of Transformation (t).	47
(4.1) Heights from Ground DEM Versus those from Vertical Control Points.	91
(4.2) Heights from Global DEM Versus those from Vertical Control Points.	92
(4.3) Heights from DBM Versus those from Ground Heights.	95
(4.4) Comparison between Google Earth Coordinates and GPS Coordinates in Easting, Northing, Length and Direction.	97
(4.5) Accuracy of Orthorectification Process with DEM only using 5 Control Points.	101
(4.6) Accuracy of Orthorectification Process with DEM only for 10 Check Points.	102
(4.7) Accuracy of Orthorectification Process with DEM only using 10 Control Points.	103
(4.8) Accuracy of Orthorectification Process with DEM only for 5 Check	104

Points.	
(4.9) Accuracy of Orthorectification Process with DEM and DBM using 10 Control Points.	105
(4.10) Accuracy of Orthorectification Process with DEM and DBM for 5 Check Points.	106
(4.11) Accuracy of Orthorectification Process with DEM only using 5 Control Points.	108
(4.12) Accuracy of Orthorectification Process with DEM only for 10 Check Points.	108
(4.13) Accuracy of Orthorectification Process with DEM only using 10 Control Points.	109
(4.14) Accuracy of Orthorectification Process with DEM only for 5 Check Points.	110
(4.15) Accuracy of Orthorectification Process with DEM and DBM using 10 Control Points.	111
(4.16) Accuracy of Orthorectification Process with DEM and DBM for 5 Check Points.	112
(4.17) The Allowable RMS for the Three Map Accuracy Standards.	116
(4.18) Accuracy of Vectorization Process for QUICKBIRD Image Using 5 Check Points.	117
(4.19) Accuracy of Vectorization Process for GEO EYE Satellite Image Extracted from Google Earth Program Using 5 Check Points.	117
(4.20) A Database for the Streets Network.	118
(4.21) A Database for the Buildings.	119
(4.22) Data of Water Pressure Zones of the Study Area.	128
(4.23) Diameters of the Water Primary Feeder Pipes.	131
(4.24) Data of Sewage Zones of the Study Area.	133
(4.25) Data of the Primary Sewage Pipes.	136

INTRODUCTION

Remote sensing has developed historically in parallel with other technological advancement such as optics, sensor electronics, satellite platforms, transmission systems and computer data processing. The first Landsat 1 provided the first detailed, high resolution, multispectral images of the entire land surface and the Landsat series continues today. The most outstanding developments began with the launching of SPOT in 1986 by France. After that a series of satellites were launched as IKONOS, QUICKBIRD, WORLD-VIEW and GEOEYE providing photos to the earth's surface with high resolution up to 40 cm nowadays (*Chuvienco, E., and Huete, A., 2010*).

Different satellite images are currently available, suitable for various types of applications. Satellite image data enable direct observation of the land surface at repetitive intervals and therefore allow mapping of the extent and monitoring of the changes in land cover. Evaluation of the static attributes of land cover (types, amount, and arrangement) and the dynamic attributes (types and rates of changes) on satellite image data may allow the types of change to be regionalized and the proximate sources of change to be identified or inferred. This information, combined with results of case studies or surveys, can provide helpful input to informed evaluations of interactions among the various driving forces (<http://www.ciesin.columbia.edu/TG/RS/RS-home.html>).

The growing availability of high resolution Google-Earth satellite images led to evaluations that are aimed at the definition of the mapping scale they can reasonably be defined for. At this high resolution, details such as buildings and other infrastructure are easily visible. Google will have access to details of 50 cm (20 in) which will be available commercially (<http://en.wikipedia.org/wiki/GeoEye-1>).

Maps can be created from these images by the Orthorectification process which is the process of geometrically correcting an image so that it can be represented on a planar surface, conform to other images or conform to a map. Orthorectification is the process by which geometry of an image is made planimetric. It is necessary

when accurate area, distance and direction measurements are required to be made from the imagery (*Erdas field guide, Fifth Edition, 1999*).

The Database can be created using Geo Database as an example of Object based type of Databases as it saves both the spatial shape type and its attributes in the same file.

(*Chuvieco, E., and Huete, A., 2010*).

The Remote Sensing and GIS can be integrated to provide thematic maps for spatial features with attributes up to date information. Also analysis using GIS for Infra-Structure Planning purposes more speedy and low costs can be done.

Objectives of the Research

The main objective of this research was to Study the integration of Remote Sensing and GIS for providing thematic maps for spatial features with up to date attributes information for Infra-Structure Planning purposes more speedy and low costs. Another objective of this research to Study the possibility of using free products of Google Earth program as Google Earth control points as alternative source to GPS control points or even with it, Global DEM (SRTM) as alternative source to ground DEM especially for flat terrain areas and finally using satellite image extracted from Google Earth program GEO EYE satellite image in this case (Google Earth program doesn't have the same spatial resolution satellite images for all areas) as alternative source to QUICKBIRD satellite images.

Two experiments were conducted to evaluate the planimetric accuracy of the results. The first one based on GEO EYE satellite image extracted from Google Earth program. The second one based on QUICKBIRD satellite image. All results were in UTM (Universal Transverse Mercator) system.

Structure of the Thesis

The remainder of the material of this research will be presented in the next five chapters, whose contents are summarized in the subsequent paragraphs:

Chapter 1 Discusses the Remote Sensing Data Concepts and Characteristics, Introduction of Remote Sensing. Brief history of Remote Sensing will also be discussed. Introduction to satellite imagery will be briefly outlined. Types and classes of Remote Sensing data also Satellite sensor characteristics and High Resolution Remote Sensing Satellites will be discussed in details and finally different applications of Remote Sensing.

Chapter 2 Discusses orthorectification of the satellite images and Digital Elevation Models, Definition of satellite imagery, Satellite images collection geometric errors, Definition and uses of DEM, The different sources of digital elevation models generation including Aerial and Space Images, Existing Topographic Maps, SAR, LIDAR, ground surveying, Global Positioning System (GPS) and Traditional Surveying Techniques also The factors affect the quality of DEM-derived products and the process of Vectorizing features.

Chapter 3 Discusses the Geographic Information Systems (GIS). The definition of Geographic Information Systems, Components of GIS, GIS Tasks and GIS spatial data representation (Raster and Vector) and Finally, GIS Database Design concept.

Chapter 4 Discusses the practical part of the research including the available data to provide thematic maps of spatial features with up to date attributes information for Infra-Structure Planning purposes starting with orthorectifying high-resolution satellite imagery then producing maps from these images and creating Geodatabase containing both spatial and attribute information of the study area. Then GIS analysis was applied for Infra-Structure Planning process especially for Water and Sewage networks. Several experiments were conducted to evaluate the planimetric accuracy of these maps.

Chapter 5 lists the conclusions obtained on the basis of the attained results. Recommendations for further future studies are provided.

Previous Trials and Experiences

(Alexandrov, A., et al., at 2004) has been studied the use of QUICKBIRD satellite imagery for updating cadastral information. Single panchromatic imagery

from QuickBird, with 61 cm resolution in nadir is processed. A DTM from existing contours in *.SHP (shape file) type with contour interval 5 m is generated. After Least Square adjustment the results of the ground displacement for normally distributed check points were as follows: mean \pm 0.82 m, maximal 1.64 m. The geometrical accuracy of the orthorectification of high resolution satellite images met the requirements for topographic map at scale of 1:5000 according to the local technical specifications.

(**Aguilar, M., et al., at 2005**) has been studied the Geometric correction of the QUICKBIRD high resolution panchromatic images . The ancillary data were generated by high accuracy methods: (1) Check and control points were measured with a differential global positioning system (DGPS) and, (2) a dense digital elevation model (DEM) with grid spacing of 2 m generated from a photogrammetric aerial flight at an approximate scale of 1/5000 (RMSE_Z<0.32 m) was used for image orthorectification. Two 3D geometric correction methods were used to correct the satellite data (3D rational function refined by the user and the 3D Toutin physical model). The number of control points by orthorectified imagery (9, 18, 27, 36 and 45 control points) was studied as well. This study showed the high importance of the quality of ancillary data (DEM and GCPs) on the accuracy of the final products. When the dense DEM was used for the image orthorectification by CCRS (Canada Centre for Remote Sensing) model, RMSE of between 0.48 m and 0.61 m were obtained. These values correspond to approximately 0.8 or 1 pixel.

(**Roberto. C., et al., at 2005**) has been Orthorectify High Resolution satellite images with space derived DSM . This study showed the orthorectification of high resolution satellite images and assessed the final accuracy which where achieved when Digital Surface Models (DSM) provided by other remotely sensed data. By using a photogrammetric processing, a DSM was obtained from an EROS (Earth Resources Observation System) high resolution stereo pair acquired over a portion of the city of Bologna (Italy). After the accuracy assessment of the terrain model through the comparison with external Digital Elevation Model (DEM), a broad range of orthorectification procedures with high resolution satellite images (IKONOS, QUICKBIRD and EROS) have been therefore investigated by the authors. The accuracy in final positioning provided by the orthorectification of QuickBird imagery

with the EROS-derived elevation dataset was evaluated using a evenly spaced set of Ground Control Points from GPS survey. The achieved accuracy could met the requirements needed in technical cartography specifications (to scale as large as 1:10000) updating of well recognizable features or entities and generic mapping procedures.

(**Volpe, F., at 2005**) has been studied the Geometrical processing of QUICKBIRD high resolution satellite data . This study showed that geometrical processing of QUICKBIRD data can be carried out with several approaches starting from each of the three QuickBird base products. The results could be obtained in terms of accuracy were strongly depend on the starting product, on the morphology of the area and on the quality of the ancillary information (GCPs and Digital Elevation Model) that were involved in the processing. The results showed similar trends and accuracy levels for all the images belong to the same group and a clear influence of the quality of the ancillary data on the achievable geometrical accuracy. It is important to note that the analyzed approach was just one of the possible solutions to the issue of the geometrical processing of QUICKBIRD data.

(**Alkan, M., et al., at 2008**) has Integrate a high resolution QUICKBIRD images with GOOGLE EARTH . In this study, Zonguldak city which is located in North-West part of Turkey was selected as the test field. The high resolution (60 cm) images of American QUICKBIRD satellite were used as pads. Besides, 1:1000 scale digital topographic maps were used for the extraction of details like roads and buildings with cartography and to provide the currency of satellite images. The data which were acquired from satellite images and cartography have been integrated with each other in a GIS. In GOOGLE EARTH, the information from high resolution satellite images and cartography do not exist for Zonguldak region that's why the results obtained from this study have been planned for the integration to the GOOGLE EARTH in Zonguldak city. The results of this study were proved that the high resolution satellite images and cartographic data in GIS environment and they are harmonious with GOOGLE EARTH.

(**Ahmed R., et al., at 2008**) has been studied the Planimetric accuracy of orthorectified QUICKBIRD imagery using non-parametric sensor models . This study

has showed that the non-parametric sensor models were useful for orthorectification of QUICKBIRD imagery to produce orthoimages. In the framework of the investigation, accuracy evaluation of the planimetric position of the obtained satellite orthoimages was done. The results showed that Generation of orthoimages with high accuracy can be done effectively from Ortho Ready Standard panchromatic product using non-parametric models this does not require the data of imaging sensor and orbit elements. The user could also order smaller Ortho Ready Standard panchromatic scenes which are cheaper instead of full scenes and The RPC (Rational Polynomial Coefficients) non-parametric model could also used for orthorectifying QUICKBIRD imagery of flat terrain with accuracies 4.875m, 1.499m and 2.028m according to the three methods of orthorectification (1- using the RPC supplied with data only, 2- using the RPC supplied with data + 2GCPs and 3- using built RPC from 3D GCPs). These accuracies of the orthorectification had met theoretically the requirements for orthoimages at scale 1:10000, 1:3000 and 1:5000 or smaller.

(Alkan M., and Marangoz M.A., at 2009) has been studied the Creation of cadastral maps for rural and urban areas by using high resolution satellite imagery. This study showed that the advantages and disadvantages of using QUICKBIRD and IKONOS imagery for producing cadastral maps. In this study, high resolution IKONOS and QUICKBIRD images of rural and urban test areas in Zonguldak and Bartın have been chosen. Firstly, pan-sharpened IKONOS and QUICKBIRD images have been produced by fusion of high resolution PAN and MS images. The parcel, building and road network objects have been extracted automatically from these datasets by initially dividing it into segments and then classified by using spectral, spatial and contextual information. On the other hand, these objects have been manually digitized from high resolution images. These vectors have been produced automatically and manually and compared with the existing digital cadastral maps and reference vector maps (scale 1:5000) of the test area. The success of object-oriented image analysis results was tested by GIS software; the results showed that QUICKBIRD image produced suitable mapping results. The main problems in the study area are the shadows of neighbored buildings. Besides, QUICKBIRD image produced non-suitable mapping results for parcels objects in city area.

Chapter 1

Remote Sensing Data Concepts and Characteristics

1.1 Introduction to Remote Sensing

Remote Sensing is defined as the measurement of object properties on the earth's surface using data acquired from aircraft and satellites. It is therefore an attempt to measure something at a distance rather than in close. Since there is no direct contact with the object of interest, so it must rely on propagated signals of some sort, for example optical, acoustical, or microwave (*Schowengerdt, R., 2007*).

The system of Remote Sensing consists of seven parameters (Energy Source or Illumination, Radiation and the Atmosphere, Interaction with the Target, Recording of Energy by the Sensor, Transmission, Reception, and Processing, Interpretation, Analysis and Application) as shown in Figure (1-1).

The term “remote sensing” is most commonly used in connection with electromagnetic techniques of information acquisition. These techniques cover the whole electromagnetic spectrum from low-frequency radio waves through the microwave, submillimeter, far infrared, near infrared, visible, ultraviolet, x-ray, and gamma-ray regions of the spectrum (*Elachi, C., and van Zyl J., 2006*).

There are two kinds of remote sensing (passive and active). Passive sensors detect natural radiation that is emitted or reflected by the object or surrounding area being observed. Reflected sunlight is the most common source of radiation measured by passive sensors. Examples of passive remote sensors include film photography, Infrared, charge-coupled devices and radiometers. On the other hand active collection emits energy in order to scan objects and areas whereupon a sensor then detects and measures the radiation that is reflected or backscattered from the target. RADAR is an example of active remote sensing where the time delay between emission and return is measured, establishing the location, height, speed and direction of an object (http://en.wikipedia.org/wiki/Remote_sensing).

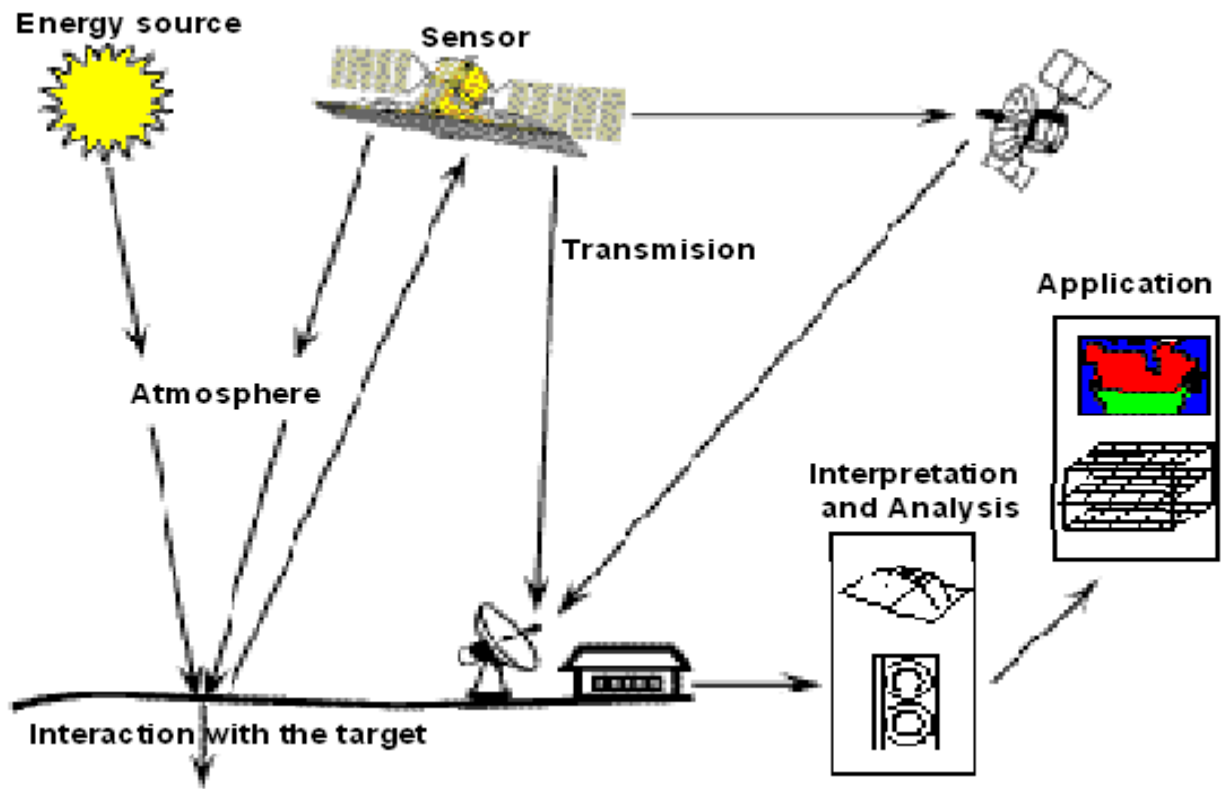


Figure (1.1): Remote Sensing System Components.

(Canada Centre for Remote Sensing Remote Sensing Tutorial).

1. 2 Brief History of Remote Sensing

Remote sensing has developed historically in parallel with other technological advancement such as optics, sensor electronics, satellite platforms, transmission systems and computer data processing.

In 1839, the first ever photos were taken in France and in 1840 the French began using photos to produce topographic maps. In 1858 the first aerial photos were taken from a height of 80m over Bievre, France using cameras mounted on a hot air balloon. By 1915 the British Royal Air Force was collecting aerial reconnaissance photos with cameras designed specially for aircraft. The launch of Sputnik by the Soviet Union in 1957 was the start of a long series of civil and military missions that enables us to explore our planet.

The first Earth Resources Technology Satellite (ERTS) launched on 1972 and was later renamed Landsat 1 provided the first detailed, high resolution, multispectral images of the entire land surface and the Landsat series continues today. The most outstanding

developments began with the launching of SPOT in 1986 in France. A series of satellites were launched providing a continuous photos to the earth's surface with high resolution up to 40 cm nowadays as shown in Figure (1-2) (*Chuvieco, E., and Huete, A., 2010*).

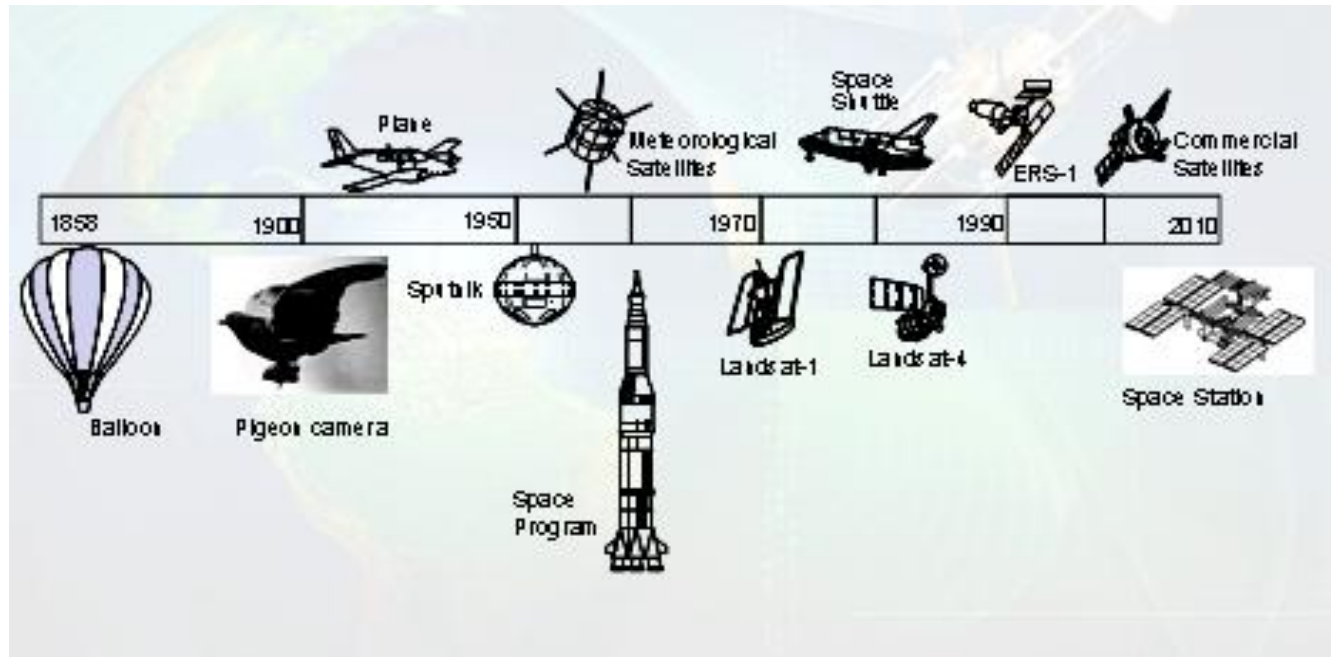


Figure (1.2): Historical Development of Remote Sensing Systems.

(*Chuvieco, E., and Huete, A., 2010*).

1.3 Introduction to Satellite Imagery

Several remote sensing satellites are currently available, providing imagery suitable for various types of applications. Satellite image data enables direct observation of the land surface at repetitive intervals and therefore allow mapping of the extent and monitoring the changes in land cover.

Evaluation of the static attributes of land cover (types, amount, and arrangement) and the dynamic attributes (types and rates of change) on satellite image data may allow the types of change to be regionalized and the proximate sources of change to be identified or inferred. This information, combined with results of case studies or surveys, can provide helpful input to informed evaluations of interactions among the various driving forces (<http://www.ciesin.columbia.edu/TG/RS/RS-home.html>).

Remote sensing satellite imagery has many applications in mapping land-use and cover, agriculture, soil mapping, forestry, city planning, archaeological investigations, military observation, and surveying (<http://www.physicalgeography.net/fundamentals/2e.html>).

1.4 Satellite Sensor Characteristics

The basic function of most satellite sensors is to collect information about the reflected radiation along a pathway, which is known as the field of view (FOV). A small sampled area of ground is called the instantaneous field of view (IFOV).

The IFOV is also described as the pixel size of the sensor. This sampling or measurement occurs in one or many spectral bands of the Electro Magnetic spectrum. The data collected by each satellite sensor can be described in terms of spatial, spectral, radiometric and temporal resolution (*Sanderson, R., 2006*).

1.4.1 Spatial Resolution

The spatial resolution (also known as ground resolution) identifies the smallest object that can be detected on an image or the minimum separation at which objects appear independent and isolated. In optical electronic sensors, the term instantaneous field of view (IFOV) is commonly used instead. The IFOV is defined as the angular section observed by the sensor, in radians, at a given moment of time. The sensor spatial resolution is the size of the projected IFOV on the ground.

The spatial resolution of optical electronic sensors depends on orbit height, speed of data collection and the numbers of detectors nowadays the higher spatial resolution sensors currently have an active range from 0.4 to 4.0 m as shown in Figure (1-3).

Spatial resolution plays a major role in image interpretation because it affects the level of detail achieved. The selection of the most convenient spatial resolution is closely related to the suitable scale for the particular problem under study. The smaller the size of the pixel, the smaller the probability that the pixel will be a mix of two or more cover types which known as the mixed pixel (*Chuvieco, E., and Huete, A., 2010*).

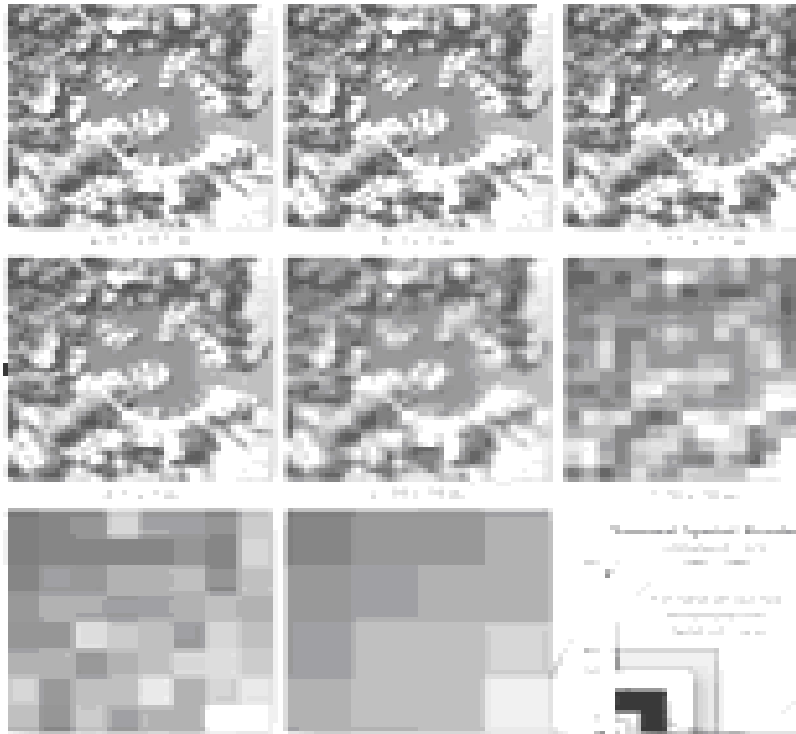


Figure (1.3): Examples of Different Spatial Resolutions.

(Chuvienco, E., and Huete, A., 2010).

1.4.2 Spectral Resolution

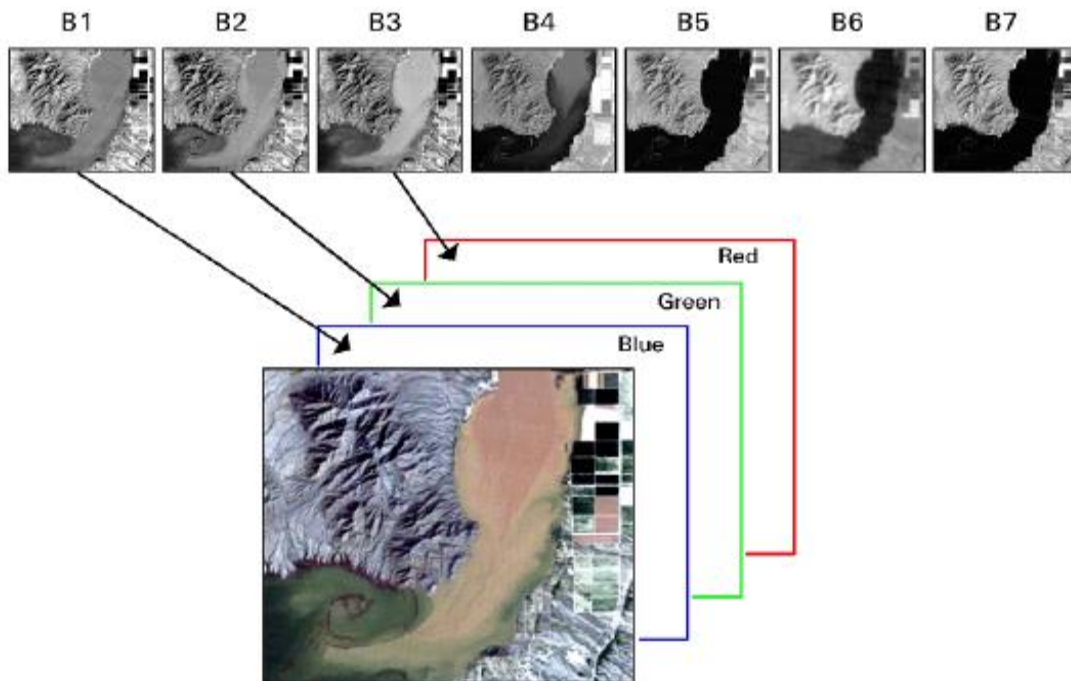
The spectral resolution of a sensor system is the number and width of spectral bands in the sensing device. The simplest form of spectral resolution is a sensor with one band senses visible light. An image from this sensor would be similar in appearance to black and white aerial photographs. A sensor with three spectral bands in the visible region of the EM spectrum would collect similar information to that of the human vision system. The Landsat TM sensor has seven spectral bands located in the visible and near to mid infrared parts of the spectrum (Sanderson, R., 2006).

A panchromatic image consists of only one band. It is usually displayed as a grey scale image, i.e. the displayed brightness of a particular pixel is proportional to the pixel digital number which is related to the intensity of solar radiation reflected by the targets in the pixel and detected by the detector.

Thus, a panchromatic image may be similarly interpreted as a black-and-white aerial photograph of the area, though a lower resolution. Multispectral and hyperspectral

images consist of several bands of data. For visual display, each band of the image may be displaying one band as a grey scale image, or in combination of three bands as a color composite image. Interpretation of a multispectral color composite image will require the knowledge of the spectral reflectance signature of the targets in the scene. Figure (1-4) shows example of multi spectral resolution images (*Sanderson, R., 2006*).

The finer the spectral resolution, the narrower the wavelength range for a particular channel or band (*Canada Centre for Remote Sensing Remote Sensing Tutorial*).



Landsat TM Color Composite Image

Figure (1.4): Example of Multi Spectral Resolution.

(*Remote Sensing Engineer Manual, 2003*).

1.4.3 Temporal Resolution

One of the most valuable aspects of unmanned satellite remote-sensing systems is their inherent repeating coverage of the same area on the earth. The interval between revisits depends on the particulars of the satellite orbit for sensors that have a fixed view direction (nadir), such as the Landsat Thematic Mapper. If more than one system is in orbit at the same time, it is possible to increase the revisit frequency.

The high resolution commercial satellites, IKONOS and QUICKBIRD, are even more “agile,” i.e. they can point off-nadir within a short time. They can thus obtain two in-track views at different angles of the same area, within minutes, to make a stereo pair. Without pointing, their revisit times are 1 to 3 days, depending on the latitude (more frequent at high latitudes) (*Schowengerdt, R., 2007*).

Table (1-1) shows examples of revisit intervals for some Remote Sensing systems.

Table (1.1): Example of Revisit Intervals and Equatorial Crossing Times for Several Satellites Remote Sensing Systems. (*Schowengerdt, R., 2007*).

Satellite	Revisit Interval	Daylight Equatorial Crossing Time
Landsat	18 days (L-1, 2, 3)/16 days (L-4, 5, 7)	9:30 A.M./10:15 A.M
SPOT	26 days (nadir only); 1 day or 4– 5 days	10:30 A.M.
IKONOS	minutes (same orbit), 1–3 days (pointing)	10:30 A.M.
QUICKBIRD	minutes; 1–3 days	10:30 A.M.
IRS-1A, B	22 days	10:30 A.M.

1.4.4 Radiometric Resolution

Radiometric resolution refers to the dynamic range, or numbers of possible data file values in each band. This is referred to a number of bits through which the recorded energy is divided. For instance, in 8-bit data, the data file values range from 0 to 255 for each pixel, but in 7-bit data, the data file values for each pixel range from 0 to 128 and so on as shown in table (1-2) (*Erdas field guide Fifth Edition, 1999*).

The finer the radiometric resolution of a sensor the more sensitive for detecting small differences in reflected or emitted energy (*Canada Centre for Remote Sensing Remote Sensing Tutorial*).

Table (1.2): Examples of Bits Number and Pixel Ranges and Gray Scale Divisions
(Lillesand, T., and Kiefer, R., 2008).

Bits Number	Digital Number (DN)	Gray Scale Divisions
6	0 to 63	64
7	0 to 127	128
8	0 to 255	256
9	0 to 511	512
10	0 to 1023	1024

1.5 Types and Classes of Remote Sensing Data

Satellite-sensor platforms are characterized by the wavelength bands employed in image acquisition, spatial resolution of the sensor, the coverage area and the temporal converge, i.e. how frequent a given location on the earth surface can be imaged by the imaging system (<http://www.crisp.nus.edu.sg/~research/tutorial/spacebrn.html>).

The remote sensing satellite imagery can be classified as following

- 1) According to the spatial resolution
 - a) Low resolution systems (approx. 1 km or more)
 - b) Medium resolution systems (approx. 100 m to 1 km)
 - c) High resolution systems (approx. 5 m to 100 m)
 - d) Very high resolution systems (approx. 5 m or less)
- 2) According to the spectral regions used in data acquisition
 - a) Optical imaging systems (include visible, near infrared, and shortwave infrared systems)
 - b) Thermal imaging systems
 - c) Synthetic aperture radar (SAR) imaging systems
- 3) According to the number of spectral bands used
 - a) Panchromatic (single wavelength band, "black-and-white", grey-scale image) systems that acquired by sensor measures energy reflectance in one portion of electromagnetic spectrum
 - b) Multispectral (several spectral bands) systems: captures image data at specific wavelengths across the electromagnetic spectrum. The wavelengths may be separated

by filters or by the use of instruments that are sensitive to particular wavelengths, including light from frequencies beyond the visible light range, such as infrared. Multi-spectral imaging can allow extraction of additional information that the human eye fails to capture with its receptors for red, green and blue. It was originally developed for space-based imaging (http://en.wikipedia.org/wiki/Multi-spectral_image).

c) Hyperspectral (hundreds of spectral bands) systems. Collects and processes information from across the electromagnetic spectrum. Unlike the human eye, which just sees visible light, hyperspectral imaging can see visible light as well as from the ultraviolet to infrared. Hyperspectral capabilities recognize different types of coral, prey, or predators, all which may appear as the same color to the human eye (http://en.wikipedia.org/wiki/Hyperspectral_imaging).

The following section shows an overview of common high resolution remote sensing satellites

1.6 High Resolution Remote Sensing Satellites

1.6.1 Landsat

Seven landsat satellites have now been successfully launched commencing with landsat-1 in July 1972. All platforms have operated from a repetitive, circular, sun-synchronous, near-polar orbit and on each day-side pass, scan a ground swath 185 km wide beneath the satellite. The first three satellites carried the Multi-spectral Scanner (MSS) as the main imaging instrument with a Return Beam Vidicon (RBV) as a subsidiary. Landsats 4 and 5 had the Thematic Mapper (TM) as the main sensor together with an MSS. The newest satellite in the series Landsat 7 carries the enhanced thematic mapper plus (ETM+) (*Landsat Satellites Historical*).

Landsats 1, 2, and 3 operated in a near-polar orbit at an altitude of 920 km. These satellites circled the Earth every 103 minutes, completing 14 orbits a day. With ground Track speed of 6.46 km/sec (*Chuvienco, E., and Huete, A., 2010*).

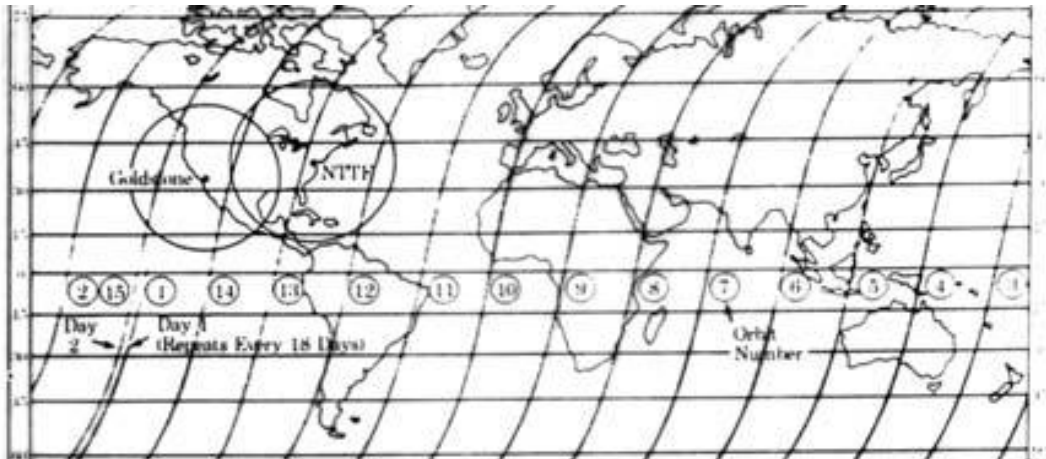


Figure (1.5): Landsat 1, 2 and 3 Daily Orbit Pattern.

(Chuvieco, E., and Huete, A., 2010).

Figure (1-5) shows north to south orbits for a single day, the orbits cross the equator at angle 9.2° from normal (or inclination angle of 99.2°) with 2760 km on equator between two successive orbits. The sensor has only 185 km swath width, so there are large gaps in image coverage between successive orbits. In each new day, the satellite orbit is progressed slightly west-ward just to over shoot the orbit of the previous day. The satellites had the capability of covering the globe once every 18 days or about 20 times per year. At the 103 minute orbital period, the 2760 km equatorial spacing between successive orbits caused the satellites to keep precise pace within the sun's west-ward progress as the earth rotated.

As a result of that, the satellite always crossed the equator at precisely the same local sun time to take the advantage of early morning skies that are generally clearer than later in the day (Lillesand, T., and Kiefer, R., 2008).

Landsats 1, 2, and 3 have two types of sensors: a three-camera return-beam vidicon (RBV) to obtain visible light and near infrared photographic images of Earth and four-channel multispectral scanner (MSS) to obtain radiometric images of Earth (http://en.wikipedia.org/wiki/Landsat_1).

The RBV system consists of three television-like cameras. The nominal ground resolution of cameras was about 80 m and the spectral sensitivity of each camera was essentially to that of a single layer of color infrared film:

Band (1) 0.475 to 0.575 μm (green), band (2) 0.580 to 0.680 μm (red) and band (3) 0.690 to 0.830 μm (near infrared)

The RBV system did not contain film, but instead their images were exposed by a shutter device and stored on a photosensitive surface within each camera. This surface was then scanned in a raster form by an internal electron beam to produce a video signal such as in a conventional television camera (*Lillesand, T., and Kiefer, R., 2008*).

The MSS instrument is an electromechanical scanning system which scans side to side during the passage of the satellite from north to south. Radiation from the earth's surface is directed to a set of six detectors in each of the four bandwidths, allowing six lines of data to be collected with each sweep of the mirror system. This radiation is converted into a digital signal in the range of zero to 63 which is then transmitted to the ground station. The Instantaneous Field of View (IFOV) of the MSS sensor on Landsats 1-3 was 79 m², however over sampling of the data in the scan line direction resulted in data collected at approximately 57 m. The approximate ground area of pixels of unprocessed data is therefore 57 m by 79 m (*Landsat Satellites Historical*).

Landsat 3 carried a MSS sensor with an additional band, designated band 8, that responded to thermal (heat) infrared radiation as shown in table (1-3) (<http://landsat.gsfc.nasa.gov/about/mss.html>).

Table (1.3): MSS Bands and its Applications.

(*Landsat Satellites Historical*).

Bands	Wavelength (μm)	Applications
4	0.5 to 0.6 (visible green)	Emphasises movement of sediment-laden water and Delineates areas of shallow water.
5	0.6 to 0.7 (visible red)	Emphasises cultural features, such as city areas. Also used for some vegetation types.
6	0.7 to 0.8 (near infrared)	Emphasises vegetation, the boundary between land and water, and landforms.
7	0.8 to 1.1 (near infrared)	Provides the best penetration of atmospheric haze, and Also emphasises vegetation.
8	10.41 to 12.6 (thermal)	Emphasises temperature variations. only on Landsat 3

Landsat 4, 5 and 7 have Earth coverage similar to Landsat 1-3. However, the lower altitude results in a different swathing pattern. Landsat 5 and 7 (and Landsat 4 prior to its decommissioning) operate in a repetitive, circular, sun-synchronous, near-polar orbit at a

nominal altitude of 705.3 km (438.4 miles) measured at the equator and Inclination 98.2°. The descending orbital node time is 9:45 AM +/- 15 minutes at the equator with an orbital period of 98.9 minutes, completing 14.5 orbits per day and viewing the entire Earth every 16 days see Figure (1-6) (<http://landsat.gsfc.nasa.gov/about/wrs.html>).

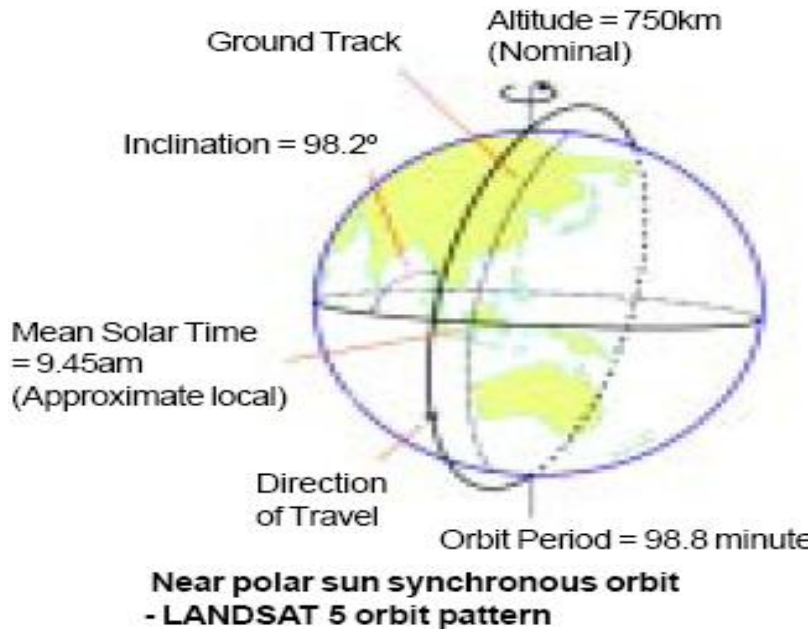


Figure (1.6): Landsat 4 and 5 Daily Orbital Pattern.

(Landsat Satellites Historical).

Landsats 4 and 5 carried both the MSS and a new, improved thematic mapper (TM) sensor. The MSS sensors onboard Landsats 4 and 5 were identical to the one that was carried on Landsat 3 (*Landsat Fact Sheet, 2003*).

The Thematic Mapper (TM) is an advanced, multispectral scanning, Earth resources sensor designed to achieve higher image resolution, sharper spectral separation, improved geometric fidelity and greater radiometric accuracy and resolution than the MSS sensor. TM data are sensed in seven spectral bands simultaneously. Band 6 senses thermal (heat) infrared radiation. A TM scene has an instantaneous field of view (IFOV) of 30 square meters in bands 1-5 and 7 while band 6 has an IFOV of 120 m² on the ground. Table (1-4) shows the TM bands and its applications (<http://landsat.gsfc.nasa.gov/about/tm.html>).

The use of more sensitive detectors, better optics and a lower orbit has enabled the collection of radiation in 7 spectral bands, with improved ground resolution, and with data quantized to 256 intensity levels and radiometric resolution of 8 bits. Data is collected using banks of 16 detectors in each band and 16 lines of data are collected during both the forward and backward sweeps of the oscillating mirror system (*Landsat Satellites Historical*).

Table (1.4): TM Bands and its Applications.

(*Landsat Satellites Historical*).

Bands	Wavelength (μm)	Applications
1	0.45 - 0.52 (visible blue)	Coastal water mapping, differentiation of soil from vegetation and forest type mapping.
2	0.52 – 0.60 (visible green)	Vegetation vigor assessment.
3	0.63 - 0.69 (visible red)	Vegetation discrimination also has high iron oxide reflectivity.
4	0.76 – 0.90 (near infrared)	Determining biomass content, delineation of water bodies and for soil moisture discrimination.
5	1.55 - 1.75 (middle infrared)	Vegetation and soil moisture content, differentiation of cloud from snow.
6	10.40 – 12.50 (thermal infrared)	Vegetation heat stress analysis, soil moisture discrimination, thermal mapping.
7	2.08 - 2.35 (middle infrared)	Discrimination of rock types and hydrothermal clay mapping.

On Landsat 7, the latest in the series, the Enhanced Thematic Mapper (ETM+) sensor provides 7 bands of multi-spectral data at 30 meters resolution, plus a panchromatic band at 15 m, over a swath 183 km wide. There is also a 60 m thermal infrared band (*Landsat Satellites Historical*).

1.6.2 SPOT

The SPOT program consists of a series of optical remote sensing satellites with the primary mission of obtaining Earth imagery for land use, agriculture, forestry, geology, cartography, regional planning, water resources and GIS applications. It is committed to commercial remote sensing on an international scale and has established a global network of control centers, receiving stations, processing centers and data distributors. SPOT satellites are operated by the French Space Agency, Centre National d'Etudes Spatiales (CNES) (<http://www.crisp.nus.edu.sg/~research/tutorial/spot.html>).

The SPOT orbit is polar, circular, sun-synchronous and phased. A polar orbit in conjunction with the rotation of the earth around the polar axis, the inclination of the orbital plane (98 degrees) allows the satellite to fly over any point of the earth during a 26 day cycle with altitude of 822 km, orbital period of 101 minutes and revisit time of 1 to 3 days. The SPOT satellite has westward drift between successive ground tracks of 2823 km (*Chuvienco, E., and Huete, A., 2010*).

The SPOT1, 2 and 3 payloads were identical and comprised two identical HRV (High Resolution Visible) imaging instruments which scanned in either the Panchromatic or Multispectral modes. The position of each HRV entrance mirror can be commanded by ground control to observe a region of interest not necessarily vertically beneath the satellite. Thus, each HRV offers an oblique viewing capability, the viewing angle being adjustable through +/- 27degrees relative to the vertical as shown in Figure (1-7) (<http://www.crisp.nus.edu.sg/~research/tutorial/spot.html>).

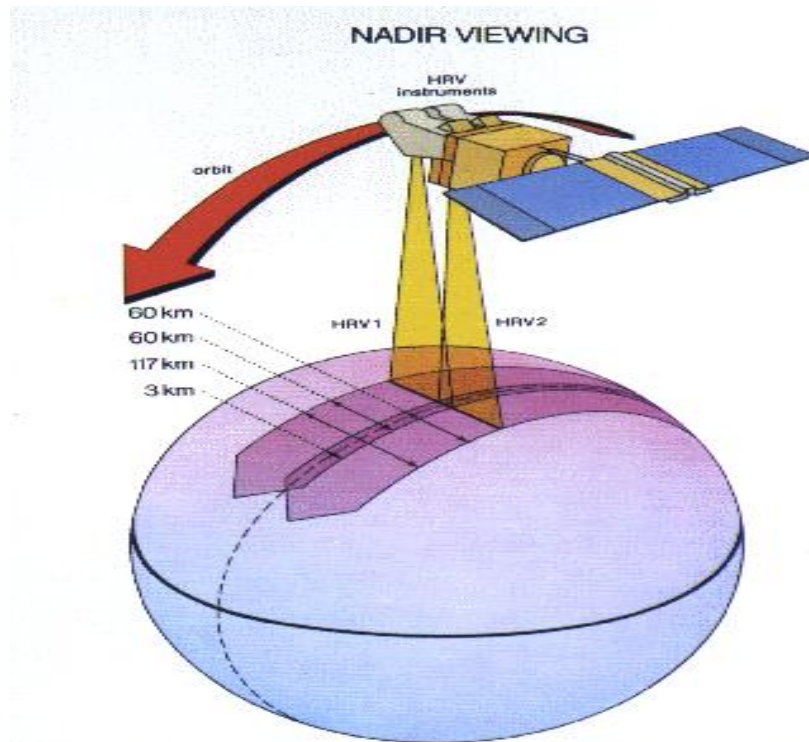


Figure (1.7): SPOT 1, 2 Twin HRV Imaging Systems.

(Landsat <http://www.crisp.nus.edu.sg/~research/tutorial/spot.htm>).

Two spectral modes of acquisition are employed as (<http://www.spotimage.fr/home/system/welcome.html>):

- (1) Panchromatic (P) has Instrument Field of View of 4.13° , spatial Resolution of 10 m and cover visible range of (0.51 to $0.73 \mu\text{m}$)
- (2) Multispectral (XS) has Instrument Field of View of 4.13° , spatial Resolution of 20 m and cover over three bands. Band (XS1) 0.50 - $0.59 \mu\text{m}$ (Green), band (XS2) 0.61 - $0.68 \mu\text{m}$ (Red), band (XS3) 0.79 - $0.89 \mu\text{m}$ (Near IR). Both HRVs can operate in either mode, either simultaneously or individually and have ground swath of 60 km.

SPOT 4 satellite includes the following instruments (http://www.csc.noaa.gov/crs/rs_apps/sensors/spot.html):

1. Two High Resolution Visible and Infrared HRVIR imaging instruments similar to HRV system in spot 1, 2 and 3, the HRVIR system includes two identical sensors capable of imaging a total nadir swath width of 120 km. Among the major improvements in the system is the addition of a 20 m resolution band in the mid-IR

portion of the spectrum between 1.58 and 1.75 μm . This band improves the vegetation monitoring, mineral discriminating and soil moisture mapping capability of data also replacing the panchromatic band of spot 1, 2 and 3 with the (red) band from these systems (0.61 to 0.68 μm) as shown in table (1-6) (*Lillesand, T., and Kiefer, R., 2008*).

Table (1.5): HRVIR Bands and its Resolutions.

(Landsat <http://www.crisp.nus.edu.sg/~research/tutorial/spot.htm>).

Bands	Wavelength (μm)	Resolution (m)
XI1	0.50 - 0.59 (Green)	20
XI2	0.61 - 0.68 (Red)	20
XI3	0.79 - 0.89 (Near IR)	20
XI4	1.53 - 1.75 (MID IR)	20
M	0.61 - 0.68 (Red)	10

2. The VEGETATION 1 (VEG1) instrument, which has a ground swath of 2,250 kilometers. VEG1 uses the same spectral bands as the HRVIR instruments (B2, B3, and mid-IR) plus an additional band for oceanographic applications, this system is useful when large area coverage is important. Table (1-7) shows the VEGETATION bands and its Resolution (<http://www.spotimage.fr/home/system/welcome.html>).

Table (1.6): VEGETATION Bands and its Resolution.

(<http://eoedu.belspo.be/en/satellites/spot.htm>).

Bands	Wavelength (μm)
B0	0.43 – 0.47 μm (Blue)
B2	0.61 – 0.68 μm (Red)
B3	0.79 – 0.89 μm (Near IR)
MIR	1.58 – 1.75 μm (MID IR)

The main system of Spot 5 consists of high resolution imaging instruments delivering a product improved compared to Spot 4 first dedicated instrument for along track stereo acquisition, higher ground resolution of 5 meters and 2.5 meters (instead of 10 m) in panchromatic mode and higher resolution in multispectral mode of 10 m (instead of 20 m) in all 3 spectral bands in the visible and near infrared ranges. The spectral band in the short wave infrared band (essential for VEGETATION data) is maintained at a resolution of 20 m due to limitations imposed by the geometry of the

CCD sensors used in this band. The field width of each instrument: 60 km, same as Spot 1, 2, 3 and 4. Spot 5 spectral bands are the same as those of Spot 4. The panchromatic band does, however, return to the values used for Spot 1-2-3 (0.51 – 0.73 μm). As requested by many users, this ensures continuity of the spectral bands established since Spot 1. Spatial resolutions are, on the other hand, improved within the limits of technical feasibility as the field width of each instrument will be also kept identical (<http://eoedu.belspo.be/en/satellites/spot.html>).

The SPOT 5 satellite includes the following instruments (<http://eoedu.belspo.be/en/satellites/spot.htm>):

1) HRG sensor. Two HRG (High Resolution Geometric) instruments are capable of generating data at four resolution levels with the same 60 km swath with images in the SWIR band of 20 m and multispectral images (green, red and near-infra-red) of 10 m and panchromatic images of 5 m also super mode panchromatic images of 2.5 m as shown in the following table.

Table (1.7): HRG Bands and its Resolutions.

(<http://eoedu.belspo.be/en/satellites/spot.htm>).

Bands	Wavelength (μm)	Resolution (m)
B1	0,50 - 0,59 μm	10
B2	0,61 - 0,68 μm	10
B3	0,79 - 0,89 μm	10
SWIR	1,58 - 1,75 μm	10
PAN	0,51 - 0,73 μm	5m (or 2.5m)

2) HRS sensor. This is an instrument with the ability to acquire stereo pair images simultaneously, a considerable advantage for the quality of digital elevation model (DEM) production. It has spectral band with resolution of 10 m, along the track sampling and panchromatic of 5 m. the imaging swath (centered on the satellite track) is 120 km.

3) VEGETATION 2 sensor. Unchanged with comparison to the one installed onboard SPOT 4.

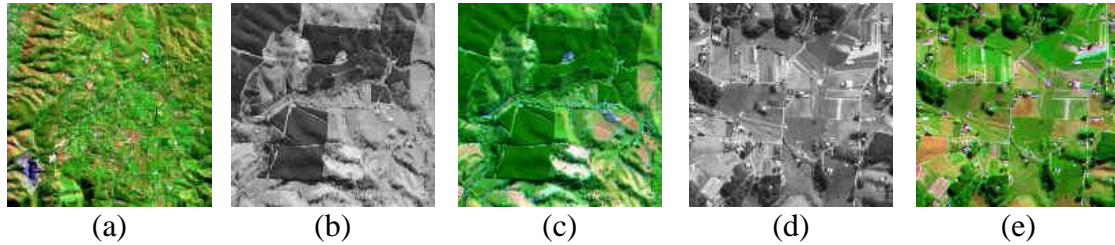


Figure (1.8): SPOT 5 Images Samples (a) 10 m Multispectral; (b) 5 m Panchromatic; (c) 5 m Multispectral; (d) 2.5 m Panchromatic; (e) 2.5 m Multispectral.

(http://www.geoimage.com.au/geoweb/spot/spot_overview.htm).

SPOT satellites data are preprocessed in panchromatic or multispectral mode to one of the following levels:

- 1) Level 1A - Detector normalization which is performed in each spectral band for radiometric corrections. This is the least processed form of data with no geometric corrections applied. When viewed, the image is a square. The scene is oriented along the satellite's orbital path, not in a map projection.
- 2) Level 1B - Radiometric and minimal geometric processing is performed to correct distortion from the Earth's rotation and the panoramic effects associated with oblique viewing angles. When viewed, the image is a parallelogram. The scene is oriented along the satellite's orbital path, not in a map projection.
- 3) Level 2A - Detector normalization is performed in each spectral band for radiometric corrections. The scene is a map projection, geocoded using satellite ephemeris data, and without auxiliary ground control points. The terrain distortion is not corrected.
- 4) Level 2B – Geocoded product using ground control points. Product is in a map projection.
- 5) Level 3A – Orthorectified product using ground control points and digital elevation model (http://www.csc.noaa.gov/crs/rs_apps/sensors/spot.html).

1.6.3 EgyptSat-1

EgyptSat-1 is the first Egyptian Earth remote-sounding satellite. it was launched on 17 April 2007. This satellite has a polar, circular and sun-synchronous with altitude of 670

km and inclination of 98.0° from the equator. The orbital period is 98.0 minute and it makes one revolution around the earth every eight hours crossing over Egypt two times every day. The revisit time is 72 hours. Egyptsat-1 is weighing only 100 kg and is carrying two devices: An infrared sensing device and a high resolution multispectral imager together with store and forward communications payload with 8m resolution (<http://en.wikipedia.org/wiki/EgyptSat1>) and (<http://www.n2yo.com/satellite/?s=31117>).

EgyptSat-1 was launched for important missions such as (http://en.wikipedia.org/wiki/EgyptSat_1):

- 1) Providing images for Egyptian deserts to recognize its geology and environment
- 2) Observing the reduction of agriculture lands on Egypt
- 3) Observing the pollution in national Egyptian water and the reduction of shore lines in Egypt

1.6.4 IRS

IRS (Indian Remote Sensing) Indian has the largest constellation of Remote Sensing Satellites, which are providing services both at the national and global levels. From the Indian Remote Sensing (IRS) Satellites, data is available in a variety of spatial resolutions up to 2.5 m. After the successful launch of IRS-1A and IRS-1B, the second two satellites IRS-1C and IRS-ID were launched on 1997 with temporal resolution of 24 days and 744 km swath width (<http://www.fas.org/spp/guide/india/earth/irs.html>).

The IRS-1C and IRS-ID satellites has three sensors on board first (LISS-III) Linear Imaging Self-Scanning remote sensing instruments which has a spatial resolution of 23 m, with the exception of the (SW Infrared band), which is 70 m. Bands 2, 3, and 4 have a swath width of 142 kilometers; band 5 has a swath width of 148 km and The panchromatic sensor which has 5.8 m spatial resolution, as well as stereo capability see table (1-9). Its swath width is 70 m also WIFS has a 188 m spatial resolution (*Erdas field guide Fifth Edition, 1999*).

Table (1.8): The IRS-1C and IRS-ID Bands and its Resolutions.

(<http://www.fas.org/spp/guide/india/earth/irs.html>).

Band	Wavelength (μm)	Resolution (m)
1 (Green)	0.52 to 0.59 μm	23
2 (Red)	0.62 to 0.68 μm	23
3 (Near IR)	0.77 to 0.86 μm	23
4 (SWIR)	1.55 to 1.70 μm	23
PAN	0.5 to 0.75 μm	5.8

IRS-P5 (CARTOSAT-1) has an improved sensor system that provides 2.5 m resolution with fore-aft stereo capability. This mission caters to the needs of cartographers and terrain modeling applications. The satellite will provide cadastral level information up to 1:5000 scale and will be useful for making 2-5 m contour maps (<http://www.fas.org/spp/guide/india/earth/irs.html>). With regard to applications in planning and management, IRS data is being used for urban planning (http://india.gov.in/sectors/science/indian_remote.php).

1.6.5 ALOS

ALOS (Advanced Land Observation Satellite) was launched on January 24, 2006. This satellite has a polar, circular and sun-synchronous with altitude of 692 km and inclination of 98.2° from the equator. ALOS is one of the world's largest earth observation satellites whose function is to collect global and high resolution land observation data and data will be made available at conditions similar to those of Earth Remote Sensing satellite missions, namely for scientific use as well as commercial applications. It can collect enough data by itself for mapping on a scale of 1:25000, without relying on points of reference on the ground. Some of its objectives are cartography, disaster monitoring, natural resource surveys and technology development.

ALOS characteristics:

The spatial resolution is 2.5 m panchromatic (2.5-m PAN) and 10-meter multispectral (10-m MS)

The spectral resolution has three remote-sensing instruments. the Panchromatic Remote-sensing Instrument for Stereo Mapping (PRISM) for digital elevation mapping (DEMs), the Advanced Visible and Near Infrared Radiometer type 2 (AVNIR-2) for precise land coverage observation, and the Phased Array type L-band Synthetic Aperture Radar (PALSAR) for day-and-night and all-weather land observation. Table (1-10) shows the ALOS different bands and its resolutions

Table (1.9): ALOS Bands and its Resolutions.

(<http://www.fas.org/spp/guide/india/earth/irs.html>).

Band	Wavelength (μm)	Resolution (m)
1 (Blue)	0.42-0.50 μm	10
2 (Green)	0.52-0.60 μm	10
3 (Red)	0.61-0.69 μm	10
4 (Near IR)	0.76-0.89 μm	10
PAN	0.52-0.77 μm	2.5

The radiometric resolution is collecting data with an 11-bit (0-2047) and its temporal resolution is 2 days revisit time (<http://www.satimagingcorp.com/satellite-sensors/alos.html>).

1.6.6 EROS

EROS (Earth Remote sensing Observation Satellite) A was launched on December 5, 2000. This satellite has a polar, circular and sun-synchronous with altitude of 480 km and inclination of 97.3° from the equator. The equatorial crossing time is nominally 9:45 AM. Using its body rotation function, the satellite is able to turn up to 45 degrees in any direction. The revolutions around the earth are 15 every 24 hours (*Chen, L., and Teo, T., 2002*).

EROS A is equipped with a camera NA30 and it's a push-broom scanner with two CCD arrays, including a total of 7800 detectors in the focal plane. The detectors are sensitive in the spectral range 0.5 – 0.9 μm produces a standard image resolution of 1.8 meters (*Westin, T., and Forsgren, J., 2002*). With a swath of 12.5-km and sub-meter resolution using hyperspectral sampling techniques. The radiometric resolution is collecting data

with an 11-bit (0-2047) and its temporal resolution is 2 to 4 days revisit time (*Chen, L., and Teo, T., 2002*).

EROS B was launched on April 25, 2006. This satellite has a polar, circular and sun-synchronous with altitude of 500 km and inclination of 97.2° from the equator. This satellite has superior capabilities, including a larger camera of CCD/TDI type (Charge Coupled Device/Time Delay Integration), with standard panchromatic resolution of 0.70 m improved pointing accuracy and a faster data communication link. The swath is 7 km. The radiometric resolution is collecting data with an 11-bits and its temporal resolution is 2 to 4 days revisit time

(http://www.satmagazine.com/cgi-bin/display_article.cgi number=1307290351) and (http://www.satmagazine.com/cgi-bin/display_image.cgi 1705129920).

EROS A and EROS B have several Applications such as Mapping, urban planning, military, change detection, disaster management, oceanography, geology

(http://www.terralink.co.nz/products_services/satellite/eros_satellite_images/).

EROS C was planned for launch in 2010. EROS C's highest resolution of 0.7-m and the satellite offers higher quality resolution and a higher data link rate than either EROS A or B (http://www.satmagazine.com/cgi-bin/display_article.cgi?number=1307290351).

1.6.7 IKONOS

IKONOS was launched on September 24, 1999. This satellite has a polar, circular and sun-synchronous with altitude of 680-km and inclination of 98° from the equator. The equatorial crossing time is nominally 10:30 AM. The revolutions around the earth are 14.7 every 24 hours with speed over the ground equals to 7 kilometers per second. The image swath is 11.3 kilometers at nadir and 13 kilometers at 30° off-nadir (*Tiejun, W., 2005*).

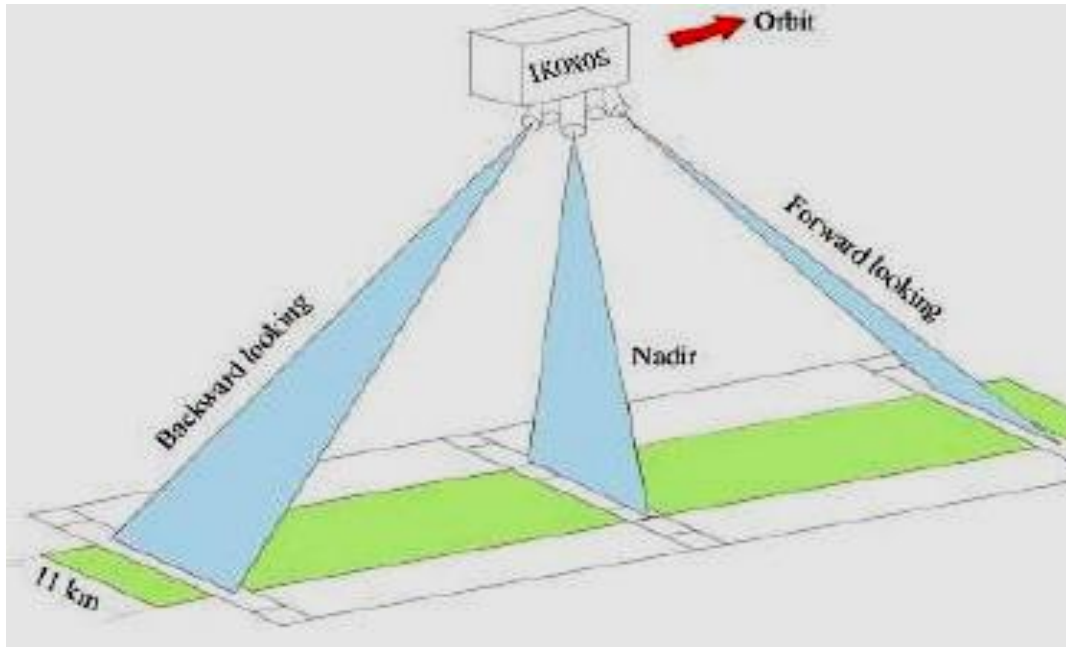


Figure (1.9): IKONOS Sensor Principle.

(Tiejun, W., 2005).

IKONOS characteristics:

The spatial resolution: (the ground sampling distance GSD) of the IKONOS sensor is 0.82 m at (nadir) for panchromatic images and 3.28 m at (nadir). At 30 degrees off nadir the GSD is 1 m and 4 m.

The spectral resolution is collecting imagery in four multispectral bands (red, green, blue and near infrared)

Table (1.10): IKONOS Bands and its Resolutions.

(Tiejun, W., 2005).

Band	Wavelength (μm)	Resolution (m)
1 (Blue)	0.445-0.516 μm	4
2 (Green)	0.506-0.595 μm	4
3 (Red)	0.632-0.698 μm	4
4 (Near IR)	0.757-0.853 μm	4
PAN	0.45-0.90 μm	1

The radiometric resolution is collecting data with an 11-bit (0-2047) sensitivity. From time-to-time the data are rescaled down to 8-bit (0 - 255) to decrease file size.

The temporal resolution: At 40 degrees latitude the revisit time is 2.9 days at 1 m GSD and 1.5 days at 1.5 GSD. The revisit times are shorter for higher latitudes and longer for latitudes closer to the equator (*Tiejun, W., 2005*).

1.6.8 QUICKBIRD

QUICKBIRD was launched on October 18, 2001. This satellite has a polar, circular and sun-synchronous with altitude of 450 Km and inclination of 97.2° from the equator. The equatorial crossing time is nominally 10:30 AM (descending node). The orbital Period is 93.4 minutes around the earth with speed over the ground equals to 7.1 Km/sec (25,560 Km/hour). The image swath is 16.5 Km x 16.5 Km at nadir and 13.8 kilometers and 544 km centered on the satellite ground track (to ~30° off-nadir) (<http://www.satimagingcorp.com/satellite-sensors/quickbird.html>) and (<http://www.gras.ku.dk/Products/SatelliteImages/QuickBird.aspx>).

QUICKBIRD characteristics:

In standard collection mode, the QUICKBIRD sensor is tilted along and across track in the range 0°-15° in order to image desired areas. The resolution on the ground in panchromatic mode is, in this range, between 61 and 66 cm (*Volpe, F., 2004*).

While Standard and Ortho Imagery products are resampled to a 60 or 70 cm resolution and for multispectral delivered at the resolution in which the data were collected (ranging from 2.44 m at nadir to 2.88 m at 25° off-nadir), while Standard and Ortho Imagery products are resampled to a 2.4 or 2.8 m pixel spacing (<http://www.eurimage.com/products/quickbird.html>).

At this resolution, details such as buildings and other infrastructure are easily visible. However, this resolution is insufficient for working with smaller objects such as a license plate on a car. The imagery can be imported into remote sensing image processing software, as well as into GIS packages for analysis. The imagery can also be used as a backdrop for mapping applications, such as Google Earth and Google Maps. Google Earth is a free, downloadable virtual globe program (<http://www.statemaster.com/encyclopedia/QuickBird>).

The spectral resolution:

Spectral information is collected by QUICKBIRD not only in the panchromatic band but also, with a resolution starting from 2.44 meters, in one infrared and three visible bands. Since the three visible bands collect spectral information in the blue, green and red part of the electromagnetic spectrum, it is possible from their RGB combination to generate natural colours views that can be used as a starting point for both technical and non-technical analysis.

By combining the infrared band with the green and the red bands, it is possible to generate false colour images when a more technical analysis of the territory is required. Natural and false colour views can be improved in terms of geometrical resolution by merging with the high-resolution panchromatic band, generating pan-sharpened multispectral images that preserve both the colour information contained in the multispectral images and geometric resolution of the panchromatic band. Colour information, especially in pan-sharpened products, is a key factor for the discrimination of small features, and in any case for a better interpretation of the imagery (*Volpe, F., 2004*).

Table (1.11): QUICKBIRD Bands and its Resolutions.

(*Volpe, F., 2004*).

Band	Wavelength (μm)	Resolution (m)
1 (Blue)	0.45-0.52 μm	2.40
2 (Green)	0.52-0.60 μm	2.40
3 (Red)	0.63-0.69 μm	2.40
4 (Near IR)	0.76-0.90 μm	2.40
PAN	0.45-0.90 μm	0.60

The radiometric resolution:

For each band, the spectral information is collected using a range of 2048 (11 bit) possible levels. This feature allows, through the use of proper processing techniques, more detailed information extraction (*Volpe, F., 2004*).

The temporal resolution is 1 to 3.5 days depending on latitude (<http://www.eurimage.com/products/quickbird.html>).

1.6.9 WORLDVIEW -1

WorldView-1 was launched on September 18, 2007. This satellite has a polar, circular and sun-synchronous with altitude of 496 km and inclination of 97.2 ° from the equator. The equatorial crossing time is nominally 10:30 AM. The image swath is 17.6 Km at nadir. The orbital period is 94.6 minutes (*Eurimage products and services WorldView-1, 2009*).

WorldView-1 characteristics: The spatial resolution is 0.50 m at nadir of panchromatic (black and white) images and 0.55 meters at 20° off-nadir. The radiometric resolution is collecting data with an 11-bit (0-2047) sensitivity. The temporal resolution is 1.7 days revisit rate for true-nadir and 5.9 days at 20° off-nadir (*Eurimage products and services WorldView-1, 2009*).

Due to the high accuracy of WorldView-1, 1:12000 scale orthomosaics are offered worldwide without GCP's. Customers can provide higher accuracy of scales (1:4800/5000) for WorldView-1 imagery where GCP's can be collected (<http://www.eurimage.com/products/wv-1.html>).

1.6.10 GeoEye-1

GeoEye-1 was launched on September 6, 2008. This satellite has a polar, circular and sun-synchronous with altitude of 684 kilometers / 425 miles and inclination of 98° from the equator. The equatorial crossing time is nominally 10:30 AM. The speed over the ground equals About 7.5 km/sec or 17,000 mi/hr. The image swath is 15.2 kilometers. It has the world's highest-resolution commercial color imaging satellite offers extraordinary detail, high accuracy and enhanced stereo for DEM generation (<http://www.satimagingcorp.com/satellite-sensors/geoeye-1.html>).

GeoEye-1 characteristics:

The spatial resolution is 0.41-meter panchromatic (black & white) and 1.65-meter multispectral resolution. The spectral resolution is collecting imagery in four multispectral bands (red, green, blue and near infrared) and one panchromatic band as shown in the following table

Table (1.12): GeoEye-1 Bands and its Resolutions.

(http://www.usgsquads.com/prod_satellite_imagery.htm).

Band	Wavelength (μm)	Resolution (m)
1 (Blue)	0.45–0.51 μm	1.65
2 (Green)	0.51–0.58 μm	1.65
3 (Red)	0.65–0.69 μm	1.65
4 (Near IR)	0.78–0.92 μm	1.65
PAN	0.45–0.80 μm	0.41

The radiometric resolution is collecting data with an 11-bit (0-2047) sensitivity. The temporal resolution is less than 3 days (http://www.usgsquads.com/prod_satellite_imagery.htm).

Google, which has its logo on the side of the rocket, has exclusive online mapping use of its data. While GeoEye-1 is capable of imagery with details the size of 41 cm (16 in), that resolution will only be available to the U.S. Government. Google will have access to details of 50 cm (20 in) which will be available commercially (<http://en.wikipedia.org/wiki/GeoEye-1>).

1.7 Applications of Remote Sensing

1.7.1 Mapping

Constitutes an integral component of the process of managing land resources, and mapped information is the common product of analysis of remotely sensed data. Natural features and manufactured infrastructures, such as transportation networks, urban areas, and administrative boundaries can be presented spatially with respect to referenced coordinate systems, which may then be combined with thematic information and topographic maps are essential for planning, evaluating, and monitoring, for military or civilian reconnaissance, or land use management, particularly if digitally integrated into a geographic information system as an information base.

Mapping applications of remote sensing include the following:

A. Planimetry

Planimetry consists of the identification and geolocation of basic land cover (e.g. forest, marsh), drainage, and anthropogenic features (e.g. urban infrastructure, transportation

networks) in the x, y plane. Planimetric information is generally required for large-scale applications - urban mapping, facilities management, military reconnaissance and general landscape information. Very high resolution is usually a requirement for accurate planimetric mapping. Concerns of the mapping community with regard to use of satellite data are spatial accuracy and the level of detail of extractable information content. The concern for information content focuses not only on interpretability of features, but on the ability to determine the correct spatial location of a feature. The spatial resolution improved from Landsat 80 m to now GeoEye-1 0.40 m so large scale maps can be produced from satellite images as shown in table (1.13)

Table (1.13): Examples of the Expected Map Scales Results for Different Satellites.

(*Thomas, 2002*)

Satellite	Resolution (m)	Map scale
Landsat MSS	80	1:200000
Landsat TM	30	1:100000
Spot 1-4	20	1:50000
Spot 5	5	1:10000
IKONOS	1	1:5000
QUICKBIRD	0.6	1:5000
WorldView-1	0.5	1:2500
GeoEye-1	0.5	1:2500

B. Digital Elevation Models (DEM's)

Present mapping programs are rarely implemented with only planimetric considerations. The demand for digital elevation models is growing with increasing use of GIS and with increasing evidence of improvement in information extracted using elevation data (for example, in discriminating wetlands, flood mapping, and forest management). The incorporation of elevation and terrain data is crucial to many applications, particularly if radar data is being used, to compensate for foreshortening and layover effects and slope induced radiometric effects. Elevation data is used in the production of popular topographic maps. Generating DEMs from remotely sensed data can be cost effective and efficient. A variety of sensors and methodologies to generate such models are available and proven for mapping applications. Two primary methods of generating elevation data are Stereogrammetry techniques using airphotos (photogrammetry), VIR imagery, or radar data (radargrammetry) and Radar interferometry involves the gathering of precise

elevation data using successive passes (or dual antenna reception) of spaceborne or airborne SAR. High accuracies have been achieved in demonstrations using both airborne (in the order of a few centimeters) and spaceborne data (in the order of 10m).

C. Topographic Mapping

Topographic maps consist of elevation contours and planimetric detail of varied scale, and serve as general base information for civilian and military use. Topographic maps can be produced using Remote Sensing techniques with different scales. SRTM and ASTER are sources of small scale Topographic maps. Satellite images stereo pairs, LIDAR and RADAR are sources of large scale Topographic maps (*Canada Centre for Remote Sensing Remote Sensing Tutorial*).

1.7.2 Geology

Geologic mapping involves the identification of landforms, rock types and rock structures (folds, faults, fractures) and the portrayal of geologic units and structures on a map. Satellite images provide geologist several advantages as large area coverage, the ability to analyze multispectral bands quantitatively in terms of digital numbers which enhance the discern compositional properties of earth materials and the capability of merging different types of remote sensing data products or combining them with topographic elevation data.

1.7.3 Agriculture

A. Crop Area Estimation

For estimating the area covered by the major crops of the season satellite remote sensing should be produced for at least three phenological phases of the crops (establishment, maximum vegetative and active reproductive phase). GPS based ground truth collection of crop field (at least 10%) should be collected. This helps in the accuracy of crop classification and correspondingly in the crop area estimation.

B. Crop Stress Monitoring

Crop stress in large areas can be detected by periodic monitoring the crop health from satellite remote sensing imageries. Once crop stress symptoms are found in substantial areas on the imageries, the exact type of stress can be ascertained by actual field visits

and remedial measures are suggested for recovering the crops from their respective stresses.

1.7.4 Forestry

As forest fire hazard zone mapping. High resolution satellite remote sensing offers one of the best techniques for forest fire detection, mapping and damage assessment in almost near real time and cost effective manner. The spot of forest fire can be detected by high resolution satellite imageries using infrared scanners (AVHRR detectors). Remote sensing technique can be also profitably exploited for quick evaluation and mapping of the damaged area through classification and change detection imageries.

1.7.5 Rangeland Resource Monitoring

While high resolution satellite remote sensing data in visible and near infrared bands help in identifying and classifying plant communities from their characteristic spectral signatures and assessing crop stress through spectral indices, the thermal infrared band helps to assess soil and canopy temperatures. Radar remote sensing helps in estimating soil moisture changes of the rangeland.

1.7.6 Water Resources

A. Assessment of Land Surface Water

Estimation of land surface water in volume unit has two observable parameters the areal spreads of water surface and the corresponding depths of water. Remote sensing technique is ideal for estimating the areal spread of the water bodies using visible, near infrared and microwave bands. Volume of water in water body can be directly estimated by remote sensing technique using the reservoir's topographic data of the driest period using the scanning altimeter as it was done by the Seasat SAR for the ocean surface.

B. Assessment of Subsurface Water

Geologists try to infer indirectly the subsurface hydrological conditions by monitoring some of the relevant surface indicators through visible, near-infrared and thermal infrared spectral bands.

1.7.7 Urbanization (Land Use Land Cover Changes)

With the availability of satellite remote sensing data, land use land cover classification system can be performed. Satellite remote sensing data of the study area acquired by the

multispectral thematic mappers are produced and processed. The enhanced images are then classified using GPS ground truth data. The classified map is then transferred to GIS which will occupy several layers in the database, each layer being on a specific class.

1.7.8 Environmental Assessment

A. Desertification

Desertification monitoring work aims at generating information on the sustained decline of productivity of useful crops from a dry area. Satellite remote sensing offers the most cost effective technique for identification, monitoring and mapping of the desertification processes. The classified satellite data at periodic intervals helps to prioritize areas on the basis of their degrees and rates of desertification.

B. Deforestation

Deforestation monitoring and forest resources assessment at periodic intervals are very much needed at regional and hemispherical levels for planning appropriate strategies to arrest any likely future climate change. From high resolution satellite imageries one can not only estimate the total forested area but can also find out the open and closed forest areas. Data from periodic classified satellite imageries can show us whether the forest area is decreasing with time. (*Panda., B., 2005*).

Chapter 2

Orthorectification of Satellite Images

2.1 Definition of Satellite Imagery

A digital image is a numeric translation of the original radiance received by the sensor forming a 2D array of numbers. The energy received from the instantaneous field of view (IFOV) is converted to a digital value. The value codes of the basic units of information are known as pixels. The brightness of a pixel as seen in the display is a function of its numeric value. This value is denoted as a digital number (*DN*; *Lillesand and Kiefer, 2008*) which is defined as a nonvisual numeric value that can be translated to visual intensity or a gray level by means of a digital analog converter. There are many digital numbers in an image as the radiometric resolution of the sensor and usually that range in the number of bits per pixel as shown in Figure (2.1) (*Chuvieco and Huete, 2010*).

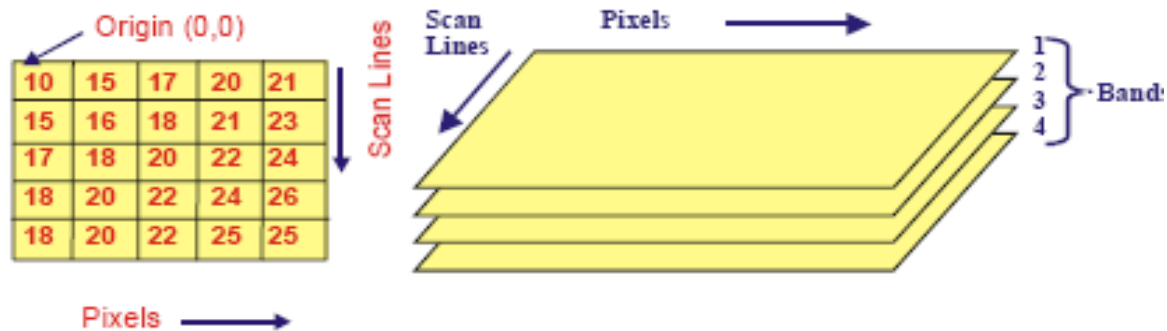


Figure (2.1): Structure of a Digital Multispectral Image.

(*Chuvieco and Huete, 2010*).

2.2 Satellite Images Collection Geometric Errors

Digital images collected from airborne or spacecraft sensors often contain systematic and unsystematic geometric errors. Some of these errors can be corrected by using ephemeris of the platform and known internal sensor distortion characteristics (systematic errors) Other errors can only be corrected by matching image coordinates of physical features recorded by the image to the geographic coordinates of the same features collected from a map or global positioning system GPS (unsystematic errors) random errors (<http://www.gis.usu.edu/Geography-Department/rsgis/RSCC/v6.2/syserr.html>).

2.2.1. The Systematic Errors:

The systematic errors are (<http://www.gis.usu.edu/Geography-Department/rsgis/RSCC/v6.2/syserr.html>).

A. Scan Skew which caused by the forward motion of the platform during the time required for each mirror sweep. The ground swath is not normal to the ground track but is slightly skewed, producing cross-scan geometric distortion

B. Mirror-Scan Velocity Variance. The mirror scanning rate is usually not constant across a given scan, producing along-scan geometric distortion

C. Panoramic Distortion. The ground area imaged is proportional to the tangent of the scan angle rather than to the angle itself. Because data are sampled at regular intervals, this produces along-scan distortion

D. Platform Velocity. If the speed of the platform changes, the ground track covered by successive mirror scans changes, producing along-track scale distortion

E. Earth Rotation. Earth rotates as the sensor scans the terrain. This results in a shift of the ground swath being scanned, causing along-scan distortion

F. Perspective For some applications it is desirable to have images represent the projection of points on a plane tangent to Earth with all projection lines normal to the plan. This introduces along-scan distortion (*Chuvienco and Huete, 2010*).

2.2.2. The Random Errors:

The random errors are (<http://www.gis.usu.edu/Geography-Department/rsgis/RSCC/v6.2/syserr.html>).

A. Altitude Variance: If the sensor platform departs from its normal altitude or the terrain increases in elevation, this produces changes in scale.

B. Platform Attitude: One sensor system axis is usually maintained normal to Earth's surface and the other parallel to the spacecraft's direction of travel. If the sensor departs from this attitude, geometric distortion results.

2.3 Digital Elevation Model (DEM)

A digital elevation model (DEM) is defined as "any digital representation of the continuous variation of relief over space," (*Burrough, P., 1986*).

Elevation data can be represented digitally in many ways, including a gridded model where elevation is estimated for each cell in a regular grid, a triangular irregular network, and contours. Representation of the DEM as a grid is quite common, as this format lends itself well to computer computations. DEM is the 3D representation of a part of the earth surface in global or local scale as digital format with the help of SRP (Sampling Reference Points) and the modeling algorithm (*Arzu, S., and Metin S., 2009*).

2.3.1. Different DEM Data Sources:

2.3.1.1 Aerial and Space Images

Aerial images are the most effective way to produce and update topographic maps. It has been estimated that about 85% of all topographic maps have been produced by photogrammetric techniques using aerial photographs. Aerial photographs are also the most valuable data source for large-scale production of high-quality DTM. Such photographs are taken by metric cameras mounted on aerial planes (*Li, Z., and et al., 2005*). Figure (2.2) shows example of aerial camera.

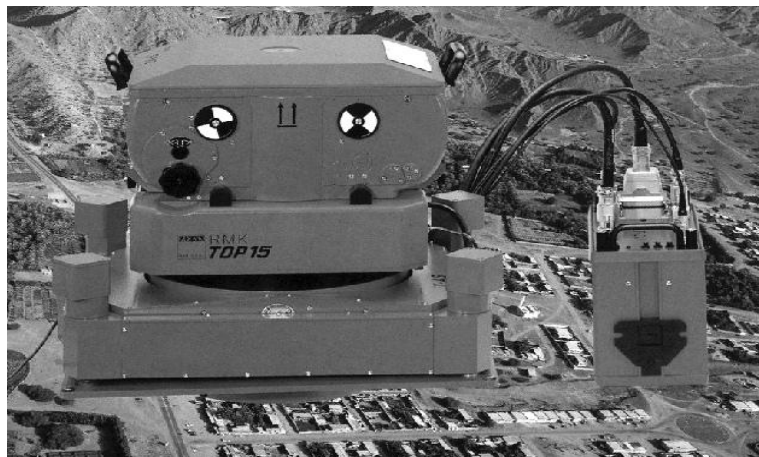


Figure (2.2): An Aerial Camera.

(*Li, Z., and et al., 2005*).

2.3.1.2. Existing Topographic Maps

Every country has topographic maps may be used as another main data source for digital terrain modeling. In many developing countries, these sources may be poor due to the

lack of topographic map coverage or the poor quality of the height and contour information contained in the map. One important concern with topographic maps is the quality of the data contained in them, especially the metric quality, this is then specified in terms of accuracy. In general, it is expected that the height accuracy of any point interpolated from contour lines will be about $1/2$ to $1/3$ of the contour interval (Li, Z., and *et al.*, 2005).

2.3.1.3. Synthetic Aperture Radar Imaging (SAR)

SAR is a microwave imaging radar developed in the 1960s to improve the resolution of traditional (real aperture) radar based on the principle of Doppler frequency shift. Imaging radar is an active sensor providing its own illumination in the form of microwaves. It receives and records echos reflected by the target, and then maps the intensity of the echo into a grey scale to form an image as shown in Figure (2.3). Unlike optical and infrared imaging sensors, imaging radar is able to take clear pictures day and night under all weather conditions (Li, Z., and *et al.*, 2005).

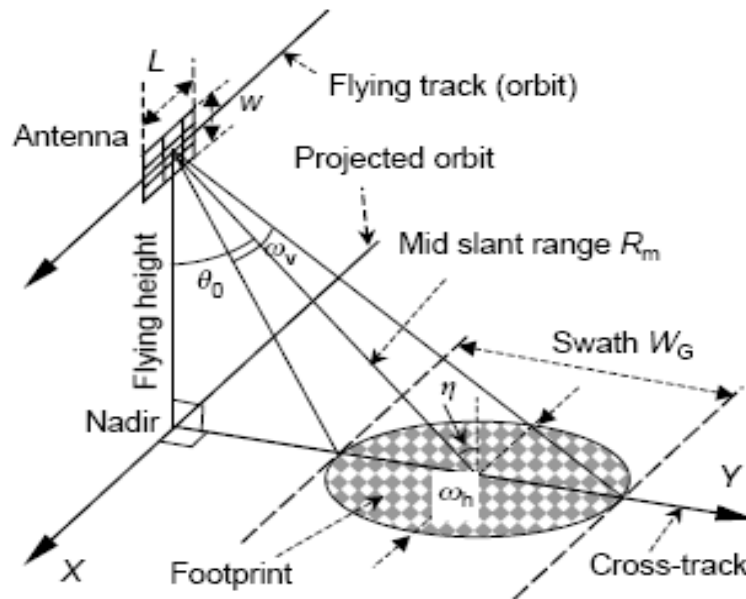


Figure (2.3): Synthetic Aperture Radar Imaging Geometry.

(Li, Z., and *et al.*, 2005).

2.3.1.4. Airborne Laser Scanning (LIDAR)

LIDAR is an active remote sensing technique. This technology involves the use of pulses of laser light directed toward the ground and measuring the time of pulse return. The return time for each pulse back to the sensor is processed to calculate the variable distances between the sensor and the various surfaces present on (or above) the ground as shown in Figure (2.4). Modern LIDAR acquisition begins with a photogrammetric aircraft equipped with Airborne GPS (for x, y, z sensor location), an Inertial Measuring Unit (for measuring the angular orientation of the sensor with respect to the ground), a rapidly pulsing (15000 pulse/sec) laser, a highly accurate clock, substantial onboard computer support and robust data storage.

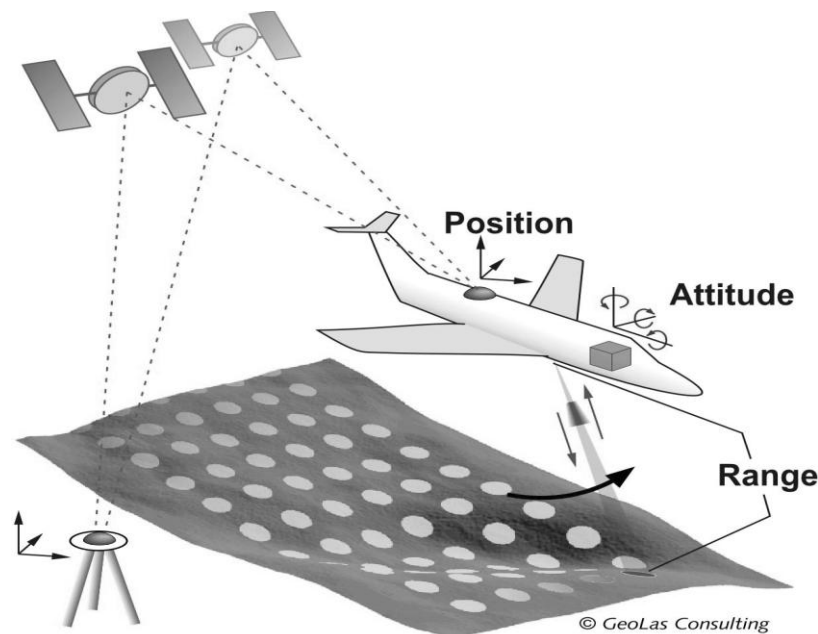


Figure (2.4): Principle of Airborne Laser Scanning.

(Li, Z., and et al., 2005).

The ALS system produces data that can be characterized as sub-randomly distributed 3-D point clouds. The processing of ALS data often aims at either the removal of unwanted measurements (in the form of either erroneous measurements or objects) or the modeling of data for a given specific model (e.g. a DTM) as a subset of a measured digital surface model (DSM). In the process of acquiring ALS data, the following steps are involved, which is, filtering, classification, and modeling. The height accuracy is in the range of 10

to 60 cm (typically 15 to 20 cm) while planimetric accuracy is 0.1 to 3 m (typically 0.3 to 1 m) (*Lillesand, T., and Kiefer, R., 2008*).

2.3.1.5. Global Positioning System (GPS)

It's a system used to find the coordinates on the earth's surface consists of three parts: space segment (24 satellites around the earth), control segment (5 control stations around the earth) and ground segment (receivers to receive signals from the satellites). The receivers can be positioned on the points to find its coordinates using static method for observation or on moving vehicles using kinematic method for observation to find the coordinates of the surveyed terrain. These coordinates can be used to construct high accurate DEMs with relatively short time.

2.3.1.6. Traditional Surveying Techniques

Traditional surveying techniques determine the position (coordinates) of a point through the measurement of distances and angles. The traditional instruments are levels, theodolites and computerized total stations. The accuracy of the Traditional field surveying techniques is very high but it's time consuming and expensive so it's suitable for relatively small areas.

Finally, Table (2.1) shows a Comparison of Various DEM data sources from the data accuracy, speed and costs point of views.

Table (2.1): Comparison of Various DEM Acquisition Techniques.

(*Li, Z., and et al., 2005*).

Acquisition Method	Accuracy of data	Speed	Cost
Traditional surveying	High	Very slow	Very high
GPS survey	Relatively high	Slow	Relatively high
SAR	Low	Very fast	Low
LIDAR	High	Fast	High
Existing Topographic Maps	Relatively low	Slow	Low

2.3.2 The Quality of DEM

The quality of DEM is a measure of how accurate elevation is at each pixel (absolute accuracy) and how accurately is the morphology presented (relative accuracy). Several factors play an important role for quality of DEM-derived products: (http://en.wikipedia.org/wiki/Digital_elevation_model).

- A. Terrain roughness
- B. Sampling density (elevation data collection method)
- C. Grid resolution or pixel size
- D. Interpolation algorithm

Modeling algorithm with known planimetric positions and elevations yields an interpolation problem. Interpolation is the prediction of unobserved point elevations by using observation values distributed around the unobserved point in the concept of DEM. The various methods used for interpolation of elevation are based on the elevations of for the determination of surface models of DEM. Selected interpolation models must be realistic and well adjusted with the topographic characteristics of surface.

- E. Vertical resolution
- F. Terrain analysis algorithm

2.4 Orthorectification of Satellite Imagery

The process of correcting the image from systematic and non-systematic errors (distortions) that acquired from the image acquisition process is known as image orthorectification and registration (*Lillesand, T., and Kiefer, R., 2008*).

Orthorectification is a process of geometrically correcting an image so that it can be represented on a planar surface, conform to other images or conform to a map. That is, it is the process by which geometry of an image is made planimetric.

It is necessary when accurate area, distance and direction measurements are required to be taken from the imagery. It is achieved by transforming the data from one grid system into another grid system using a geometric transformation.

Orthorectification is not necessary if there is no distortion in the image. For example, if an image file is produced by scanning or digitizing a paper map that is in the desired projection system, then that image is already planar and does not require orthorectification unless there is some skew or rotation of the image. Scanning and digitizing produce images that are planar, but do not contain any map coordinate information. These images need only to be geo-referenced, which is a much simpler process than rectification (<http://www.wamis.org/agm/pubs/agm8/Paper-5.pdf>).

Usually, orthorectification is the conversion of data file coordinates to some other grid and coordinate system, called a reference system. Rectifying or registering image data on disk involves the following general steps, regardless of the application:

- A) Locate GCPs
- B) Compute and test a transformation
- C) Create an output image file with the new coordinate information in the header. The pixels must be resampled to conform to the new grid (*Erdas field guide, Fifth Edition, 1999*).

2.4.1. Ground Control Points (GCPs)

GCPs are points of known ground location that can be accurately located on the digital image. Some features that might be used as good control points such as highway intersections, buildings corners, sharp edges of walls and distinct shoreline features. Imprecise location of these points on the image or a sectorized distribution will produce an erroneous geometric correction. For this reason, finding GCPs is the most crucial phase of the correction process and the one that demands more human input. Three aspects are essential in the selection of GCPs (number, location and distribution).

In correction process numerous GCPs are located both in terms of their two image coordinates (column, row numbers) on the distorted image and in terms of their ground coordinates, Typically measured from a map, or GPS located in the field, in terms of UTM coordinates or latitude and longitude coordinates (*Lillesand, T., and Kiefer, R., 2008*).

2.4.2. The Transformation Process

Transformation may be one of the following types:

2.4.2.1. Polynomial Transformation.

2.4.2.2. Affine Transformation.

2.4.2.3. Projective Transformation.

2.4.2.4. Piecewise Transformation.

2.4.2.5. Digital Differential Rectification.

2.4.2.6. Direct Linear Transformation.

The following paragraphs discuss these types of transformation:

2.4.2.1. Polynomial Transformation

It may be categorized to two types as follows:

a) Linear Transformation

The transformation of coordinates from one system to another (image to map) using a linear algebraic formula (first order polynomial transformation). First-order polynomial transformations can be used to project raw imagery to a planar map projection, convert a planar map projection to another planar map projection, and when rectifying relatively small image areas. The first order transformation can also be used for data that are already projected onto a plane but may not be rectified to the desired map projection (<http://www.gis.usu.edu/Geography-Department/rsgis/RSCC/v6.2/syserr.html>).

b) Non-Linear Transformation

Transform of coordinates from one system to another (image to map) using a non-linear algebraic formula (Nth order polynomial). These transformations can correct nonlinear more complicated distortions. Second-order transformations can be used to convert Latitude/Longitude data to a planar projection, for data covering a large area (to account for the Earth's curvature) and with distorted data (for example, due to camera lens distortion). Third-order transformations are used with distorted aerial photographs, on scans of warped maps and radar imagery. Fourth-order transformations can be used on very distorted aerial photographs (*Erdas field guide, Fifth Edition, 1999*) and (<http://www.gis.usu.edu/Geography-Department/rsgis/RSCC/v6.2/syserr.html>).

The higher orders of transformation the more GCPs needed. For instance, three points define a plane. Therefore, to perform a 1st-order transformation, which is expressed by the equation of a plane, at least three GCPs are needed. Similarly, the equation used in a 2nd-order transformation is the equation of a parabola. Six points are required to define a parabola. Therefore, at least six GCPs are required to perform a 2nd-order transformation. The minimum number of points required to perform a transformation of order (t) equals (*Erdas field guide, Fifth Edition, 1999*).

$$\frac{((t - 1)(t - 2))}{2} \quad (2.1)$$

Table (2.2) shows the minimum number of GCPs required to perform each transformation started from the first order. These numbers of GCPs are computed using equation (2.1).

Table (2.2): Number of GCPs Needed for each Order of Transformation (t).

(*Erdas field guide, Fifth Edition, 1999*).

Order of transformation (N)	Number of GCPs
1	3
2	6
3	10
4	15
5	21
6	28
7	36
8	45
9	55
10	66

Due to the polynomial transformation, the original image is shifted, rotated, scaled and squeezed so that it best fits to the given reference points. Although polynomials are very easy to use for rectifications, they can cause problems and errors in the transformed image. They do not adequately correct relief displacements nor do they consider the special geometry of the imaging system (*Novak K., 1992*).

Coefficients are used in a first-order polynomial as follows (*Novak K., 1992*).

$$x_o = a_o + a_1x + a_2y, y_o = b_o + b_1x + b_2y \quad (2.2)$$

Where:

x and y are source coordinates (input)

x_o and y_o are rectified coordinates (output)

2.4.2.2. Affine Transformation

Affine transformation transforming all polylines into polylines and all polygons into polygons while preserving their intersection properties.

An affine transformation is any transformation that preserves collinearity condition (i.e., all points lying on a line initially still lie on the same line after transformation) and keep ratios of distances (e.g., the midpoint of a line segment remains a midpoint after transformation) (<http://mathworld.wolfram.com/AffineTransformation.html>).

In affine geometry, affine transformations (translations, rotations . . .) play a central role; by definition, an affine transformation is an invertible linear image followed by a translation, that is, image coordinates $(x, y) \longrightarrow (x_o, y_o)$, (*Projective Transformation, 2005*).

$$x_o = ax + by + c, y_o = dx + ey + f, \text{ and } ad - bc \neq 0. \quad (2.3)$$

Where:

x, y are the image coordinates, x_o, y_o are the transformed coordinates, a, b, d and e are the rotation and scale factor parameters, c, f are the translation parameters.

Affine transformations do not alter the degree of a polynomial, parallel lines/planes are transformed to parallel lines/planes, and intersecting lines/plane are transformed to intersecting lines and planes. However, affine transformations do not preserve lengths and angle measures and as a result they will change the shape of geometric features (<http://cse.taylor.edu/~btoll/s99/424/res/mtu/Notes/geometry/geo-tran.htm>).

2.4.2.3. Projective Transformation

If the object's surface describes sufficiently a precise plane, a projective rectification should be used. To perform a projective rectification, a geometric transformation between image plane and the projective plane is necessary (Albertz, J., and Kreiling, W., 1989).

While projective transformations, similar to affine transformations, it does not change the degree of a polynomial, two parallel (*i.e.* intersecting) lines/planes can be transformed to two intersecting (*i.e.* parallel) lines/planes as shown in Figure (2.5) (<http://cse.taylor.edu/~btoll/s99/424/res/mtu/Notes/geometry/geo-tran.html>).

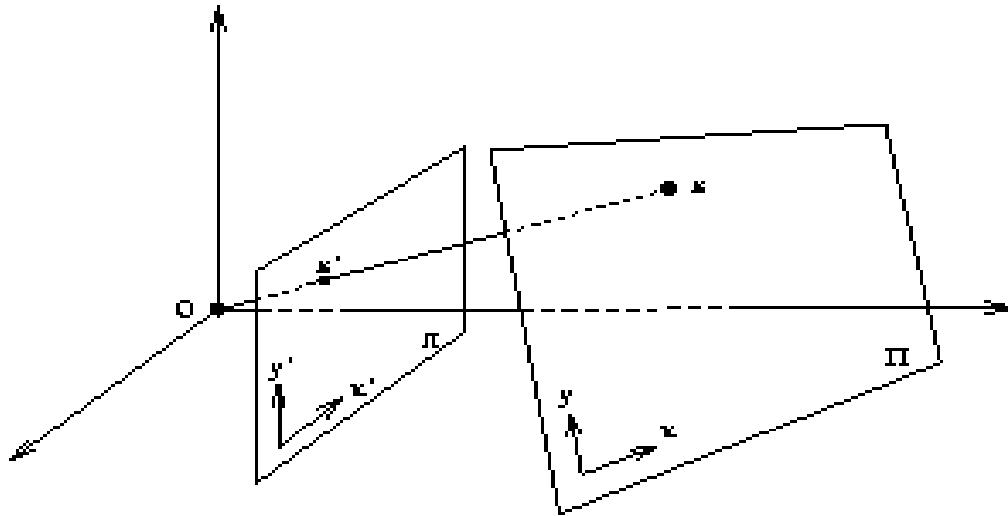


Figure (2.5): The Projective Transformation Concept.

(http://homepages.inf.ed.ac.uk/rbf/CVonline/LOCAL_COPIES/EPsrc_SSAZ/node7.html).

Image acquisition is a projective process and if lens and sensor nonlinearities do not exist, the relation between two images of a rather flat scene can be described by a projective transformation as follows (Novak K., 1992).

$$x = \frac{a_1x' + a_2y' + a_3}{c_1x' + c_2y' + 1}, \quad y = \frac{b_1x' + b_2y' + b_3}{c_1x' + c_2y' + 1} \quad (2.4)$$

Where:

$a_1, a_2, a_3, b_1, b_2, b_3, c_1$ and c_2 are eight unknown parameters of transformation, which can be determined if the coordinates of four non-collinear corresponding control points in the images are known. If correspondences are known to contain noise, more than four correspondences should be used in a least squares or clustering method to obtain the transformation parameters (*Transformation Functions for Image Registration, 2003*).

The elements of exterior and interior orientation are not needed as they implicit in these parameters. This projective transform is typically used to rectify airphotos with flat terrain (*Novak K., 1992*).

2.4.2.4. Piecewise Transformation

If control points in the reference image are triangulated, by knowing the correspondence between control points in sensed and reference images, corresponding triangles in the sensed image can be obtained as shown in Figure (2.6).

Piecewise methods are that map areas within corresponding triangles to each other. If a linear transformation function is used to map a triangle in the sensed image to the corresponding triangle in the reference image, the transformation becomes piecewise linear. The transformation will be continuous, but it will not be smooth.

When the regions are small or local geometric difference between the images is small, piecewise linear may be sufficient. However, if local deformations are large, tangents at the two sides of a triangle edge may be quite different, resulting in an inaccurate registration. The choice of triangulation will affect the registration result. As a general rule, elongated triangles should be avoided and preference should be given to triangles without acute angles.

Algorithms that maximize the minimum angle in triangles is known as Delaunay triangulation. Better approximation accuracy will be achieved if 3-D points obtained for control points in the reference image and X or Y coordinate of corresponding control points in the sensed image are used to obtain the triangles as shown in Figure (2.6) (*Transformation Functions for Image Registration, 2003*).

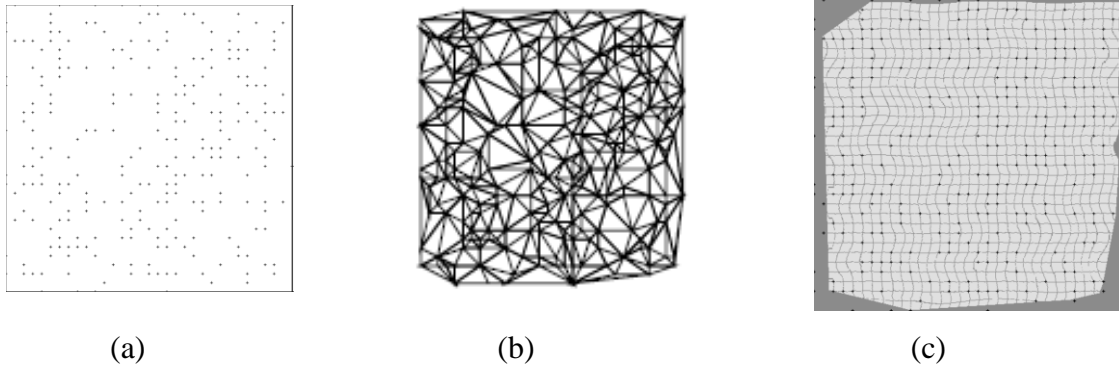


Figure (2.6): (a) A set of Random Spaced Control Points, (b) Triangulation of Control Points and (c) Piecewise Linear Resampling of Image Using the Control Points.

(Transformation Functions for Image Registration, 2003).

Because the piecewise transformation is based on a triangulation of the available control points, it has the ability to represent the changes in displacement across an image more effectively than polynomial-based transformation which globally averages the control points to calculate a best fit surface. This is especially true in images with non-uniform displacements (<http://www.ctmap.com/assets/pdfprojects/geotin.pdf>) and (Ochis H., and Russell E., 2000).

2.4.2.5. Digital Differential Rectification

The term differential rectification has its origin in the approach of rectifying small parts of a photograph. Conventional analog or analytical ortho-projectors do this by optical image transfer. For digital differential rectification, each pixel is separately transferred from the original image to the resulting image (Novak K., 1992).

Differential rectification is generally called as ortho-rectification in literature. Elements of exterior and interior orientations and digital elevation model of the stereo model area are required to perform the transformation. Additional parameters which are modeled to correct errors of the sensors may be added to increase the precision and accuracy of the transformation as the following collinearity condition equations as (Novak K., 1992).

$$x = x_0 - c \frac{r_{11}(X - XL) + r_{12}(Y - YL) + r_{13}(Z - ZL)}{r_{31}(X - XL) + r_{32}(Y - YL) + r_{33}(Z - ZL)} \quad (2.5)$$

$$y = y_0 - c \frac{r_{21}(X - XL) + r_{22}(Y - YL) + r_{23}(Z - ZL)}{r_{31}(X - XL) + r_{32}(Y - YL) + r_{33}(Z - ZL)} \quad (2.6)$$

Where:

x_0, y_0 are the principal point coordinates, x, y are the image coordinates, r_{11} to r_{33} are the rotation parameters, c is the principal distance, X, Y, Z are the ground coordinates and X_0, Y_0, Z_0 are the exposure station coordinates.

Polynomials cannot correct relief displacements, because no information concerning the height of the ground control points are used (*Rocchini, D., 2004*).

Digital differential rectification is the best rectification technique which corrects all distortions caused by sensors and others. The disadvantage of this technique is, it requires too many priory data for transformation (*Temiz, M., and Küliür, S., 2008*).

2.4.2.6. Direct Linear Transformation (DLT)

Direct linear Transformation was applied for the first time in 1971 by Abdel-Aziz and karara. In this method the space coordinate system is optional. It is useful to transform image space to ground space. DLT equation is as follows (*B.Behdinian, 2000*).

$$x = \frac{a_{11} X + a_{12} Y + a_{13} Z + a_{14}}{a_{31} X + a_{32} Y + a_{33} Z + 1} \quad (2.7)$$

$$y = \frac{a_{21} X + a_{22} Y + a_{23} Z + a_{14}}{a_{31} X + a_{32} Y + a_{33} Z + 1} \quad (2.8)$$

These equations with 11 coefficients are (a_{11} to a_{33}) transform (x, y) from image space to ground space. By omitting Z , the equations convert to these equations:

$$x = \frac{a_{11} X + a_{12} Y + a_{13}}{a_{31} X + a_{32} Y + 1} \quad (2.9)$$

$$y = \frac{a_{21} X + a_{22} Y + a_{23}}{a_{31} X + a_{32} Y + 1} \quad (2.10)$$

Where:

(x, y) are image coordinate and (X, Y, Z) are ground coordinate that comes from GCPS.

By solving this equation, 11 unknown parameters will be determined. First of all, 4 coordinate of map should be found and then each pixel on the image which has the same coordinate system as the map, the gray value is determined by DLT transformation function and locating the corresponding image position on the raw image followed by resampling beside each needs high value that can be extracted from DEM file (*B.Behdinian, 2000*).

2.4.3. The Resampling Process

The resampling is used to determine the digital values to place the new pixel locations of the corrected output image as shown in Figure (2.7). The resampling process calculates the new pixel values from the original digital pixel values in the uncorrected image.

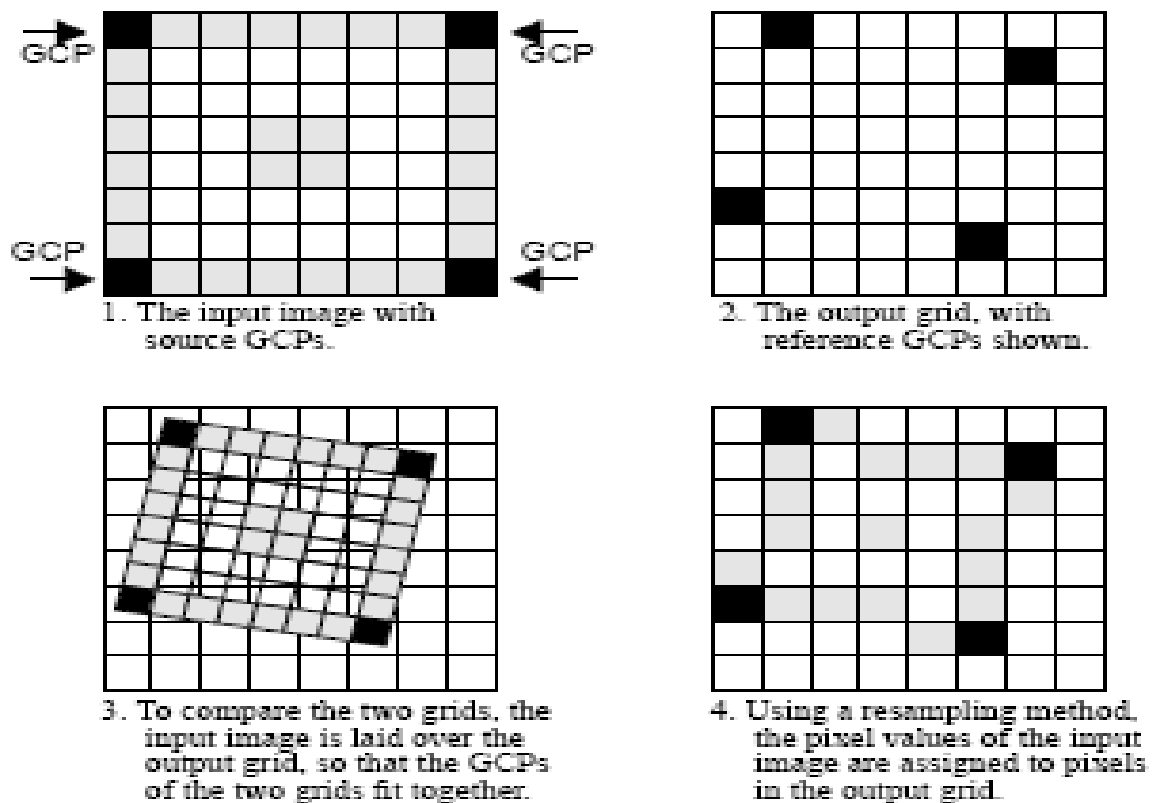


Figure (2.7): The Resampling Process.

(<http://www.gis.usu.edu/Geography-Department/rsgis/RSCC/v6.2/nn.html>).

The Resampling process has three techniques as follows:

2.4.3.1. The Nearest Neighbor Technique.

Uses the value of the closest input pixel for the output pixel value. To determine the nearest neighbor, the algorithm uses the inverse of the transformation matrix to calculate the image file coordinates of the desired geographic coordinate. The pixel value occupying the closest image file coordinate to the estimated coordinate will be used for the output pixel value in the rectified image as shown in Figure (2.8)

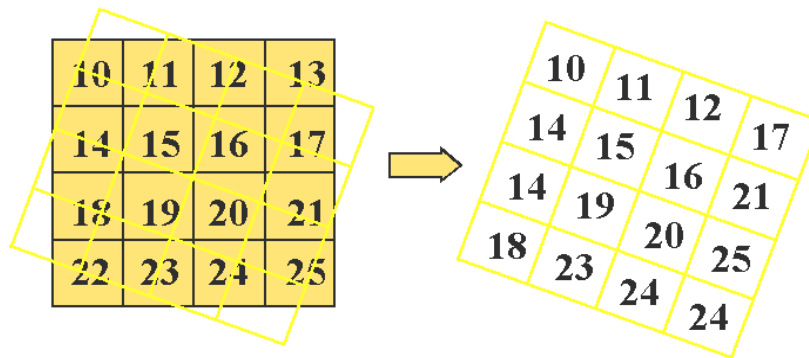


Figure (2.8): The Nearest Neighbor Resampling Technique.

(<http://www.gis.usu.edu/Geography-Department/rsgis/RSCC/v6.2/nn.html>).

Its advantages are that the output values are the same as the original input values. Other methods of resampling tend to average surrounding values. This may be an important consideration when discriminating between vegetation types or locating boundaries, since original data are retained, this method is recommended before classification and is easy to compute and therefore fastest to use.

Its disadvantages are that data values may be lost, while other values may be duplicated and this loss of data may result in breaks in linear features such as roads, streams, and boundaries (<http://www.gis.usu.edu/Geography-Department/rsgis/RSCC/v6.2/nn.html>).

2.4.3.2. The Bilinear Interpolation Technique.

Uses the weighted average of the nearest four pixels to the output pixel. The averaging process alters the original pixel values and creates entirely new digital values in the

output image as shown in Figure (2.9). This may be undesirable if further processing and analysis, such as classification based on spectral response, is to be done. If this is the case, resampling may best be done after the classification process.

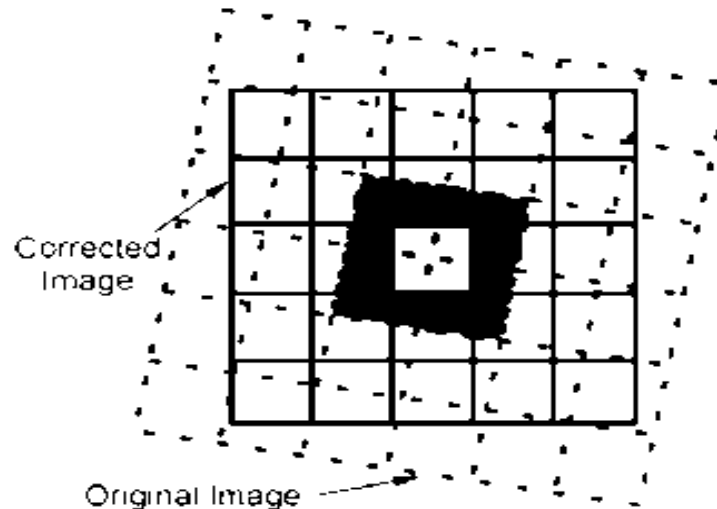


Figure (2.9): The Bilinear Interpolation Resampling Technique.

(<http://www.gis.usu.edu/Geography-Department/rsgis/RSCC/v6.2/nn.html>).

Its advantages are due to Image smooth and higher spatially accuracy than nearest neighbor method.

Its disadvantages are alters original data and reduces contrast by averaging neighboring values together and is computationally more expensive than nearest neighbor (<http://www.gis.usu.edu/Geography-Department/rsgis/RSCC/v6.2/bl.html>).

2.4.3.3. The Cubic Convolution Technique.

Uses the weighted average of the nearest sixteen pixels to the output pixel. The output is similar to bilinear interpolation, but the smoothing effect caused by the averaging of surrounding input pixel values as shown in Figure (2.10). As bilinear interpolation, this method results in completely new pixel values. However, these two methods produce images which have a much sharper appearance and avoid the blocky appearance of the nearest neighbor method (<http://www.gis.usu.edu/Geography-Department/rsgis/RSCC/v6.2/cc.html>).

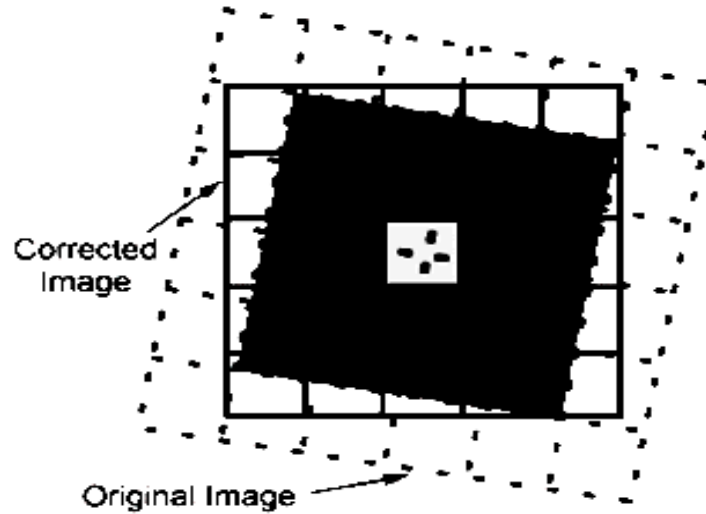


Figure (2.10): The Cubic Convolution Resampling Technique.

(<http://www.gis.usu.edu/Geography-Department/rsgis/RSCC/v6.2/nn.html>).

2.4.4 Accuracy Investigation of Orthorectification Process

The RMS is the error used to determine the accuracy of the Orthorectification Process. It is the difference between the desired outputs coordinates for the GCPs and its actual output coordinate, when the point is transformed with the geometric transformation as shown in Figure (2.11). Root Mean Square Error (RMS) (*Erdas field guide, Fifth Edition, 1999*).

$$(R_i) = \sqrt{(X_r - X_i)^2 + (Y_r - Y_i)^2} \quad (2.11)$$

Where:

X_i and Y_i are the input source coordinates, X_r and Y_r are the retransformed coordinates.

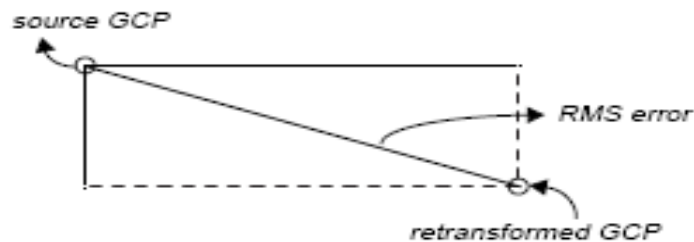


Figure (2.11): RMS Error of Point.

(*Erdas field guide, Fifth Edition, 1999*).

Total Root Mean Square Error (RMS):

From the residuals, the following calculations are made to determine the total RMS error, the X RMS error, and the Y RMS error (*Erdas field guide, Fifth Edition, 1999*).

$$R_x = \sqrt{\frac{1}{n} \sum X R_i^2} \quad (2.12)$$

$$R_y = \sqrt{\frac{1}{n} \sum Y R_i^2} \quad (2.13)$$

$$Tot. RMS = \sqrt{R_x^2 + R_y^2} \quad (2.14)$$

Where:

R_x = X-RMS error, R_y = Y-RMS error, T = total RMS error, n = the number of GCPs, i = GCP number, $X R_i$ = the X-residual for GCP i and $Y R_i$ = the Y residual for GCP i .

The vertical root-mean-square error (RMSE) statistic is used to describe the vertical accuracy of a DEM, encompassing both random and systematic errors introduced during production of the data. The RMSE is defined as (*Erdas field guide, Fifth Edition, 1999*).

$$RMSE = \sqrt{\sum \frac{(z_i - z_t)^2}{n}} \quad (2.15)$$

Where:

Z_i = interpolated DEM elevation of a test point, Z_t = true elevation of a test point, n = number of test points. Accuracy is computed by a comparison of linear interpolated elevations in the DEM with corresponding known elevations. Test points should be well distributed, representative of the terrain and have true elevations with accuracies well within the DEM accuracy criteria. Acceptable test points include, in order of preference: field control, aerotriangulated test points, spot elevations, or points on contours from

existing source maps with appropriate contour interval (*National Mapping Program*) and (*MERCURI, P., et al., 2006*).

2.5 Features Vectorization

When vector data is not readily available for setting up a GIS database. Vector data is normally created from existing paper maps or natural source images, such as aerial photos or satellite imagery. Vectorization of features refers to the creation of vector data from hardcopy materials or raster images that are traced using a digitizer keypad on a digitizing tablet or a mouse on a displayed image. Any image not already in digital format must be digitized before it can be read by the computer and incorporated into the database. Most satellite images data are already in digital format upon receipt, so it is not necessary to digitize them.

However, you may also have maps, photographs, or other nondigital data that contain information you want to incorporate into the study. Or, you may want to extract certain features from a digital image to include in a vector layer. Tablet digitizing and screen digitizing enable you to digitize certain features of a map or photograph, such as roads, bodies of water, voting districts, and so forth (*Erdas field guide, Fifth Edition, 1999*). Vectorization has many different ways as follows:

2.5.1. Manual Vectorization

This is traditionally the most common way to convert paper-based sources of spatial information (e.g. maps) to digital vector data. The paper map is attached by tape to a digitizing tablet as shown in Figure (2.12). Usually between 4-6 initial points with known coordinates are logged on tablet. Optimally these points are such locations as the intersections of graticule lines. In the absence of an overlying grid system, points are taken from identifiable locations such as street intersections or landmarks.

A digitizer is much like a mouse with an attitude. The mouse in this case is called a cursor or a puck and it normally has a small transparent Lucite portion that sticks out. The puck has a nicely defined crosshair target so you can see exactly where it's pointing.

A board (the tablet or table portion of the digitizer) replaces the cushioned mouse pad and this board includes a very fine mesh of electrified wires that crisscross up and down and right and left at very precise distances. These wires are sensors that know exactly where that target on your cursor is at any given time and because the board and the cursor talk to each other the digitizer software can record the position of the cursor in exact millimeters or small portions of an inch (*Demers, M., 2009*).

Once all the features are traced the newly acquired data is transformed from table units (the coordinates of the digitizing table) to real world units using algorithm. This algorithm takes the known table coordinates of the initial points and warps the data to match the real world coordinates assigned to those points (<http://gislounge.com/methods-for-creating-spatial-databases/>).



Figure (2.12): Digitizing Table.

(*Erdas field guide, Fifth Edition, 1999*).

2.5.2. Semi-Manual Semi-automatic Vectorization (On Screen Digitizing).

On-screen digitizing is an interactive process in which a map is created using previously digitized or scanned information. This method of geocoding is commonly called "heads-up" digitizing because the attention of the user is focused up on the screen, and not on a digitizing tablet. This technique may be used to trace features from a scanned map or image to create new layers or themes (<http://www.ncgia.ucsb.edu/cctp/units/unit14/14.html>).

On-screen digitizing involves using an image as a background layer on a computer screen, then using the mouse to add points, lines, and areas. To create layers, users trace over the features that are visible on the screen. This concept is like electronic tracing paper. Other existing layers (points, lines, & areas) can be used as reference for on-screen digitizing as shown in Figure (2.-13) (http://www.palmbeach.k12.fl.us/maps/gis/slide_4.html).

As compared with the other forms of spatial data input On-screen digitizing is more direct requires less equipment and doesn't require you constantly relocate tic marks (little x's that identify the corners) on the maps or aerial photographs that you're inputting (*Demers, M., 2009*).

And has many advantages over manual table digitizing as it's more comfortable, more accurate and faster, you get more information and it is less expensive (http://www.creaf.uab.es/Miramón/new_note/notes/tablescr.html).

On-screen digitizing does have some drawbacks. Most of those drawbacks result from the need to scan the raw imagery and maps to make them compatible as digital background for the On-screen digitizing process. With today's scanners you don't have to worry about this issue especially when compared with the variable distortion of the imagery or paper maps themselves which may occur when digitizing over multiple sessions under uncontrolled temperature and humidity (*Demers, M., 2009*).



Figure (2.13): On Screen Digitizing.

(http://www.creaf.uab.es/Mirammon/new_note/notes/tablescr.html).

2.5.3. Automatic Vectorization

It's the processes of converting features on raster images to vector features automatically using computer software's (automatic feature extraction). This operation depends on the classification of the raster image and converting these classes to features. The accuracy of classification depend on the classification method and the pixel size (resolution) of the raster image so this method is more accurate in the case of aerial images (small pixel size 10 cm) than in the case of satellite images (relatively large pixel size 50 cm). Recently this operation is made by the help of high accurate DEMs like LIDAR DEMs.

Chapter 3
Geographic Information Systems
(GIS)

3.1 The Definition of Geographic Information Systems

Geographic: the collected data is associated with some location in space (spatially located).

Information: attributes or the characteristics (data) can be used to symbolize and provide further insight into a given location (information relevant to decisions made by people and organizations).

System: a seamless operation linking the information to the geography which requires hardware, networks, software, data, and operational procedures. Not just software-* and not just for making maps (system that supports program and resource planning, inventory, management and evaluation activities) (*Terborgh, C., 2010*).

Towards a definition of (GIS)

Different definitions of GIS have evolved in different areas and disciplines. All GIS definitions recognize that spatial data are unique because they are linked to maps (Space matters).

Definition (1) A GIS is a toolbox "A powerful set of tools for storing and retrieving at will, transforming and displaying spatial data from the real world for a particular set of purposes" (*Burrough, P., 1986*).

"Automated systems for the capture, storage, retrieval, analysis, and display of spatial data" (*Clarke, 1995*).

Powerful means to store organize and analyze data that can be described or modeled spatially/geographically (*Black., et al, 1998*).

Definition (2) A GIS is an information system "System that is designed to work with data referenced by spatial or geographic coordinates. In other words, a GIS is both a database system with specific capabilities for spatially-referenced data, as well as a set of operations for working with the data" (*Star and Estes, 1990*).

Definition (3) GIS is an approach to science "The generic issues that surround the use of GIS technology, impede its successful implementation, or emerge from an understanding of its potential capabilities" (*Goodchild, 1992*).

Definition (4) GIS plays a role in society “Organized activity by which people measure and represent geographic phenomena, and then transform these representations into other forms while interacting with social structures” (*Nick C., 1999*).

The formal definition of GIS “A system for capturing, storing, checking, integrating, manipulating, analysing and displaying data which are spatially referenced to the Earth. This is normally considered to involve a spatially referenced computer database and appropriate applications software” (<http://www.uic.edu/classes/sids/cids422gis.ppt>).

I think that GIS can be defined as a tool for modelling for the earth’s surface as shown in Figure (3.1). This model is spatially corrected and have data base which provide information for this model which can be used for many applications according to the user purposes. Simply spatial location linked using software to data base equals GIS.



Figure (3.1): Modeling the Earth Surface Using GIS.
(<http://healthybermap.org/HGeoreswhatisgis.pps>).

3.2 Components of GIS

A GIS can be divided into five components. People, Data, Hardware, Software and Procedures. All of these components need to be in balance for successful system. No one part can run without the other as shown in Figure (3.2).

3.2.1. People

People are the component who actually makes the GIS work. They include many positions including GIS managers, database administrators, application specialists, systems analysts, and programmers. They are responsible for maintenance of the geographic database and provide technical support. People also need to be educated to make decisions on what type of system to use. People associated with a GIS can be categorized into: viewers, general users, and GIS specialists.

Viewers are the public at large whose only need is to browse a geographic database for referential material. These constitute the largest class of users.

General Users are people who use GIS for conducting business, performing professional services, and making decisions. They include facility managers, resource managers, planners, scientists, engineers, lawyers, business entrepreneurs, etc.

GIS specialists are those who make the GIS work. They include GIS managers, database administrators, application specialists, systems analysts, and programmers. They are responsible for the maintenance of the geographic database and the provision of technical support to the other two classes of users (*Lo, 2002*).

3.2.2. Procedures

Procedures include how the data will be retrieved, stored, managed, transformed, analyzed, and finally presented in a final output. The procedures are the steps for answering the questions need to be resolved. The ability of a GIS to perform spatial analysis and answer these questions (queries) is what differentiates this type of system from any other information systems.

The transformation processes includes such tasks as adjusting the coordinate system, setting a projection, correcting any digitized errors in a data set, and converting data from vector to raster or raster to vector (*Carver, 1998*).

3.2.3. Hardware

Hardware consists of the technical equipment needed to run a GIS including a computer system with enough power to run the software, enough memory to store large amounts of data, and input and output devices such as scanners, digitizers, GPS data loggers, media disks, and printers (*Carver, 1998*).

3.2.4. Software

Software there are many different GIS software packages available today. All packages must be capable of data input, storage, management, transformation, analysis, and output, but the appearance, methods, resources, and ease of use of the various systems may be very different.

Today software packages are capable of allowing both graphical and descriptive data to be stored in a single database, known as the object-relational model. Before this innovation, the geo-relational model was used. In this model, graphical and descriptive data sets were handled separately. The modern packages usually come with a set of tools that can be customized to the users needs (*Lo, 2002*).

3.2.5. Data

Data Perhaps the most time consuming and costly aspect of initiating a GIS is creating a database. There are several considerations should be taken before acquiring geographic data. They are crucial to check the quality of data before obtaining it. Errors in data set can add many unpleasant and costly hours for implementing a GIS and the results and conclusions of the GIS analysis most likely will be wrong (<http://maic.jmu.edu/sic/gis/components.html>).



Figure (3.2): Components of GIS.

(<http://maic.jmu.edu/sic/gis/components.html>).

3.3 GIS Tasks

GIS essentially perform six processes or tasks:

3.3.1. Input

Input before geographic data can be used in a GIS it must be converted into a suitable digital format. The process of converting data from analogue paper maps into computer files is called digitizing. Modern GIS technology has the capability to automate this process fully for large projects; smaller jobs may require manual digitizing.

Today many types of geographic data already exist in GIS-compatible formats. These data can be obtained from data suppliers and loaded directly into a GIS.

3.3.2. Manipulation

Manipulation it is likely that data types required for a particular GIS project will need to be transformed or manipulated in some way to make them compatible with the used system. For example, geographic information is available at different scales (street centerline files might be available at a scale of 1:100,000; postal codes at 1:10,000; and census boundaries at 1:50,000).

Before overlaying and integrating these data, they must be transformed to the same scale. This could be a temporary transformation for display purposes or a permanent one required for analysis. There are many other examples of data manipulation that are routinely performed in GIS. These include projection changes, data aggregation (for example, to convert sales territories for census building blocks), and generalization (weeding out unnecessary data).

3.3.3. Management

Management for small GIS projects, it may be sufficient to store geographic information as computer files. However, when data volumes become large and the number of users of the data becomes more than a few, then it is better to use a database management system (DBMS) to help store, organize, and manage data.

A DBMS is nothing more than computer software to manage a database an integrated collection of data. There are many different designs of DBMS, but in GIS the relational design has found most favor. In the relational design, data are stored conceptually as a collection of tables. Common fields in different tables are used to link them together. This surprisingly simple design has been so widely used mainly because of its flexibility and very wide deployment in applications both within and without GIS.

3.3.4. Query

Query once you have a functioning GIS containing the required geographic information, it can begin to ask simple questions such as: Who owns the land parcel on the corner? or How far is it between two places? or Where is land zoned for industrial use? and analytical questions such as: Where are all the sites suitable for building new houses? or What is the dominant soil type for oak forest? or best route for new highway and how will traffic be affected?

3.3.5. Analysis

Analysis GIS systems really come into their own when they are used to analyze geographic data. The processes of geographic analysis (often called spatial analysis or

geoprocessing) uses the geographic properties of features to look for patterns and trends, and to undertake "what if" scenarios. Modern GIS have many powerful analytical tools, but two are especially important as shown in Figure (3.3).

a. Proximity Analysis GIS are often used to answer such questions as:

- How many houses lie within 100 m of this water main?
- What is the total number of customers within 10 km of this store?
- What proportion of the alfalfa crop is within 500 m of the well?

For this purpose, GIS technology uses a process called buffering to determine the proximity relationship between features.

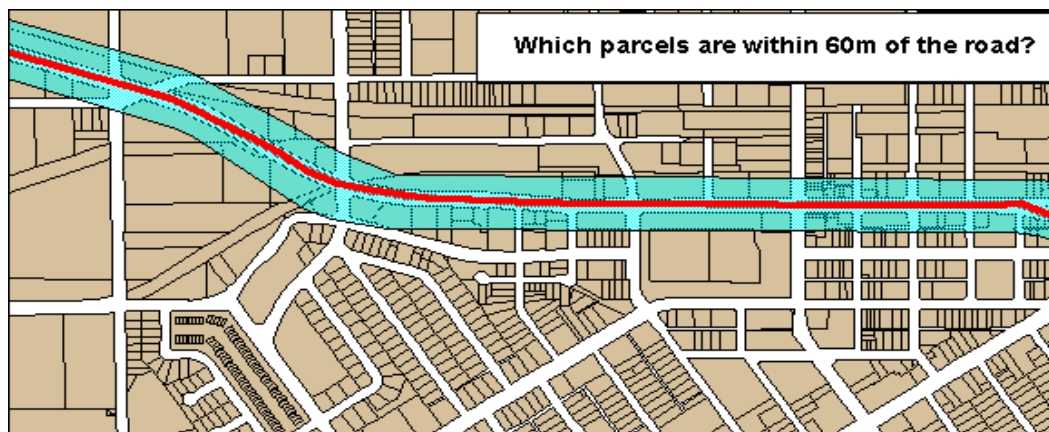


Figure (3.3): Proximity Analysis.

(<http://gis.unk.edu/Archive/What%20is%20GIS.ppt>)

b. Overlay Analysis The integration of different data layers involves a process called overlay as shown in Figure (3.4). This could be a visual operation, but analytical operations require one or more data layers to be joined physically. This overlay, or spatial join, can integrate data on soils, slope, and vegetation, or land ownership with tax assessment.

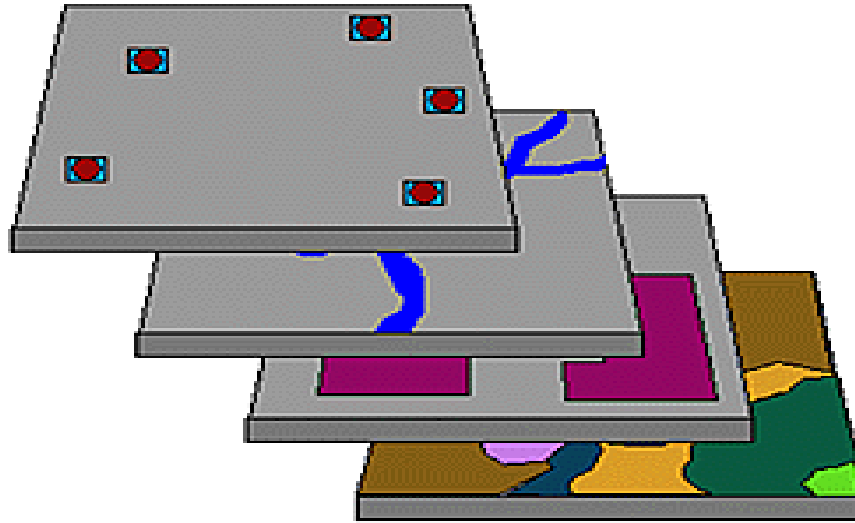


Figure (3.4): Overlay Analysis.

(<http://gis.unk.edu/Archive/What%20is%20GIS.ppt>).

3.3.6. Visualization

Visualization For many types of geographic operation, a visual result is better as a map or graph as shown in Figure (3.5). Maps are very efficient for storing and communicating geographic information. While cartographers have created maps for Millennia, GIS provides new and exciting tools to extend the art and science of cartography (<http://www.itu.edu.tr/~turkoglu/documanlar/documanlar/COURSE%202%20ABOUT%20GIS.ppt>).

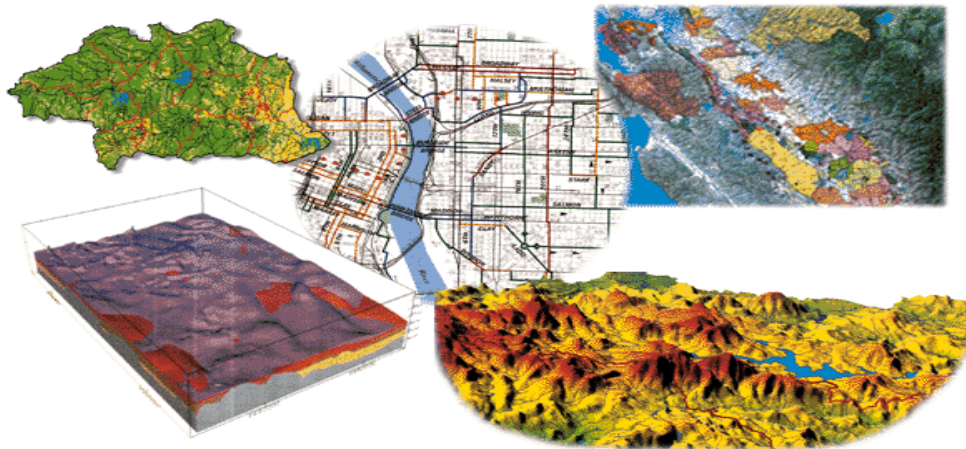


Figure (3.5): Data Visualization in GIS.

(<http://healthcybermap.org/HGeores/whatisgis.pps>).

3.4 GIS Spatial Data Representation

GIS data represents real objects (such as roads, land use and elevation) in digital form. Real objects can be divided into two abstractions: discrete objects (a house) and continuous fields (such as rainfall amount, or elevation). Traditionally, there are two broad methods used to store data in a GIS for both abstractions: Raster and Vector.

3.4.1 Raster Data Model

A raster based system displays, locates, and stores graphical data by using a matrix or grid of cells as shown in Figure (3.6). A unique reference coordinate represents each pixel either at a corner or the centroid. Each cell or pixel has discrete attribute data assigned to it. Raster data resolution is dependent on the pixel or grid size and may vary from sub-meter to many kilometers. Because these data are two-dimensional, GIS store various information such as forest cover, soil type, land use, wetland habitat, or other data in different layers. Layers are functionally related map features.

Generally, raster data requires less processing than vector data, but it consumes more computer storage space. Scanning remote sensors on satellites store data in raster format. Digital terrain models (DTM) and digital elevation models (DEM) are examples of raster data (*Koeln et al 1994 and Huxhold, 1991*).

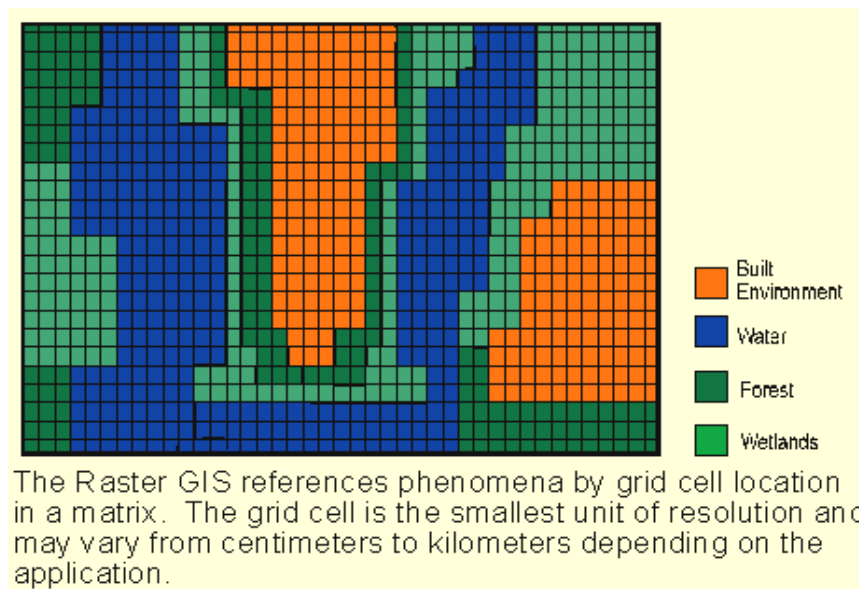


Figure (3.6): Raster Data Model.

(*Koeln et al 1994 and Huxhold, 1991*).

Elements of the raster data

A. Pixel value where each cell in a raster model carries a value, which represents the characteristic of a spatial phenomenon at the location denoted by its row and column. Depending on the coding of its cell values, a raster can be either an integer or a floating point raster. An integer value has no decimal digits, whereas a floating point value does.

B. Pixel size which determines the resolution of the raster data model. A large pixel size cannot represent the precise location of spatial features but a small pixel size increases the data volume and the data processing time.

C. Raster bands where a raster may have a single band or multiple bands. Each pixel in a multiband raster is associated with more than one pixel value. An example of multiband raster is a satellite image which may have five or more bands in each pixel location. Each pixel in single raster band has only one pixel value. An example of the single band raster is an elevation raster which has one elevation value at each pixel location (*Chang, K., 2008*).

3.4.2 Vector Data Model

A vector based system displays graphical data as points, lines or arcs, and areas with attributes. Cartesian coordinates (i.e., x and y) and computational algorithms of the coordinates define points in a vector system. Lines or arcs are a series of ordered points. Areas or polygons are also stored as ordered lists of points, but by making the beginning and end points the same node the shape is closed and defined. Topological models define the connectivity of vector based systems. Vector systems are capable of very high resolution (less than or equal to .001 cms) and graphical output is similar to hand-drawn maps.

This system works well with azimuths, distances, and points, but it requires complex data structures and is less compatible with remote sensing data. Vector data requires less computer storage space and maintaining topological relationships is easier in this system (*Koeln et al 1994 and Huxhold, 1991*).

In a GIS, geographical features are often expressed as vectors, by considering those features as geometrical shapes. Different geographical features are expressed by different types of geometry:

A. Points a simple vector map elements, Zero-dimensional points are used for geographical features that can best be expressed by a single point reference. In other words, by simple location. Examples include wells, peaks, features of interest, and trailheads. Points convey the least amount of information of these file types. Points can also be used to represent areas when displayed at a small scale. For example, cities on a map of the world might be represented by points rather than polygons. No measurements are possible with point features.

B. Lines a line is one-dimensional element and has the property of length. A line has two end points and points in between to mark the shape of the line. The shape of the line may be a smooth curve or a connection of straight line segments. Smooth curves are typically fitted by mathematical equations such as splines. Straight line segments may represent humane made features as canals and streets. Roads, streams and contour lines are example of line features (*Chang, K., 2008*).

C. Polygons it is a two-dimensional polygon have the property of area (size) and perimeter. It is consists of connected lines, a polygon may be single or has topological relationships with other polygons. A polygon may contain holes, such as national forest containing private land parcels (holes). The existence of holes means that the polygon has both external and internal boundaries. Example of polygon includes land parcels and water bodies (*Chang, K., 2008*).

3.4.3 Raster and Vector Advantages and Disadvantages

There are some important advantages and disadvantages of using a raster or vector data model to represent reality:

- A) Raster datasets contain a value for all points covered an area may require more storage space than representing data in a vector format which can store only required data.
- B) Raster data allows easy implementation of overlay operations, which are more difficult with vector data.
- C) Vector data can be displayed as vector graphics used on traditional maps, whereas raster data will appear as an image that may has a blocky appearance for object boundaries. (depending on the resolution of the raster file).
- D) Vector data is easier to register, scale, and re-project and can simplify combining vector layers from different sources.
- E) Vector data is more compatible with relational database environments, where they can be a part of a relational table as a normal column and processed using a multitude of operators.
- F) Vector file sizes are usually smaller than raster data, which may be 10 to 100 times larger than vector data (depending on resolution).
- G) Vector data is simpler to update and maintain, whereas a raster image can be completely reproduced. (Example: a new road is added).
- H) Vector data allows much more analysis capability, especially for "networks" such as roads, power, rail, telecommunications, etc. (Examples: Best route, largest port, airfields connected to two-lane highways). Raster data will not have all the characteristics of the features it displayed (http://en.wikipedia.org/wiki/Geographic_information_system).

3.5 GIS Database Design

Data are raw facts constitute building block of information. Data are the heart of the DBMS. Noting that all the data will not convey useful information. Useful information is obtained from processed data. In other words, data has to be processed in order to obtain information. Relevant information is the key to decision making. Good decision making is the key to organizational survival.

Data are a representation of facts, concepts or instructions in a formalized manner suitable for communication, interpretation or processing by humans or automatic means. The data in DBMS can be broadly classified into two types. One is the collection of information needed by the organization and the other is metadata which is the information about the database. Data are the most stable part of an organization's information system. As example a company needs to save information about employees, department and salaries. These pieces of information are called data. Generally we perform operations on data or data items to supply some information about an entity (*Sumathi and Esakkirajand, 2007*).

Data Base is a collection of information that is organized so that it can easily be accessed, managed, and updated. Databases can be classified according to types of content: full-text, numeric, and images. The database should contain all the data needed for long term storage of the data and access of the data by a large number of users generally characterizes database systems (<http://searchsqlserver.techtargget.com/definition/database>).

Database may be defined as set of related files that is created and managed by a database management system (DBMS). Today, DBMS can manage any form of data including text, images, sound and video. Database and file structures are always determined by the software. As far as the hardware is concerned, it's all bits and bytes (<http://www.techweb.com/encyclopedia/defineterm.jhtml?term=database&x=&y>).

3.5.1. Data Base Management System (DBMS)

Sometimes called a database manager, is a software package that enables users to build and manipulate a data base (*Oz, E., 2004*).

The DBMS manages user requests and requests from other programs. So that, users and other programs are free from having to understand where the data is physically located on storage media and in a multi-user system, who else may also be accessing the data. In handling user requests, the DBMS ensures the integrity of the data (that is, making sure it continues to be accessible and is consistently organized as intended) and security (making

sure only those with access privileges can access the data) (<http://searchsqlserver.techtarget.com/definition/database-management-system>).

A Database Management System (DBMS) is designed to manage a large body of information. Data management involves both defining structures for storing information and providing mechanisms for manipulating the information. In addition, the database system must provide for the safety of the stored information, despite system crashes or attempts at unauthorized access. If data are to be shared among several users, the system must avoid possible anomalous results due to multiple users concurrently accessing the same data.

Examples of the use of database systems include airline reservation systems, company payroll and employee information systems, banking systems, credit card processing systems, and sales and order tracking systems. A major purpose of a database system is to provide users with an abstract view of the data. The system hides certain details of how the data are stored and maintained. Data can be stored in complex data structures that permit efficient retrieval and users can see a simplified and easy-to-use view of data. The lowest level of abstraction, the physical level, describes how the data are actually stored and details data structures.

The next-higher level of abstraction, the logical level, describes what data are stored, and what relationships exist among these data. The highest level of abstraction, the view level, describes parts of the database those are relevant to each user; application programs used to access a database form part of the view level (<http://encyclopedia2.thefreedictionary.com/database+management+system>).

The main objectives of database management system are data availability, data integrity, data security and data independency. These will be discussed in the next subsection:

- A. Data availability refers to the fact that the data are available for wide variety of users in a meaningful format at reasonable cost, so that the users can easily access these data.

B. Data integrity refers to the correctness of the data in the database. In other words, the data available in the database is a reliable data.

C. Data security refers to the fact that only authorized users can access the data. Data security can be enforced by passwords. If two separate users are accessing a particular data at the same time, the DBMS must not allow them to make conflicting changes.

D. Data independency DBMS allows the user to store, update and retrieve data in an efficient manner. DBMS provides an abstract view of how the data is stored in the database. In order to store the information efficiently, complex data structures are used to represent the data. The system hides certain details of how the data are stored and maintained (*Sumathi and Esakkirajand, 2007*).

A database is a comprehensive collection of related data stored in logical files and collectively processed, usually in tabular form. Database Management Systems (DBMS) have been developed to manipulate, i.e. import, store, and sort and retrieve data in a database. Today, most systems use a relational database structure but other systems exist and may be well suited to particular types of data. There are three basic types with which we should be familiar in GIS. These are hierarchical data structure, network systems, and relational database structure as shown in Figure (3.7). These structures will be discussed in the next subsections.

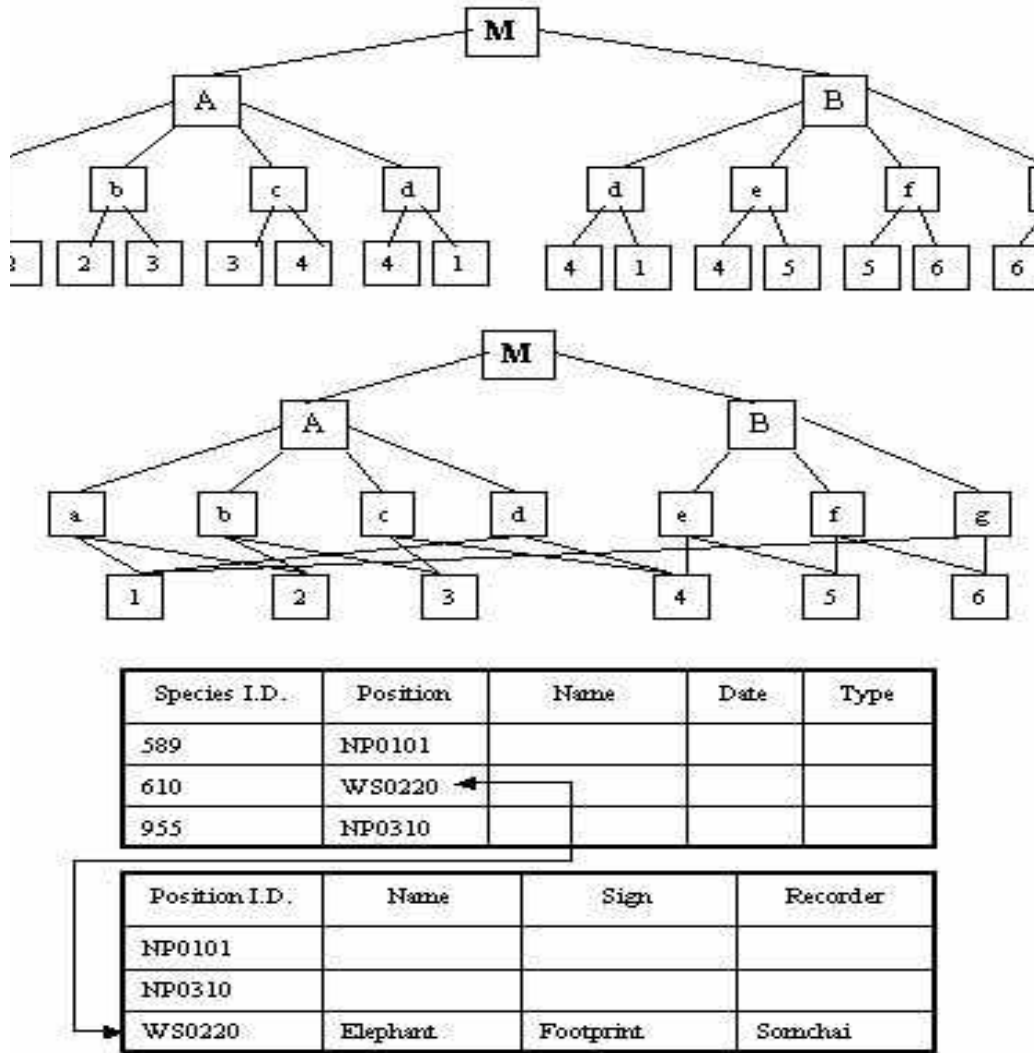


Figure (3.7): Structure of Database System a) Hierarchical Database System b) Network Database System and c) Relation Database.

(<http://www.unixspace.com/context/databases.html>).

A. Hierarchical Model organizes data in a tree structure. There is a hierarchy of parent and child data segments. This structure implies that a record can have repeating information, generally in the child data segments.

Data in a series of records, which have a set of field values attached to it. It collects all the instances of a specific record together as a record type. These record types are the equivalent of tables in the relational model, and with the individual records being the equivalent of rows. To create links between these record types, the hierarchical model uses Parent Child Relationships. These are a one to many mapping relation between

record types. This is done by using trees, like set theory used in the relational model, "borrowed" from maths. For example, an organization might store information about an employee, such as name, employee number, department, salary.

The organization might also store information about an employee's children, such as name and date of birth. The employee and children data forms a hierarchy, where the employee data represents the parent segment and the children data represents the child segment. If an employee has three children, then there would be three child segments associated with one employee segment. In a hierarchical database the parent-child relationship is one to many. This restricts a child segment to having only one parent segment. Efficient storages for data that have a clear hierarchy. Tools that store data in hierarchically organized files are commonly used for image data

(<http://www.unixspace.com/context/databases.html>).

B. Network Model is a database model conceived as a flexible way of representing objects and their relationships. Its distinguishing feature is that the schema, viewed as a graph in which object types are nodes and relationship types are arcs, is not restricted to being a hierarchy or lattice. Store data in interconnected units with few constraints on the type and number of connections. Fewer constraints than hierarchical databases Links defined as part of the database structure. Networks can become chaotic unless planned carefully (*http://en.wikipedia.org/wiki/Network_model*).

C. Relational Model organizes data in tables. Each table, is identified by a unique table name, and is organized by rows and columns. Each column within a table also has a unique name. Columns store the values for a specific attribute, e.g. cover group, tree height. Rows represent one record in the table. In a GIS each row is usually linked to a separate spatial feature, e.g. a forestry stand.

Accordingly, each row would be comprised of several columns, each column containing a specific value for that geographic feature. Data is often stored in several tables. These tables follow certain rules to store and more importantly retrieve data from these sets including the two following critical rules. First a table can't have duplicate rows this means that each row in a table should represent a unique entry. Second a table must be

searchable because each row of data is unique so to find a unique entry you can use one or more columns (containing a specific type of data) to search the rows (*Demers, M., 2009*).

Tables can be joined or referenced to each other by common columns (relational fields) usually the common column is an identification number for a selected geographic feature, e.g. a forestry stand polygon number. This identification number acts as the primary key for the table. The ability to join tables through use of a common column is the essence of the relational model. Such relational joins are usually ad hoc in nature and form the basis of for querying in a relational GIS product. Unlike the other previously discussed database types, relationships are implicit in the character of the data as opposed to explicit characteristics of the database set up. The relational database is the most widely used (*Litwin, P., 2003*).

The benefits of a database that has been designed according to the relational model are numerous. Some of them are: Data entry, updates and deletions will be efficient. Data retrieval, summarization and reporting will also be efficient. Since the database follows a well-formulated model, it behaves predictably.

Since much of the information is stored in the database rather than in the application, the database is somewhat self-documenting. Changes to the database schema are easy to make (*Litwin, P., 2003*).

3.5.1.1. Advantages of using a DBMS

In DBMS, all files are integrated into one system thus reducing redundancies and making data management more efficient. In addition, DBMS provides centralized control of the operational data. Some of the advantages of data independence, integration and centralized control are:

- A. Redundancies and inconsistencies can be reduced in conventional data systems, an organization often builds a collection of application programs created by different programmers and requiring different components of the operational data of the organization. The data in conventional data systems is often not centralized. Some

applications may require data to be combined from several systems. Combining all the data in a database would involve reduction in redundancy as well as inconsistency. It also is likely to reduce the costs for collection, storage and updating of data.

B. Better service to end Users centralizing the data in a database also often means that users can obtain new and combined information that would have been impossible to obtain. Also, use of a DBMS should allow users do not know programming to interact with the data more easily.

C. Flexibility of the system is improved Changes are often necessary to the contents of data stored in any system.

D. Cost of developing and maintaining systems is lower As noted earlier, it is much easier to respond to unforeseen requests when the data is centralized in a database than when it is stored in conventional file systems. Although the initial cost of setting up of a database can be large, one normally expects the overall cost of setting up a database and developing and maintaining application programs to be lower than for similar service using conventional systems.

E. Security can be improved Setting up of a database makes it easier to enforce security restrictions since the data is now centralized. It is easier to control who has access to what parts of the database.

F. Integrity can be improved since the data of the organization using a database approach is centralized and would be used by a number of users at a time, it is essential to enforce integrity controls (http://www.cs.jcu.edu.au/Subjects/cp3020/1997/Lecture_Notes/databases/dbms_disadv.html).

3.5.1.2. Disadvantages of using a DBMS

Although there are many advantages of DBMS, the DBMS may also have some minor disadvantages. These are:

A. Cost of Hardware & Software a processor with high speed of data processing and memory of large size is required to run the DBMS software. It means that it is important to up grade the hardware used for file-based system. Similarly, DBMS software is also very costly.

B. Cost of Data Conversion When a computer file-based system is replaced with a database system, the data stored into data file must be converted to a database file. It is very difficult and costly method to convert data of data files into a database. It is important to hire database and system designers along application programmers. Alternatively, it must take the services of some software house. So, a lot of money has to be paid for developing software.

C. Cost of Staff Training Most DBMS is often complex systems so the training for users to use the DBMS is required. Training is required at all levels, including programming, application development, and database administration. The organization has to be paid a lot of amount for the training of staff to run the DBMS.

D. Appointing Technical Staff the trained technical persons such as database administrator, application programmers, data entry operators etc. are required to handle the DBMS. You have to pay handsome salaries to these persons. Therefore, the " system cost" increases.

E. Database Damage In most of the organizations, all data is integrated into a single database. If database is damaged due to electric failure or database is corrupted on the storage media, then valuable data may be lost forever (<http://www.blurtit.com/q217827.html>).

Chapter 4

Practical Applications

The practical part of this research we discuss the integration of Remote Sensing and GIS for infra-structure planning which can be performed through large scale thematic maps with minimum costs this is done by orthorectification of high resolution satellite images (Quickbird) and Satellite images extracted from Google earth program in this case was (GEO EYE Satellite image). The study is divided into two cases as:

- **Case (1):** in this case, ground control points derived from GPS where GPS observations were carried out by placing a GPS antenna on points relative to a fixed GPS station, DEM derived from ground surveying and DBM from counting the buildings floors divided by 3m.
- **Case (2):** in this case, we study the possibility of using ground control points derived from Google earth program, Global DEM (SRTM) and DBM from counting the buildings floors divided by 3m.

4.1 Study Area Description

The area of study is selected at Qaluop city, covers approximately two squares kilometers and located in the Nile valley zone (the main middle zone) of the plane coordinate system in Egypt. It is an urban area that contains buildings, a network of roads. The terrain heights vary from 15m up to 21m above M.S.L (mean sea level).

4.1.1 Selecting the Suitable Satellite Imagery for the Desired Mapping Scale

The pixel size of the required image should be selected according the original map scale in order to preserve the planimetric accuracy of the map. The pixel size is computed using the following formula (*Thomas, 2002*).

$$\text{Pixel size} = 0.2\text{mm} * \text{map scale} \quad (4.1)$$

Pixel size = 0.2mm * map scale = 60cm for 1:3000 map scale (Quickbird satellite image)

Pixel size = 0.2mm * map scale = 50cm for 1:2500 map scale (Google earth satellite image)

or within the available spatial resolution (Google Earth doesn't have the same spatial resolution for all areas). For this reason, the following data sources have been selected to achieve the required purpose and accuracy.

4.1.2 Data Sources

The sources of data include the following:

A. A 60-centimeter spatial resolution pansharped image over the area of study was collected in May 31, 2005 by Space Imaging's Quickbird satellite and supplied in a TIFF digital format. This image has been radiometrically corrected to improve the radiometric quality by the production company before publishing. This image is classified as a high resolution satellite image and could be used for producing cadastral maps with a certain scale will be discussed next. Figure (4.1) shows the QUICKBIRD image used in the research study.



Figure (4.1): QUICKBIRD Satellite Image.

B. A Satellite image extracted from Google Earth program (GEO EYE satellite image in this case) over the area of study were collected in January 29, 2010 and supplied in a TIFF digital format. This image has been radiometrically corrected to improve the radiometric quality by the production company before publishing. This image is also considered as a high resolution satellite image. This image was downloaded from Google images downloader program (its program used for downloading images from Google

Earth program). Figure (4.2) shows the GEO-EYE satellite image used in the study and extracted from Google Earth program.



Figure (4.2): GEO EYE Satellite Image Extracted from Google Earth Program.

C. A 1/5000 topographic map of Qaluop city over the same area of study produced in 1978 from 1/15000 aerial photographs acquired in 1977. The map is published by the Egyptian Survey Authority (ESA), projected into the Universal Transverse Mercator (UTM) projection. Figure (4.3) shows an existing topographic map for the area under investigation.



Figure (4.3): 1/5000 Topographic Map of the Study Area.

4.1.3 Used Softwares

ERDAS IMAGINE 9.2 software was used in the present research. This software has the ability to orthorectify LANDSAT, SPOT, IKONOS, QUICKBIRD, WORLDVIEW and GEOEYE data in different format. The main functions of this software are:

- Enhance the image-histogram contrast
- Image to image geographic registration
- Unsupervised classification using isodata
- Orthorectification of satellite data

- Creating a surface
- Creating a mask of thematic data

ARC GIS 9.3 software was also used in the present research. The main functions of this software are:

- Producing the DBM
- Image to image geographic registration
- Creating a surface
- Creating Database for the study area
- Analysis and planning for the study area

4.2 Methodology of Investigation

The infra-structure planning of the study area was done using the above mentioned data and was implemented in several stages as follow:

- Orthorectification of the satellite images
- On screen digitizing and Production of the final thematic maps
- Checking the planimetric accuracy of the map production process
- Creation of the Database for the study area
- Analysis of the Database for the study area

4.2.1 Orthorectification of the Satellite Images

4.2.1.1 Generation of the Digital Elevation Model

To generate a DEM to be used for the orthorectification process, two cases are available Ground DEM and Global DEM (SRTM)

A) Ground DEM was performed as follows:

A.1. Rectification of QUICKBIRD satellite image using the GPS ground control points

A.2. A leveling was performed for all the streets of the study area using the leveling program on the total station (3522 point). The leveling points were projected in their planimetric locations using the rectified QUICKBIRD satellite image as shown in Figure (4.4).

A.3. The Ground DEM was built from these points by ERDAS IMAGINE 9.2 software using nonlinear rubber sheeting interpolation method. In order to distribute the slope change smoothly across triangles, the nonlinear transformation with polynomial of order larger than one is used by considering the gradient information. The fifth order polynomial transformation is chosen as the best nonlinear rubber sheeting technique in this software. It is a smooth function. The transformation function and its first order partial derivative are continuous having the following equation (*Erdas field guide, Fifth Edition, 1999*).

$$\sum_{i=0}^5 \sum_{j=0}^5 a(i)k.Xi - j.Yj \quad (4.2)$$

Where:

a (i) are the coefficients which can be computed using the common 3522 points of the two systems and the subscript $k = (i*i + j) / 2 + j$. where each 3 meters cell has a unique elevation value derived from the elevation points as shown in Figure (4.5).

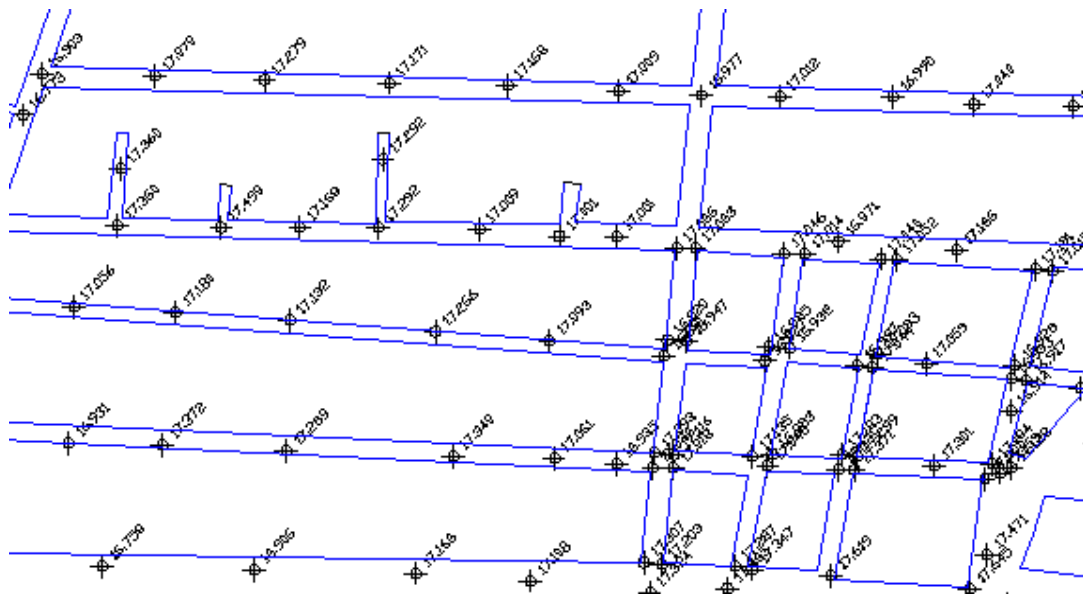


Figure (4.4): Sample of the Elevation Points from Ground Surveying.

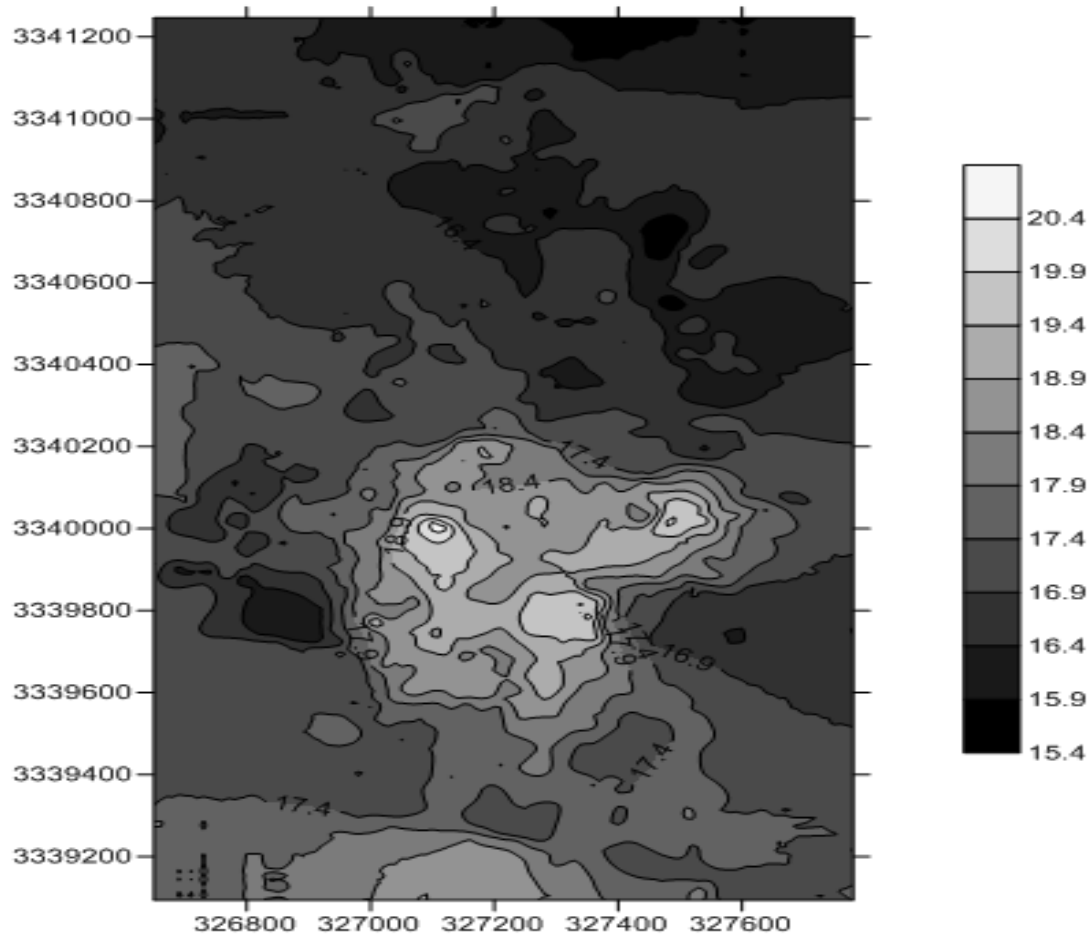


Figure (4.5): The Ground Digital Elevation Model of the Study Area.

B. A Global free downloaded DEM (SRTM) from websites is available for the study area was downloaded as points (3872 point) as shown in Figure (4.6), so the DEM was built from these points by ERDAS IMAGINE 9.2 software. This is performed by nonlinear rubber sheeting interpolation see Equation (4.2), in which each cell has a unique elevation value derived from the elevation points where cell size was 3 m as shown in Figure (4.7)



Figure (4.6): Sample of the Elevation Points from Global (SRTM) DEM.

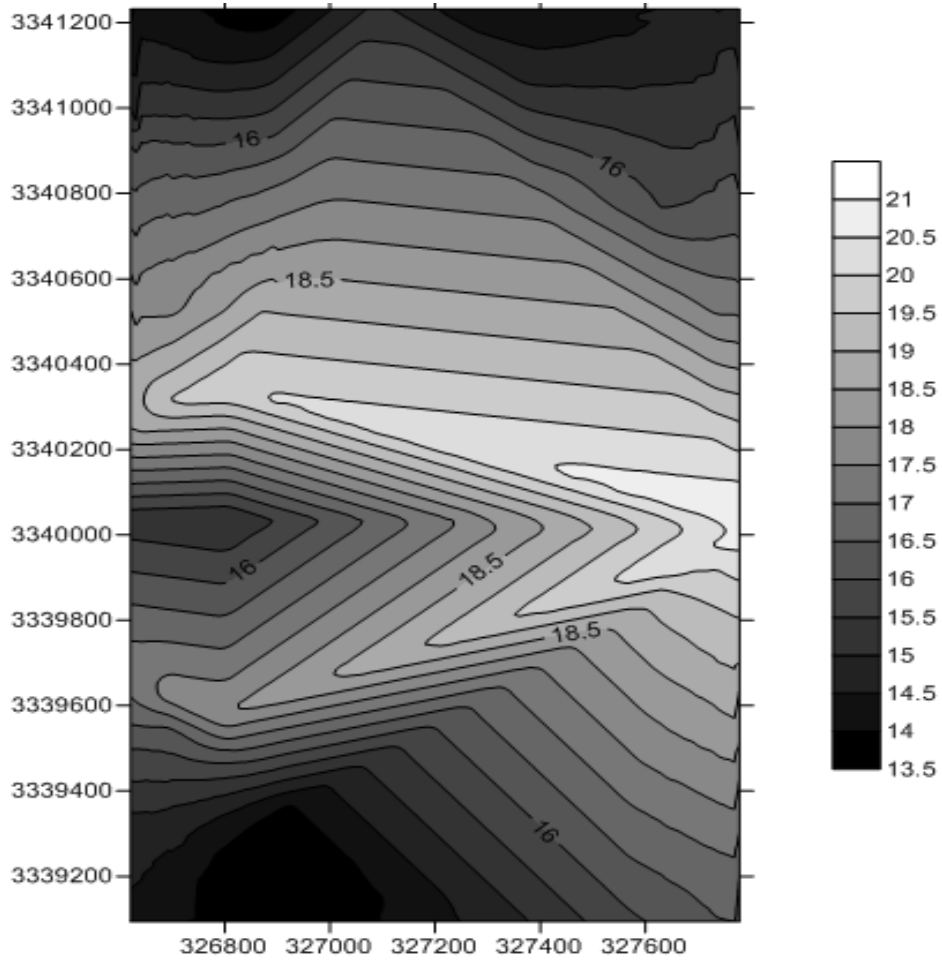


Figure (4.7): Digital Elevation Model Derived from the Global (SRTM).

4.2.1.2 Checking the Vertical Accuracy of the Ground Digital Elevation Model

Testing the Ground DEM using 20 points removed from the Ground DEM and evenly distributed across the area of interest as shown in Figure (4.8) against vertical control points derived precisely by total station data for the same 20 points, the root mean square error (RMS) of elevations of the Ground DEM have been computed using the following formula (*National Mapping Program*) and (*MERCURI, P., et al., 2006*).

$$\text{RMSE} = \sqrt{\sum \frac{(Z_i - Z_g)^2}{n}} \quad (4.3)$$

Where:

Z_i = interpolated DEM elevation of a test point, Z_g = ground true elevation of a test point, n = number of test points and were 0.16m.

Table (4.1) shows the elevations of the interpolation Ground DEM and the vertical control points derived precisely by total station.

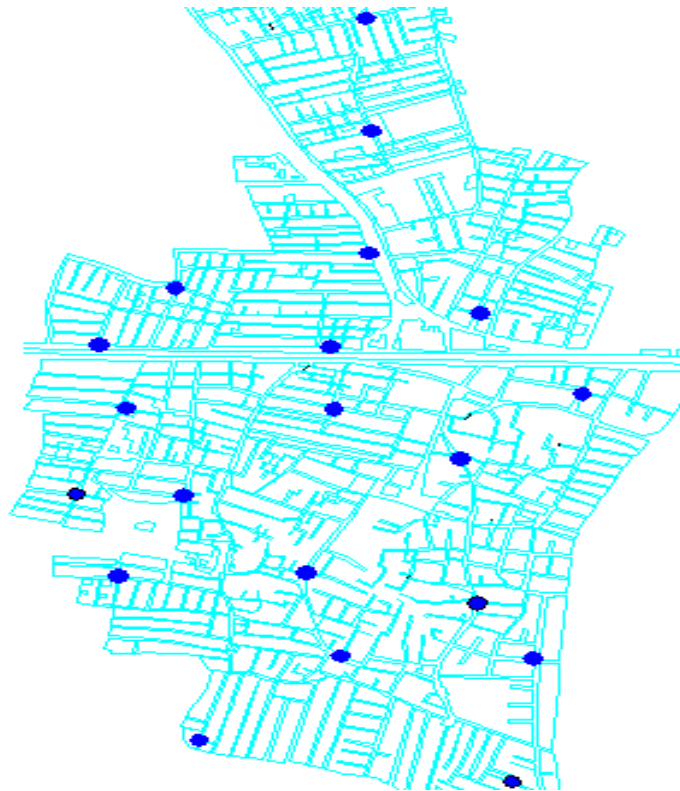


Figure (4.8): Distribution of the Check Points over the Study Area.

Table (4.1): Heights from Ground DEM Versus those from Vertical Control Points.

Point	Vertical Ground control points. (Z_G) mt	Interpolated Ground DEM Elev. (Z_i) mt	($Z_i - Z_G$) mt
1	16.72	16.90	0.18
2	16.73	16.57	-0.16
3	16.56	16.48	-0.12
4	17.34	17.41	0.13
5	16.85	16.96	0.11
6	16.84	17.08	0.14
7	18.45	18.38	0.16
8	16.77	17.05	0.18
9	16.76	16.94	0.19
10	17.29	17.10	-0.19
11	18.97	18.86	-0.11
12	17.98	17.82	-0.15
13	17.63	17.46	-0.17
14	17.51	17.71	0.19
15	17.46	17.65	0.17
16	17.06	17.14	0.12
17	17.12	16.99	-0.13
18	16.52	16.42	-0.14
19	18.68	18.84	0.16
20	16.08	16.26	0.18

4.2.1.3 Checking the Vertical Accuracy of the Global (SRTM) Digital Elevation Model

Testing the Global DEM using 20 points evenly distributed across the area of interest as shown in Figure (4.8) against vertical control points derived precisely by total station data for the same 20 points, the root mean square error (RMS) of elevations of the Global DEM have been computed using the Equation (4.3) where Z_i = interpolated DEM elevation of a test point, Z_t = true elevation of a test point, n = number of test points (*National Mapping Program*) and (*MERCURI, P., et al., 2006*) and were 1.84m.

Table (4.2) shows the elevations of the interpolation Global DEM and the vertical control points derived precisely by total station.

Table (4.2): Heights from Global DEM Versus those from Vertical Control Points.

Point	Interpolated DEM Elev. (Zi) mt	Vertical control points. (Zt) mt	(Zi-Zt) mt
1	15.68	16.88	1.20
2	18.85	16.53	-2.32
3	19.51	16.46	-3.05
4	20.10	17.34	-2.76
5	19.51	16.97	-2.54
6	19.02	16.94	-2.08
7	18.65	18.45	-0.20
8	20.43	16.97	-3.46
9	15.81	16.96	1.15
10	16.48	17.20	0.72
11	18.86	18.86	0.00
12	17.45	17.91	0.46
13	17.34	17.56	0.22
14	15.87	17.71	1.84
15	15.96	17.66	1.70
16	13.95	17.16	3.22
17	17.17	17.02	-0.16
18	16.65	16.52	-0.13
19	18.41	18.85	0.44
20	17.28	16.08	-1.20

4.2.1.4 Generation of the Digital Building Model

Although the limitation of Lidar data availability and the presence of huge number of buildings in the study area (about 8311 building), a Digital Building Model (DBM) had been generated manually, where the positions of Buildings were digitized from the rectified QUICKBIRD satellite image using the ARC GIS 9.3 program (on-screen digitizing technique).

Each building was considered as an area of interest .The building heights were measured by counting the number of floors multiplied by 3m height. The height of the first floor in each building was considered as 4m or 5m, the building average heights at the study area ranges from 3m to 42m as shown in Figure (4.9). After that all the areas in between had

been masked to the datum level (zero level). The Figure (4.10) shows 3D Building Model of the study area.



Figure (4.9): Sample of Digital Building Model of Study Area.

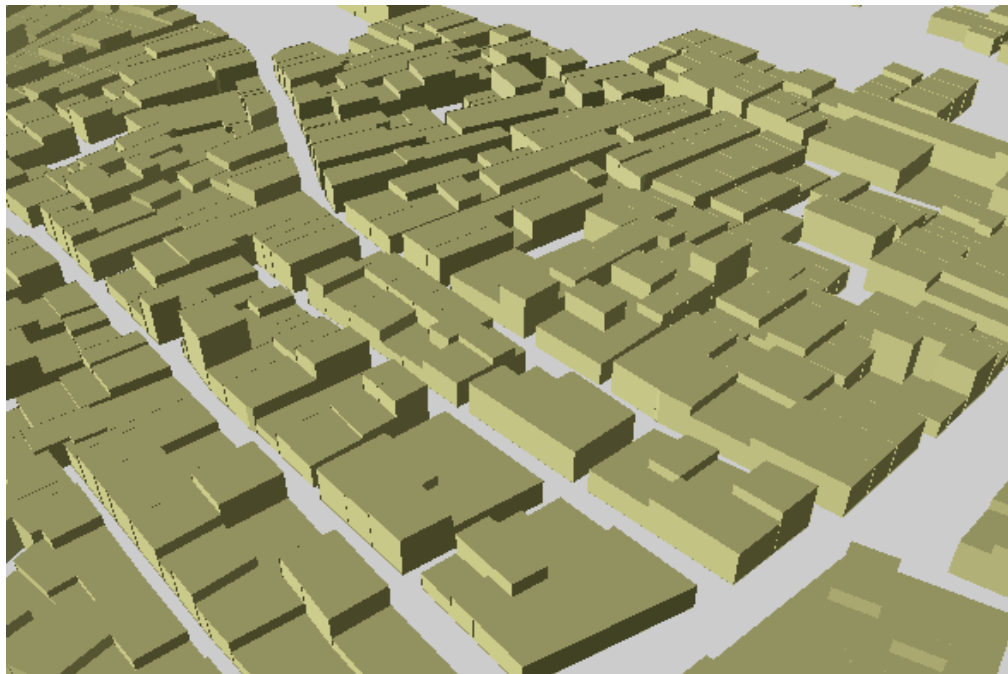


Figure (4.10): Sample of 3D Digital Building Model of Study Area.

4.2.1.5 Checking the Vertical Accuracy of the Digital Building Model

Testing the heights of the DBM generated manually from counting floors against the true building heights measured from ground using a non prism (laser) total station. Using 25 buildings evenly distributed across the area of interest, the root mean square error (RMSE) of the DBM have been computed using the following formula (*National Mapping Program*) and (*MERCURI, P., et al., 2006*).

$$\text{RMSE} = \sqrt{\sum \frac{(Z_b - Z_t)^2}{n}} \quad (4.4)$$

Where:

Z_b = DBM height of building, Z_t = true height of building, n = number of test heights and were 0.28m. Table (4-3) shows the Heights from DBM versus those from ground heights.

The error of 1 m in building heights will reduces the planimetric accuracy of the map by nearly 1 cm in case of 3 m building heights and the effect will be decreased as the building height increased (*Salah, M.,2004*).

Table (4.3): Heights from DBM Versus those from Ground Heights.

Point	DBM Height. mt	True Height. mt	Height. DIFF. mt
1	16	16.04	-0.04
2	7	7.55	-0.55
3	10	9.72	0.28
4	10	10.26	-0.26
5	7	6.54	0.46
6	10	9.80	0.20
7	7	6.97	0.03
8	13	13.07	-0.07
9	13	12.84	0.16
10	11	11.05	-0.05
11	10	10.39	-0.39
12	10	10.48	-0.48
13	11	11.13	-0.13
14	7	7.17	-0.17
15	13	13.22	-0.22
16	10	9.75	0.25
17	7	7.28	-0.28
18	10	9.56	0.44
19	10	10.31	-0.31
20	10	10.11	-0.11
21	10	9.85	0.15
22	14	14.03	-0.03
23	13	13.47	-0.47
24	10	9.95	0.05
25	7	6.93	0.07

4.2.1.6 Possibility of Using Google Earth Points as Control Points

This test was carried out to find the possibility of using Google Earth control points as alternative source to GPS control points or even with it for large scale map production. The coordinates of 20 GCPs distributed over the study area see Figure (4.11) derived from both Google Earth program and GPS have been compared. The results were tabulated in table (4.4). Figure (4.12) shows the shift in Easting direction between Google Earth and GPS 20 points, Figure (4.13) shows the shift in Northing direction between Google Earth and GPS 20 points, Figure (4.14) shows The Vector of shift between

Google Earth and GPS 20 points and Figure (4.15) shows the Direction of shift of two points p1 and p6.



Figure (4.11): Distribution of GCPs over the Study Area.

Table (4.4): Comparison between Google Earth Coordinates and GPS Coordinates in Easting, Northing, Length and Direction.

Point	G.E-E mt	G.E-N mt	GPS-E mt	GPS-N mt	E-D mt	N-D mt	LEN. mt	DIR.
P 1	326937.46	3341197.82	326938.99	3341199.25	1.53	1.43	2.1	BEARING=N47E
P2	327229.03	3341070.61	327232.22	3341071.33	3.19	0.72	3.27	BEARING=N77E
P3	327086.87	3340745.75	327090.69	3340744.42	3.82	-1.3	4.04	BEARING=S71E
P4	327421.4	3340354.4	327422.74	3340356.93	1.34	2.53	2.86	BEARING=N28E
P5	326787.58	3340278.89	326789.05	3340280.62	1.47	1.73	2.27	BEARING=N40E
P6	327589.52	3340162.1	327591.82	3340161.95	2.3	-0.2	2.3	BEARING=S86E
P7	327178.35	3340123.33	327180.06	3340124.69	1.71	1.36	2.19	BEARING=N52E
P8	326929.29	3339913.72	326929.66	3339916.23	0.37	2.51	2.54	BEARING=N08E
P9	326697.4	3339832.4	326700.22	3339832.08	2.82	-0.3	2.84	BEARING=S84E
P10	327131.89	3339728.81	327133.61	3339729.01	1.72	0.19	1.73	BEARING=N84E
P11	327190.39	3339524.08	327190.5	3339527.51	0.11	3.42	3.42	BEARING=N02E
P12	326654.96	3339574.19	326656.32	3339574.79	1.35	0.59	1.48	BEARING=N66E
P13	327067.72	3339273.48	327069.35	3339274.27	1.63	0.79	1.81	BEARING=N64E
P14	327648.83	3339081.98	327651.26	3339081.88	2.43	-0.1	2.43	BEARING=S88E
P15	327509.88	3339519.05	327510.57	3339521.31	0.69	2.27	2.37	BEARING=N17E
P16	327634.05	3339879.58	327637.3	3339879.68	3.25	0.1	3.25	BEARING=N88E
P17	327172.34	3340273.52	327174.03	3340275.84	1.69	2.32	2.87	BEARING=N36E
P18	327871.72	3340303.39	327873.4	3340303.34	1.68	-0.4	1.68	BEARING=S89E
P19	327236.81	3340499.52	327237.57	3340502.6	0.76	3.09	3.18	BEARING=N14E
P20	326916.02	3340417.28	326916.25	3340418.15	0.23	0.87	0.9	BEARING=N15E

Where: G.E-E is Google Earth Easting coordinates, G.E-N is Google Earth Northing coordinates, GPS-E is GPS Easting coordinates, GPS-N is GPS Northing coordinates, E-

D is the shift between GPS and Google Earth in Easting direction, N-D is the shift between GPS and Google Earth in Northing direction, LEN is the vector distance of shift between GPS and Google Earth, DIR is the direction of shift between Google Earth and GPS points.

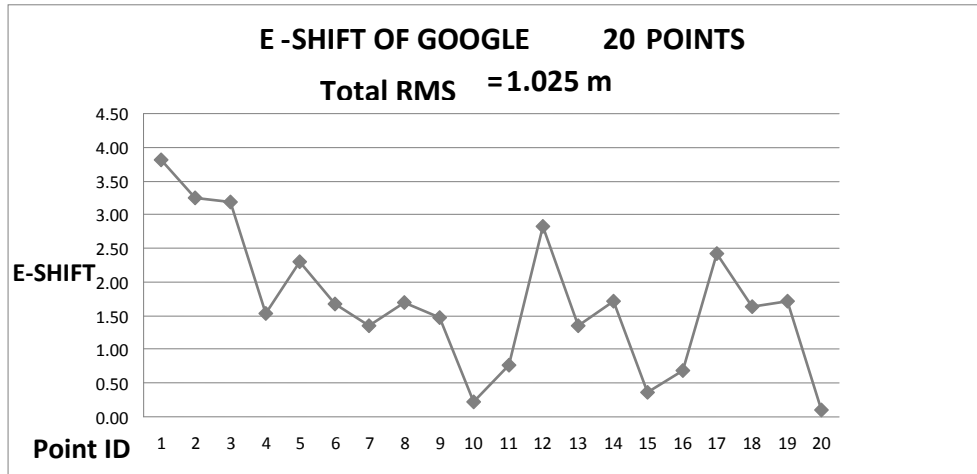


Figure (4.12): The Shift in Easting Direction between Google Earth and GPS 20 Points.

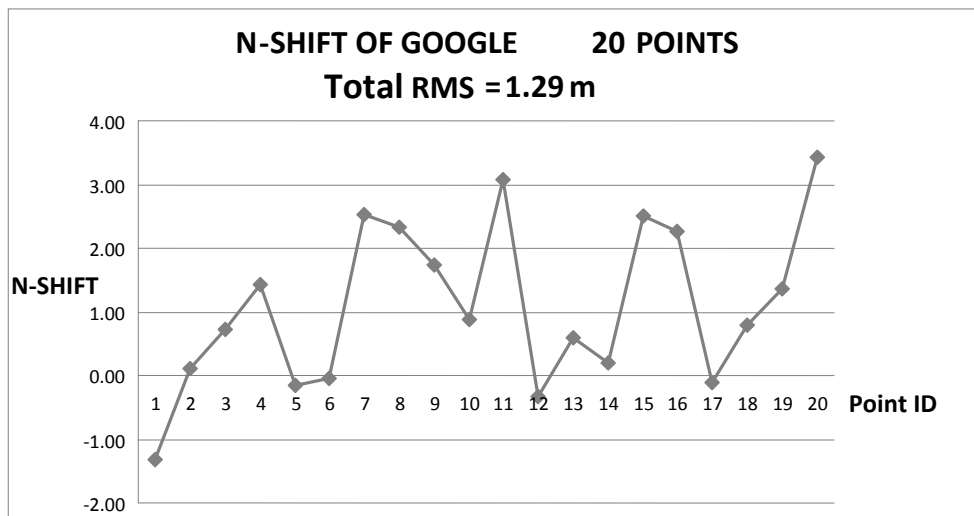


Figure (4.13): The Shift in Northing Direction between Google Earth and GPS 20 Points.

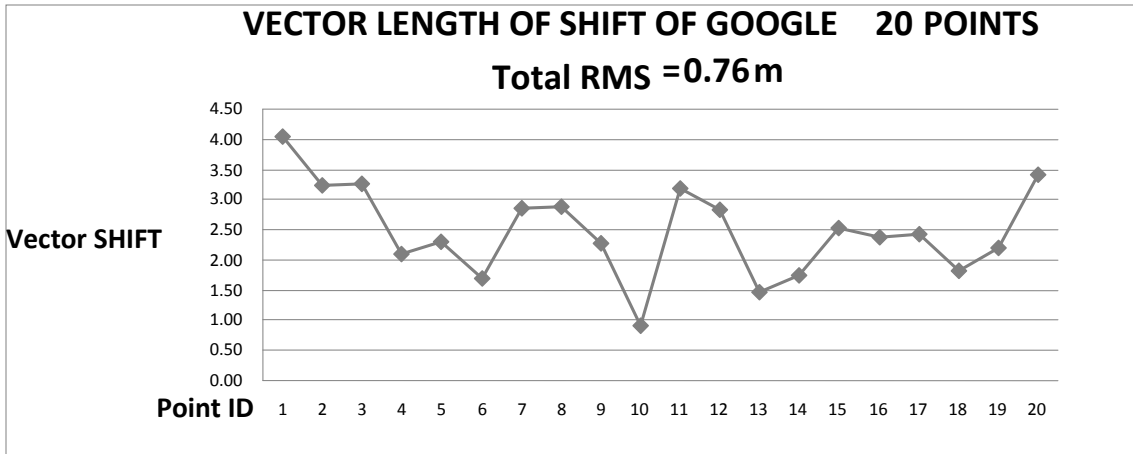


Figure (4.14): Vector Length of shift between Google Earth and GPS 20 points

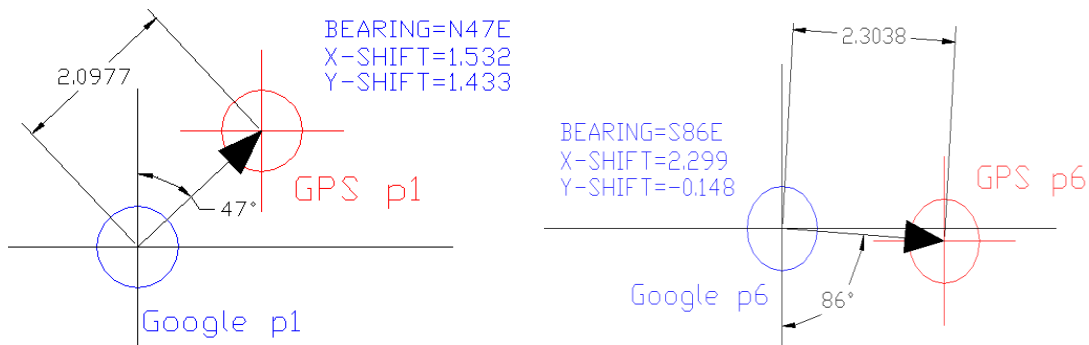


Figure (4.15): Direction of Shift of Two Points p1 and p6.

From these results Google Earth control points cant be used as alternative source to GPS points for large scale map production because it have different shift lengths in both Easting and Northing directions as shown in Figure (4.12) and Figure (4.13) also different shift directions as shown in Figure (4.15) so the transformation parameters between these control points and image points cant be computed for the orthorectification process due to this disturbances in these points.

4.2.1.7 Orthorectification of GEO EYE Satellite Image Using GPS Control Points and (Ground DEM and DBM)

This test was carried out to find the possibility of using Satellite image extracted from Google earth program in this case was (GEO EYE Satellite image) for producing large scale cadastral maps. Orthorectification of this image was performed using 15 GCPs distributed over the study area derived by GPS. The Differential rectification will be used as it is the most accurate method of orthorectification (*Temiz, M., and Külür, S., 2008*). The test was divided into three cases as follows:

Case (1): Orthorectification of GEO EYE Satellite image extracted from Google Earth program Using 5 GCPs evenly distributed over the study area and using DEM only as shown in Figure (4.16). Table (4.5) shows accuracy of Orthorectification Process using 5 Control Points and Table (4.6) shows accuracy of Orthorectification Process of 10 Check Points.

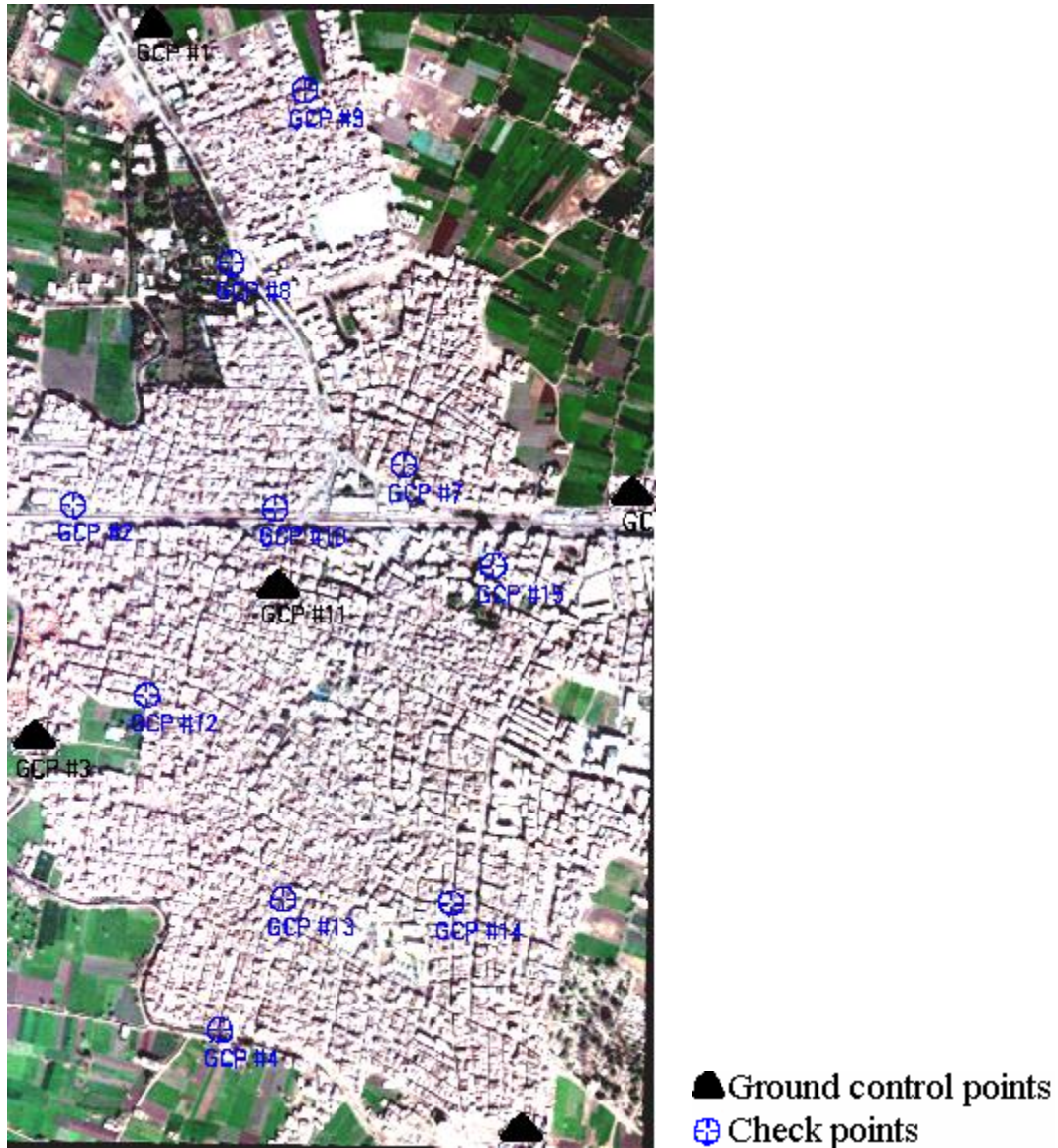


Figure (4.16): Distribution of GCPs over the Study Area (5 CPs).

Table (4.5): Accuracy of Orthorectification Process with DEM only using 5 Control Points.

Point-ID	E-image mt	N-image mt	E-GPS mt	N-GPS mt	Z mt	ΔE mt	ΔN mt	Vector mt
GCP #1	326939.63	3341198.57	326938.99	3341199.25	16.42	0.20	0.01	0.20
GCP #3	326707.60	3339830.99	326705.82	3339831.21	18.43	-0.38	0.05	0.39
GCP #5	327650.89	3339082.17	327651.26	3339081.88	17.05	0.25	0.01	0.25
GCP #6	327874.58	3340301.65	327873.40	3340303.34	16.76	-0.36	0.03	0.36
GCP #11	327179.95	3340124.32	327180.06	3340124.69	18.45	0.29	-0.10	0.31

Table (4.6): Accuracy of Orthorectification Process with DEM only for 10 Check Points.

Point-ID	E-image mt	N-image mt	E-GPS mt	N-GPS mt	Z mt	ΔE mt	ΔN mt	Vector mt
GCP #2	326788.29	3340281.40	326789.05	3340280.62	16.95	0.91	-0.52	1.04
GCP #4	327067.76	3339275.94	327069.35	3339274.27	17.80	0.99	-0.88	1.33
GCP #7	327423.00	3340356.68	327422.74	3340356.93	16.46	0.08	-0.44	0.44
GCP #8	327091.72	3340742.64	327090.69	3340744.42	16.57	-0.15	0.47	0.49
GCP #9	327231.56	3341072.70	327232.22	3341071.33	16.88	0.66	-1.35	1.50
GCP #10	327174.45	3340275.05	327174.03	3340275.84	17.35	0.06	0.05	0.08
GCP #12	326930.26	3339915.61	326929.66	3339916.23	17.20	0.07	0.15	0.17
GCP #13	327191.38	3339526.05	327190.50	3339527.51	17.72	-0.27	0.62	0.67
GCP #14	327511.73	3339520.16	327510.57	3339521.31	17.57	-0.48	0.46	0.66
GCP #15	327591.18	3340163.08	327591.82	3340161.95	16.98	0.50	-1.11	1.21

Where: E-image is the Easting coordinates of GEO EYE Satellite image extracted from Google Earth program, N-image is the Northing coordinates of GEO EYE Satellite image extracted from Google Earth program, E-GPS is the Easting coordinates of GPS, N-GPS is the Northing coordinates of GPS, Z is the elevation of the point derived from Ground DEM, ΔE is the distance between the Easting coordinates of GEO EYE Satellite image extracted from Google Earth program and the Easting coordinates of GPS, ΔN is the distance between the Northing coordinates of GEO EYE Satellite image extracted from Google Earth program and the Northing coordinates of GPS, Vector is the resulted shift of each point.

The RMS for GCPs was 0.5295m in E direction and 0.7135 m in N direction and the total RMS was 0.8885m see Equation (2.9).

Case (2): Orthorectification of GEO EYE Satellite image extracted from Google Earth program Using 10 GCPs evenly distributed over the study area and using DEM only as shown in figure (4.17). Table (4.7) shows accuracy of Orthorectification Process using 10 Control Points and Table (4.8) shows accuracy of Orthorectification Process of 5 Check Points.



Figure (4.17): Distribution of GCPs over the Study Area (10 CPs).

Table (4.7): Accuracy of Orthorectification Process with DEM only using 10 Control Points.

Point-ID	E-image mt	N-image mt	E-GPS mt	N-GPS mt	Z mt	ΔE mt	ΔN mt	Vector mt
GCP #1	326939.63	3341198.57	326938.99	3341199.25	16.42	-0.06	0.19	0.20
GCP #2	326788.29	3340281.40	326789.05	3340280.62	16.95	0.53	-0.31	0.62
GCP #3	326707.60	3339830.99	326705.82	3339831.21	18.43	-0.82	0.30	0.87
GCP #4	327067.76	3339275.94	327069.35	3339274.27	17.80	0.72	-0.72	1.02
GCP #5	327650.89	3339082.17	327651.26	3339081.88	17.05	0.15	-0.21	0.26
GCP #6	327874.58	3340301.65	327873.40	3340303.34	16.76	-0.35	0.28	0.45
GCP #8	327091.72	3340742.64	327090.69	3340744.42	16.57	-0.35	0.71	0.79
GCP #9	327231.56	3341072.70	327232.22	3341071.33	16.88	0.53	-1.01	1.14
GCP #11	327179.95	3340124.32	327180.06	3340124.69	18.45	0.11	0.05	0.12
GCP #13	327191.38	3339526.05	327190.50	3339527.51	17.72	-0.48	0.73	0.87

Table (4.8): Accuracy of Orthorectification Process with DEM only for 5 Check Points.

Point-ID	E-image mt	N-image mt	E-GPS mt	N-GPS mt	Z mt	ΔE mt	ΔN mt	Vector mt
GCP #7	327423.00	3340356.68	327422.74	3340356.93	16.46	-0.01	-0.1	0.09
GCP #10	327174.45	3340275.05	327174.03	3340275.84	17.35	-0.06	0.12	0.14
GCP #12	326930.26	3339915.61	326929.66	3339916.23	17.20	-0.12	0.19	0.22
GCP #14	327511.73	3339520.16	327510.57	3339521.31	17.57	-0.29	0.21	0.36
GCP #15	327591.18	3340163.08	327591.82	3340161.95	16.98	0.22	-0.5	0.52

The RMS for GCPs was 0.3477m in E direction and 0.5067m in N direction and the total RMS was 0.6145m.

Case (3): Orthorectification of GEO EYE Satellite image extracted from Google Earth program Using 10 GCPs evenly distributed over the study area and using DEM and DBM as shown in Figure (4.18). Table (4.9) shows accuracy of Orthorectification Process using 10 Control Points and Table (4.10) shows accuracy of Orthorectification Process of 5 Check Points.

For correcting the buildings relief displacement 15 GCPs over the building corners have been used where their positions are known on the DBM area to concentrate the correction over the buildings.

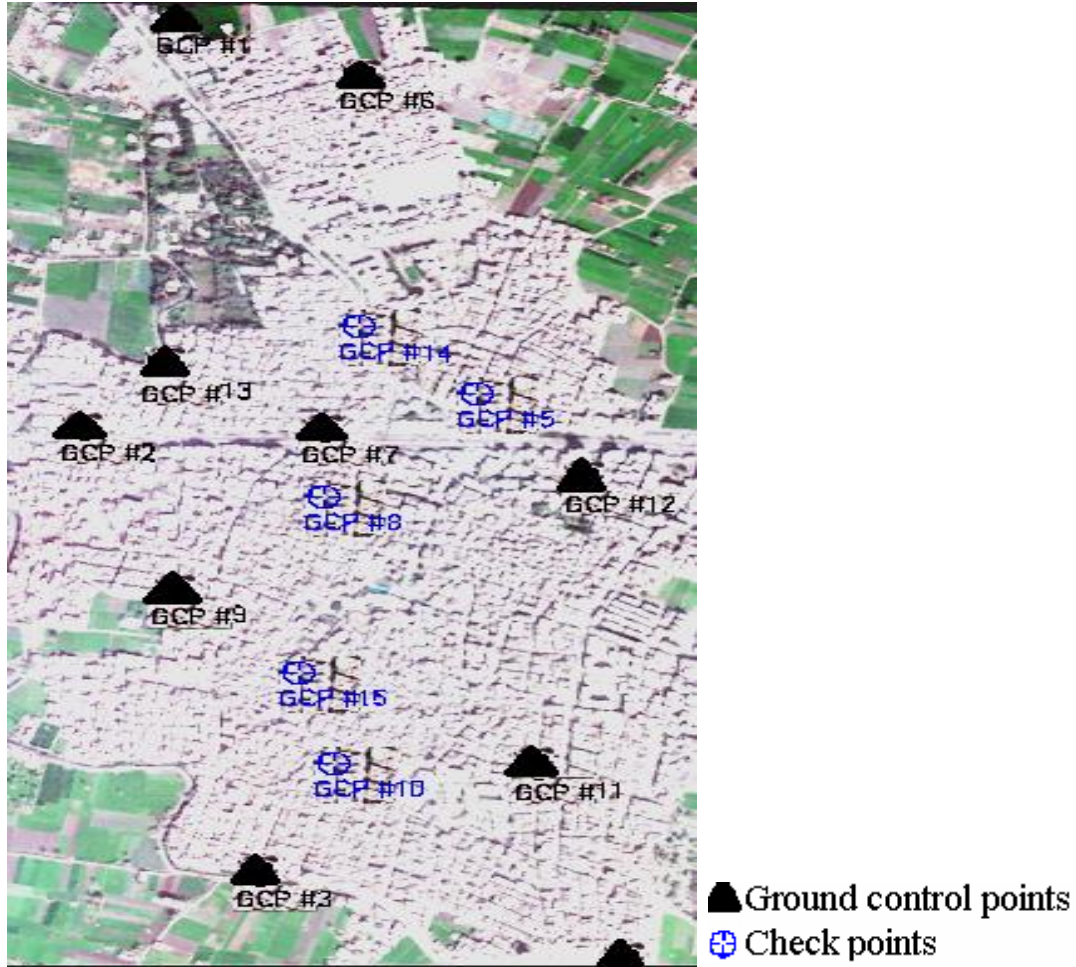


Figure (4.18): Distribution of GCPs over the Study Area (10 CPs) and DBM.

Table (4.9): Accuracy of Orthorectification Process with DEM and DBM using 10 Control Points.

Point-ID	E-image mt	N-image mt	E-GPS mt	N-GPS mt	Z mt	ΔE mt	ΔN mt	Vector mt
GCP #1	326939.14	3341198.75	326938.99	3341199.25	4.00	-0.32	0.29	0.43
GCP #2	326787.89	3340281.52	326789.05	3340280.62	10.00	0.28	-0.30	0.41
GCP #3	327067.57	3339275.13	327069.35	3339274.27	10.00	0.62	-0.23	0.66
GCP #4	327650.89	3339082.17	327651.26	3339081.88	4.00	0.08	-0.37	0.38
GCP #6	327230.88	3341073.26	327232.22	3341071.33	10.00	0.38	-0.40	0.55
GCP #7	327174.34	3340275.25	327174.03	3340275.84	7.00	-0.41	0.54	0.68
GCP #9	326930.11	3339915.93	326929.66	3339916.23	10.00	-0.51	0.38	0.64
GCP #11	327511.73	3339520.16	327510.57	3339521.31	7.00	-0.73	0.68	1.00
GCP #12	327590.64	3340163.58	327591.82	3340161.95	13.00	0.47	-0.22	0.52
GCP #13	326915.34	3340419.37	326916.25	3340418.15	11.00	0.14	-0.37	0.39

Table (4.10): Accuracy of Orthorectification Process with DEM and DBM for 5 Check Points.

Point-ID	E-image mt	N-image mt	E-GPS mt	N-GPS mt	Z mt	ΔE mt	ΔN mt	Vector mt
GCP #5	327422.79	3340356.82	327422.74	3340356.93	10.00	-0.23	0.55	0.60
GCP #8	327179.95	3340124.32	327180.06	3340124.69	7.00	-0.19	0.41	0.45
GCP #10	327190.99	3339526.08	327190.50	3339527.51	7.00	-0.48	0.83	0.96
GCP #14	327237.10	3340504.02	327237.57	3340502.60	13.00	-0.05	-0.2	0.19
GCP #15	327132.99	3339729.62	327133.61	3339729.01	10.00	0.05	-0.1	0.08

The RMS for GCPs was 0.2530m in E direction and 0.4889m in N direction and the total RMS was 0.5504m.

Figure (4.19) shows the RMS of GEO EYE Satellite image extracted from Google Earth program using 5 GCPs, 10 GCPs with DEM only and 10 GCPs with DEM and DBM.

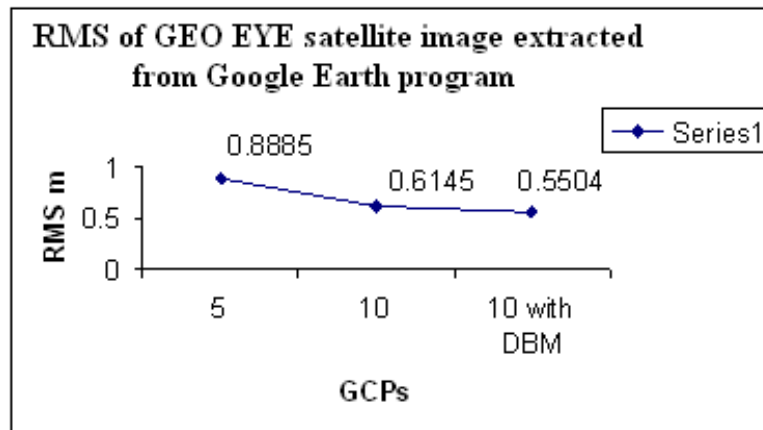


Figure (4.19): RMS of the GEO EYE Satellite Image Extracted from Google Earth Program.

4.2.1.8 Orthorectification of QUICKBIRD Satellite Imagery Using GPS Control Points and (Ground DEM and DBM)

Case (1): Orthorectification of QUICKBIRD Satellite Imagery Using 5 GCPs evenly distributed over the study area and using DEM only as shown in Figure (4.20). Table

(4.11) shows accuracy of Orthorectification Process using 5 Control Points and Table (4.12) shows accuracy of Orthorectification Process of 10 Check Points.



Figure (4.20): Distribution of GCPs over the Study Area (5 CPs).

Table (4.11): Accuracy of Orthorectification Process with DEM only using 5 Control Points.

Point-ID	E-image mt	N-image mt	E-GPS mt	N-GPS mt	Z mt	ΔE mt	ΔN mt	Vector mt
GCP #1	326938.47	3341202.27	326938.99	3341199.25	16.42	0.45	-0.07	0.46
GCP #7	327180.46	3340126.61	327180.06	3340124.69	18.45	-0.83	0.27	0.88
GCP #10	327648.17	3339083.89	327651.26	3339081.88	17.05	0.42	-0.04	0.43
GCP #13	326653.33	3339578.04	326656.32	3339574.79	17.51	0.05	-0.09	0.11
GCP #14	327873.36	3340305.22	327873.40	3340303.34	16.76	-0.09	-0.07	0.11

Table (4.12): Accuracy of Orthorectification Process with DEM only for 10 Check Points.

Point-ID	E-image mt	N-image mt	E-GPS mt	N-GPS mt	Z mt	ΔE mt	ΔN mt	Vector mt
GCP #2	327234.34	3341073.46	327232.22	3341071.33	16.88	-1.03	0.25	1.06
GCP #3	327089.12	3340747.60	327090.69	3340744.42	16.57	0.82	-0.29	0.87
GCP #4	327424.07	3340358.25	327422.74	3340356.93	16.46	-1.04	0.59	1.19
GCP #5	326790.95	3340282.92	326789.05	3340280.62	16.95	-1.99	0.41	2.03
GCP #6	327592.97	3340163.58	327591.82	3340161.95	16.98	-1.01	0.25	1.04
GCP #8	326927.02	3339919.55	326929.66	3339916.23	17.20	0.53	-0.31	0.62
GCP #9	327189.33	3339529.89	327190.50	3339527.51	17.72	-0.50	0.02	0.50
GCP #11	327508.81	3339523.42	327510.57	3339521.31	17.57	0.07	-0.04	0.08
GCP #12	327173.58	3340278.17	327174.03	3340275.84	17.35	-0.20	0.10	0.23
GCP #15	326701.92	3339834.63	326705.82	3339831.21	18.43	0.93	-0.29	0.98

The RMS for GCPs was 0.9612m in E direction and 0.3023 m in N direction and the total RMS was 1.008m.

Case (2): Orthorectification of QUICKBIRD Satellite Imagery Using 10 GCPs evenly distributed over the study area and using DEM only as shown in Figure (4.21). Table (4.13) shows accuracy of Orthorectification Process using 10 Control Points and Table (4.14) shows accuracy of Orthorectification Process of 5 Check Points.

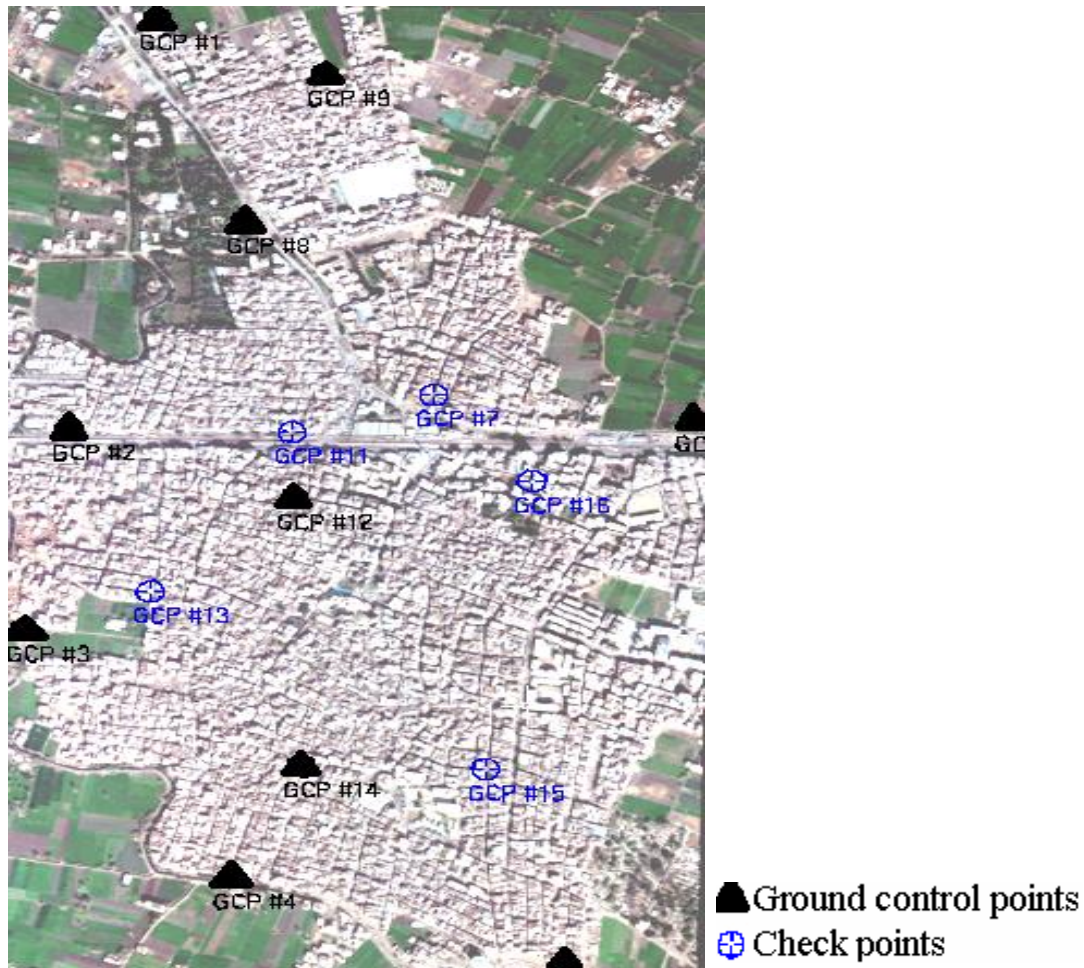


Figure (4.21): Distribution of GCPs over the Study Area (10 CPs).

Table (4.13): Accuracy of Orthorectification Process with DEM only using 10 Control Points.

Point-ID	E-image mt	N-image mt	E-GPS mt	N-GPS mt	Z mt	ΔE mt	ΔN mt	Vector mt
GCP #1	326938.47	3341202.27	326938.99	3341199.25	16.42	0.86	-0.07	0.86
GCP #2	327234.34	3341073.46	327232.22	3341071.33	16.88	-0.48	0.07	0.49
GCP #3	327089.12	3340747.60	327090.69	3340744.42	16.57	1.18	-0.38	1.24
GCP #5	326790.95	3340282.92	326789.05	3340280.62	16.95	-1.84	0.44	1.88
GCP #6	327592.97	3340163.58	327591.82	3340161.95	16.98	-0.64	0.05	0.64
GCP #7	327180.46	3340126.61	327180.06	3340124.69	18.45	-0.67	0.25	0.72
GCP #10	327648.17	3339083.89	327651.26	3339081.88	17.05	0.52	-0.03	0.52
GCP #11	327508.81	3339523.42	327510.57	3339521.31	17.57	0.17	-0.07	0.19
GCP #13	326653.33	3339578.04	326656.32	3339574.79	17.51	-0.04	-0.07	0.08
GCP #15	326701.92	3339834.63	326705.82	3339831.21	18.43	0.93	-0.21	0.95

Table (4.14): Accuracy of Orthorectification Process with DEM only for 5 Check Points.

Point-ID	E-image mt	N-image mt	E-GPS mt	N-GPS mt	Z mt	ΔE mt	ΔN mt	Vector mt
GCP #4	327424.07	3340358.25	327422.74	3340356.93	16.46	-0.67	0.39	0.78
GCP #8	326927.02	3339919.55	326929.66	3339916.23	17.20	0.58	-0.3	0.66
GCP #9	327189.33	3339529.89	327190.50	3339527.51	17.72	-0.54	0.02	0.54
GCP #12	327173.58	3340278.17	327174.03	3340275.84	17.35	0.02	0.03	0.04
GCP #14	327873.36	3340305.22	327873.40	3340303.34	16.76	0.54	-0.4	0.67

The RMS for GCPs was 0.5243m in E direction and 0.2869m in N direction and the total RMS was 0.5976 m.

Case (3): Orthorectification of QUICKBIRD Satellite Imagery Using 10 GCPs evenly distributed over the study area and using DEM and DBM as shown in Figure (4.22). Table (4.15) shows accuracy of Orthorectification Process using 10 Control Points and Table (4.16) shows accuracy of Orthorectification Process of 5 Check Points.

For correcting the buildings relief displacement 15 GCPs over the building corners have been used where their positions are known on the DBM area to concentrate the correction over the buildings.

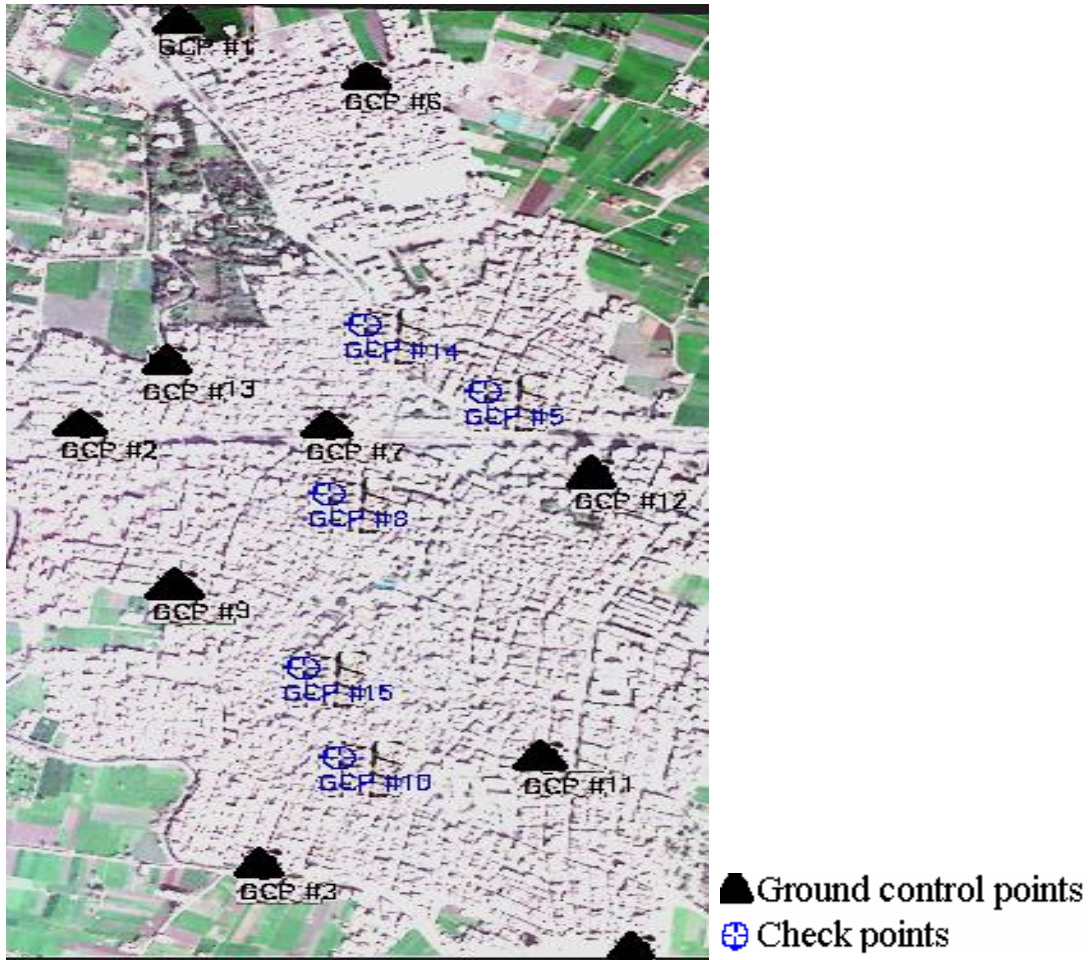


Figure (4.22): Distribution of GCPs over the Study Area (10 CPs) and DBM.

Table (4.15): Accuracy of Orthorectification Process with DEM and DBM using 10 Control Points.

Point-ID	E-image mt	N-image mt	E-GPS mt	N-GPS mt	Z mt	ΔE mt	ΔN mt	Vector mt
GCP #1	326937.72	3341199.44	326938.99	3341199.25	4.00	0.94	0.22	0.96
GCP #2	327233.51	3341070.82	327232.22	3341071.33	10.00	-0.80	-0.25	0.83
GCP #4	326792.01	3340280.13	326789.05	3340280.62	10.00	-0.50	-0.17	0.53
GCP #5	327173.64	3340276.95	327174.03	3340275.84	7.00	0.76	-0.85	1.13
GCP #6	327592.63	3340161.52	327591.82	3340161.95	13.00	-0.87	0.18	0.89
GCP #8	327510.28	3339521.30	327510.57	3339521.31	7.00	0.19	0.94	0.95
GCP #10	327649.33	3339086.56	327651.26	3339081.88	4.00	0.76	-0.55	0.94
GCP #11	327073.12	3339273.48	327069.35	3339274.27	10.00	-0.66	-0.04	0.66
GCP #13	326917.60	3340416.82	326916.25	3340418.15	11.00	0.25	0.43	0.49
GCP #15	326932.08	3339915.01	326929.66	3339916.23	10.00	-0.07	0.11	0.13

Table (4.16): Accuracy of Orthorectification Process with DEM and DBM for 5 Check Points.

Point-ID	E-image mt	N-image mt	E-GPS mt	N-GPS mt	Z mt	ΔE mt	ΔN mt	Vector mt
GCP #3	327423.76	3340356.75	327422.74	3340356.93	10.00	-0.70	-0.1	0.71
GCP #7	327180.73	3340124.51	327180.06	3340124.69	7.00	0.22	0.01	0.22
GCP #9	327191.12	3339527.82	327190.50	3339527.51	7.00	0.64	-0.2	0.67
GCP #12	327136.64	3339728.34	327133.61	3339729.01	10.00	-0.68	0.10	0.69
GCP #14	327238.81	3340502.08	327237.57	3340502.60	13.00	-0.26	-0.1	0.31

The RMS for GCPs was 0.5436m in E direction and 0.1441m in N direction and the total RMS was 0.5624m.

Figure (4.23) shows the RMS of QUICKBIRD satellite image using 5 GCPs, 10 GCPs with DEM only and 10 GCPs with DEM and DBM

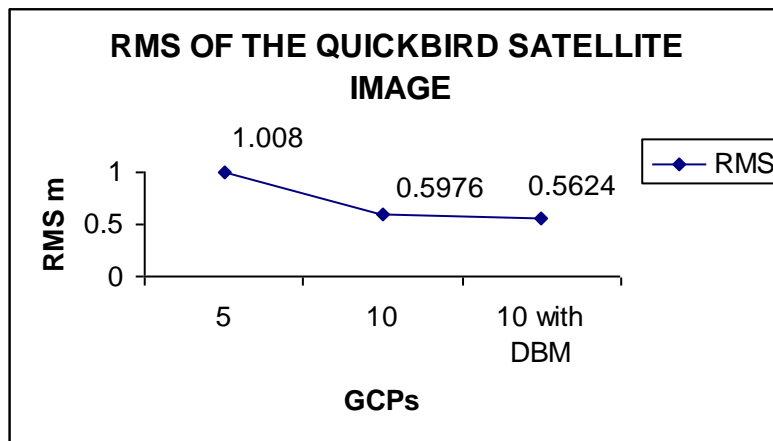


Figure (4.23): RMS of the QUICKBIRD Satellite Image.

4.2.3 On Screen Digitizing and Production of the Final Thematic Maps

The thematic maps created by on screen digitizing method using ARC-GIS 9.3 program for both images (QUICKBIRD and GEO EYE Satellite image extracted from Google Earth program). Digitizing includes streets and buildings as shown in the following figures:



Figure (4.24): On Screen Digitizing for GEO EYE Satellite Image Extracted from Google Earth Program for Streets.



Figure (4.25): On Screen Digitizing for GEO EYE Satellite Image Extracted from Google Earth Program for Buildings.



Figure (4.26): On Screen Digitizing for QUICKBIRD Satellite Image for Streets.



Figure (4.27): On Screen Digitizing for QUICKBIRD Satellite Image for Buildings.

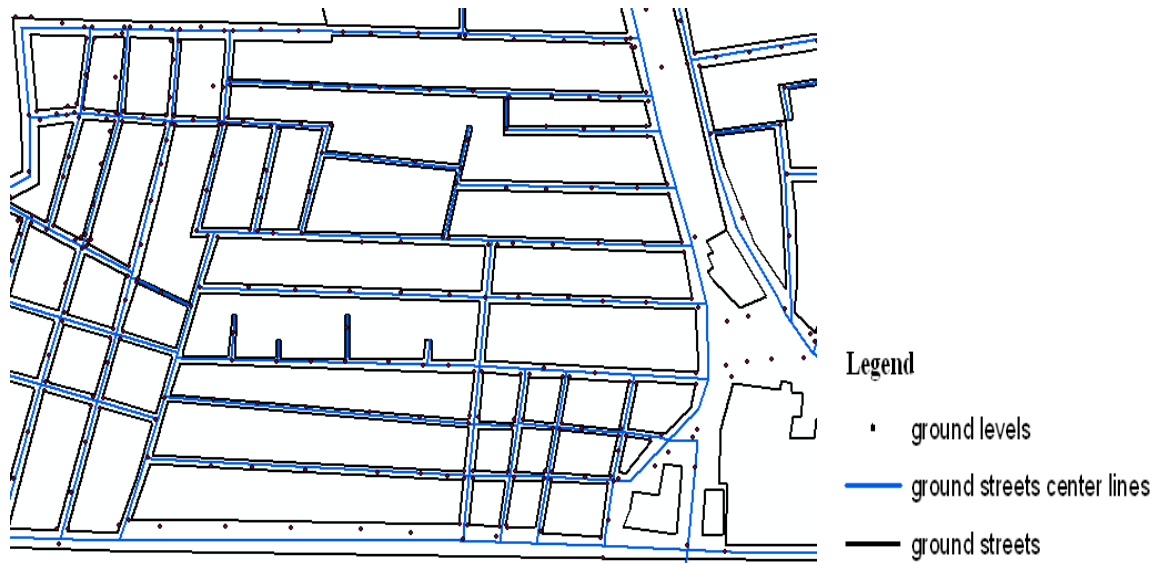


Figure (4.28): The Results of On Screen Digitizing for Both Streets and Buildings from GEO EYE Satellite Image Extracted from Google Earth Program.

4.2.4 Checking the Planimetric Accuracy of the Map Production Process

The accuracy of the final map products should be evaluated according to the three major map accuracy standards. These standards use root-mean-square error (RMSE) for evaluation. RMSE is the square root of the average of the set of squared differences between dataset coordinate values and coordinate values from an independent source of higher accuracy for identical points.

First standard is The NMAS “National Map Accuracy Standards” (*NMAS; 1947*) still the official standard for map (*Anderson and Mikhail, 1998*).

First the Horizontal Accuracy: For maps on publication scales larger than 1:20,000, not more than 10 percent of the points tested shall be in error by more than 1/30 inch (0.8mm), measured on the publication scale. While maps on publication scales of 1:20,000 or smaller not more than 10 percent of the points tested shall be in error by more than 1/50 inch (0.5mm). These limits of accuracy shall apply to positions of well-defined points that are easily plotted on the scale of the map within 1/100 inch (0.25mm) (*NMAS, 1947*).

The Vertical Accuracy as applied to contour maps on all publication scales, not more than 10 percent of the elevations tested shall be in error by more than one-half the contour interval (*NMAS, 1947*).

To determine the horizontal accuracy in actual ground meters, the following calculation must be performed. If the scale is larger than 1:20,000, use this calculation (*NMAS; 1947*).

$$0.03333 \times \text{scale} \times 2.54 / 100 = \text{ground meter} \quad (4.5)$$

For 1:2500-scale maps: $0.03333 \times 2500 \times 2.54 / 100 = 2.12$ meters.

The ASPRS Standard “American Society for Photogrammetry and Remote Sensing” Accuracy Standards for Large-Scale Maps.

For 1:2500-scale maps: $(0.03333 \times 2500 \times 2.54 / 100) / 3.333 = 0.64$ meters.

The NSSDA Standard “National Standard for Spatial Data Accuracy”

For 1:2500-scale maps: $(0.03333 \times 2500 \times 2.54 / 100) / 2 = 1.06$ meters.

Table (4.17) shows the three map accuracy standards (NMA, ASPRS and NSSDA) according to the above computations.

Table (4.17): The Allowable RMS for the Three Map Accuracy Standards.

Scale	NMAS (m)	NSSDA (m)	ASPRS (m)
1:2500	2.12	1.06	0.63
1:3000	2.54	1.27	0.85
1:4000	3.39	1.69	1.00
1:5000	4.24	2.12	1.25

The planimetric accuracy will be evaluated for both QUICKBIRD and Google Earth images.

A. Checking out the planimetric accuracy of the map produced from QUICKBIRD satellite image:

Using the same 5 check points of the orthorectification process after the vectorization to calculate the total RMSE of the final maps, the results was recorded in table (4.18) shows

that the RMS for GCPs was 0.999m in Easting direction and 0.352m in Northing direction while the total RMS was 1.05 m see Equation (2.9).

Table (4.18): Accuracy of Vectorization Process for QUICKBIRD Image Using 5 Check Points.

Point-ID	E-image mt	N-image mt	E-GPS mt	N-GPS mt	Z mt	ΔE mt	ΔN mt
GCP #3	327422.737	3340356.925	327420.270	3340357.048	2.467	-0.12	2.470
GCP #7	327237.574	3340502.604	327236.162	3340502.176	1.412	0.428	1.475
GCP #9	327180.060	3340124.690	327179.508	3340124.475	0.552	0.215	0.592
GCP #12	327133.612	3339729.006	327133.967	3339728.683	-0.355	0.323	0.479
GCP #14	327190.496	3339527.505	327190.364	3339526.547	0.132	0.958	0.967

B. Checking out the planimetric accuracy of the map produced from GOOGLE EARTH satellite image:

Using the same 5 check points of the orthorectification process after the vectorization to calculate the total RMSE of the final maps, the results are recorded in table (4.19) that the RMS for GCPs was 0.495m in Easting direction and 0.574m in Northing direction and the total RMS was 0.76 m see Equation (2.9).

Table (4.19): Accuracy of Vectorization Process for GEO EYE Satellite Image Extracted from Google Earth Program Using 5 Check Points.

Point-ID	E-image mt	N-image mt	E-GPS mt	N-GPS mt	Z mt	ΔE mt	ΔN mt
GCP #3	327422.737	3340356.925	327423.178	3340354.844	-0.441	2.081	2.124
GCP #7	327237.574	3340502.604	327238.765	3340500.284	-1.191	2.320	2.607
GCP #9	327180.060	3340124.690	327180.903	3340123.624	-0.843	1.066	1.359
GCP #12	327133.612	3339729.006	327133.523	3339728.186	0.089	0.820	0.829
GCP #14	327190.496	3339527.505	327190.464	3339526.031	0.032	1.474	1.473

From these results of tables (4.19) (4.18), we conclude that these RMS for maps extracted from both images were within the required map accuracy standard for a map scale 1:5,000 according to the three map accuracy standards see table (4.17). Also these results were within the required map accuracy standard for a map scale 1:2,500 according to both the NMAS and NSSDA standards see also table (4.17). Also satellite image

extracted from Google Earth program (GEO EYE satellite image) in this case can be used as alternative source to other satellite images for producing large scale cadastral maps.

One of the main objectives of this research was the integration of GIS with Remote Sensing. For this purpose, a GIS has to be generated using spatial and attribute data. The following subsections will discuss these issues.

4.3 Building a GIS for the Study Area

For instance spatial and attribute data for streets may include street length, surface type,...etc. another example for spatial and attribute data for building may include building owner, height, area, number of floors,...etc.

4.3.1 Creation of the Database for the Study Area

A database should be designed as a part of GIS, it's designed for storing street network and building attribute and spatial data to assist the planner for infra-structure planning. The Database was created using ARC-GIS 9.3 program. Geo Database is an example of Object based type of Databases and it saves both spatial shape type and its attributes in the same file for streets and buildings as shown in tables (4.20) and (4.21).

Table (4.20): A Database for Streets Network.

Street-ID	Street-Shape	Street-Length mt	Street-width mt	Street-type
1	Polyline	64.78	2.36	Gravel
2	Polyline	182.90	11.59	Gravel
3	Polyline	127.47	4.89	Gravel
4	Polyline	30.06	2.37	Gravel
5	Polyline	47.27	3.68	Asphalt
6	Polyline	1300.86	8.02	Asphalt
7	Polyline	117.47	9.52	Asphalt
8	Polyline	114.40	3.79	Gravel
9	Polyline	552.24	3.99	Gravel
10	Polyline	213.30	4.37	Gravel

Table (4.21): A Database for Buildings.

Building-ID	Building-Shape	Building-Owner	street ID	No. of floors	Building-height mt	Building-Area mt ²
1	polygon	M. H.	1	2	7	246.89
2	polygon	A. L.	1	4	13	208.84
3	polygon	S. S.	1	3	10	261.78
4	polygon	H. L.	1	1	4	258.11
5	polygon	J. P.	1	1	4	98.93
6	polygon	O. D.	2	2	8	81.67
7	polygon	T. X.	2	2	8	29.71
8	polygon	P. D.	2	2	7	86.94
9	polygon	O. H.	2	3	11	162.54
10	polygon	P. Q.	2	3	10	72.39

4.3.2 Analysis and Planning for Study Area

For Infra-Structure planning of the study area, the streets were classified using the created database of streets according to its widths 3 classes. The first class to display data of streets of width less than 3.5 m because it affecting the execution of the Infra-Structure networks.

Another two classes were minor roads for minor pipes width ranges from (3.5m-8m) and major roads for major pipes width ranges from (8m-17m) as shown in Figure (4.29).

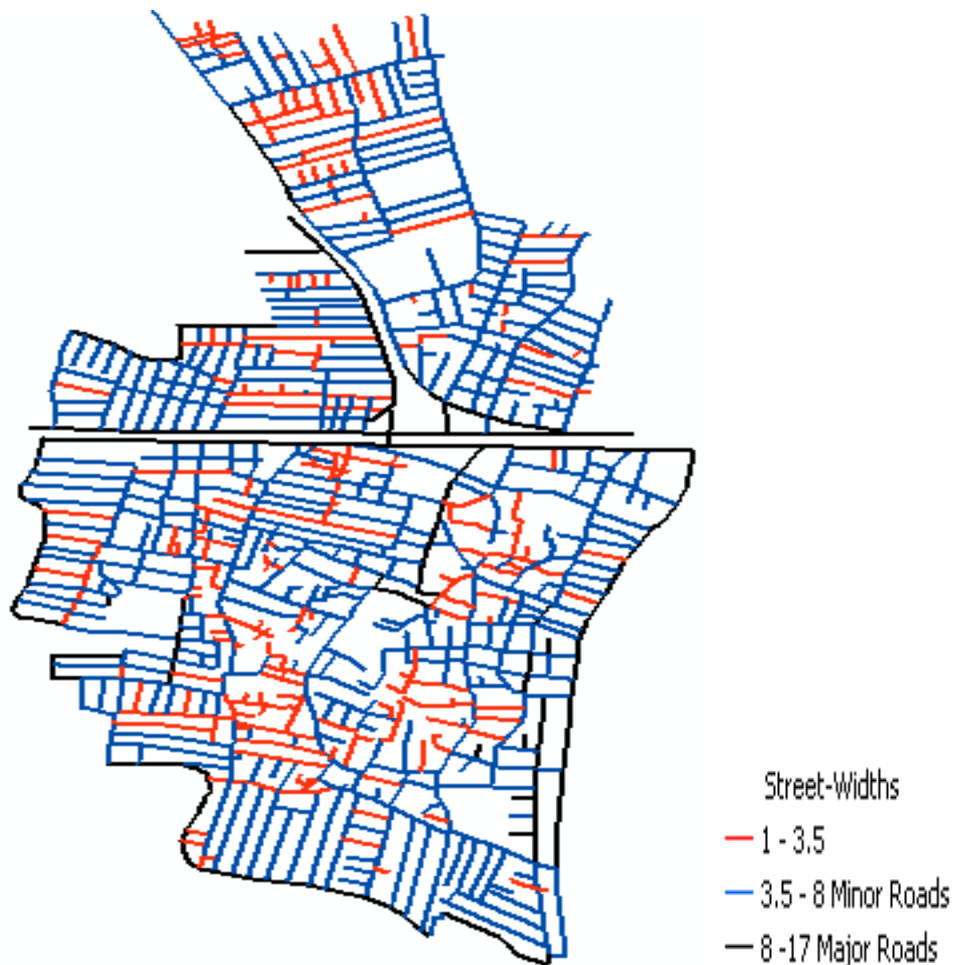


Figure (4.29): Classification of Streets According to its Widths.

Also classification of the ground levels has been done. This is useful especially for sewage network planning where gradient is required as shown in Figure (4.30). Where the ground elevations is classified into 9 classes. For instance, class 1 requirements ground with elevations ranges from 15m to 16m and so on.

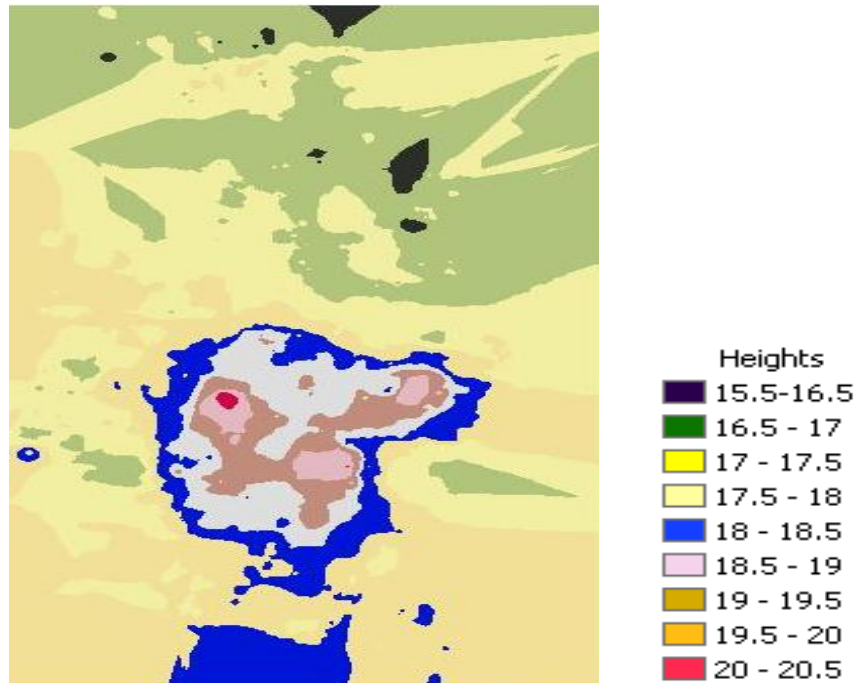


Figure (4.30): Classification of Ground Levels in the Study Area.

4.3.3. Applications of GIS

4.3.3.1. Pre-planning of Water Networks for the Study Area

An application to use the stored data for determining the most suitable location for a water tank in an area. It also includes planning of water networks in area under investigation.

A. Determining the most suitable location for the Water Tank which may serve the study area. The Water Tank is an important to be use at the maximum consumption hours and to save water at the minimum consumption hours and also to protect the pipes from the water hammer and emergency situations.

The rules which applied to find this location are:

1. The required location must be in a place which has the highest levels in the study area
2. It must also be in place owned to the country as possible
3. The roads goes to this location doesn't intersect with any water obstacles
4. The roads to this location should have suitable widths to enable the cutting works

5. The location should be near as possible to the existing water and electricity networks of the study area
6. The location should not has water or electricity works
7. The location should be near as possible to the feeding pipe which come from purification station

Using the spatial analysis tools in ARC GIS, the steps of finding the most suitable location are:

- 1- Decide: Which data set required to be input data. The elevations, Building and Streets
- 2- Drive: classifying the available data. The elevations (classification of levels in the study area), Building (classifying Distance to buildings every 10m), Streets with suitable widths (classifying Distance to streets every 10m) as shown in Figure (4.31)
- 3- Reclassify: gives high values for more suitable attribute. The elevations (highest levels in the study area) was classified as class 10, Building (Distance to buildings 10m) was classified as class10, Streets (Distance to streets 10m) was classified as class 10 as shown in Figure (4.32)
- 4- Weight and combination of these values: the highest elevation on the study area have the high weight (75%), Distance to buildings weight (12.5%) and Distance to streets weight (12.5%). The result will be a map of the most suitable locations by which we decide the most suitable location of the Water Tank as shown in Figure (4.33)

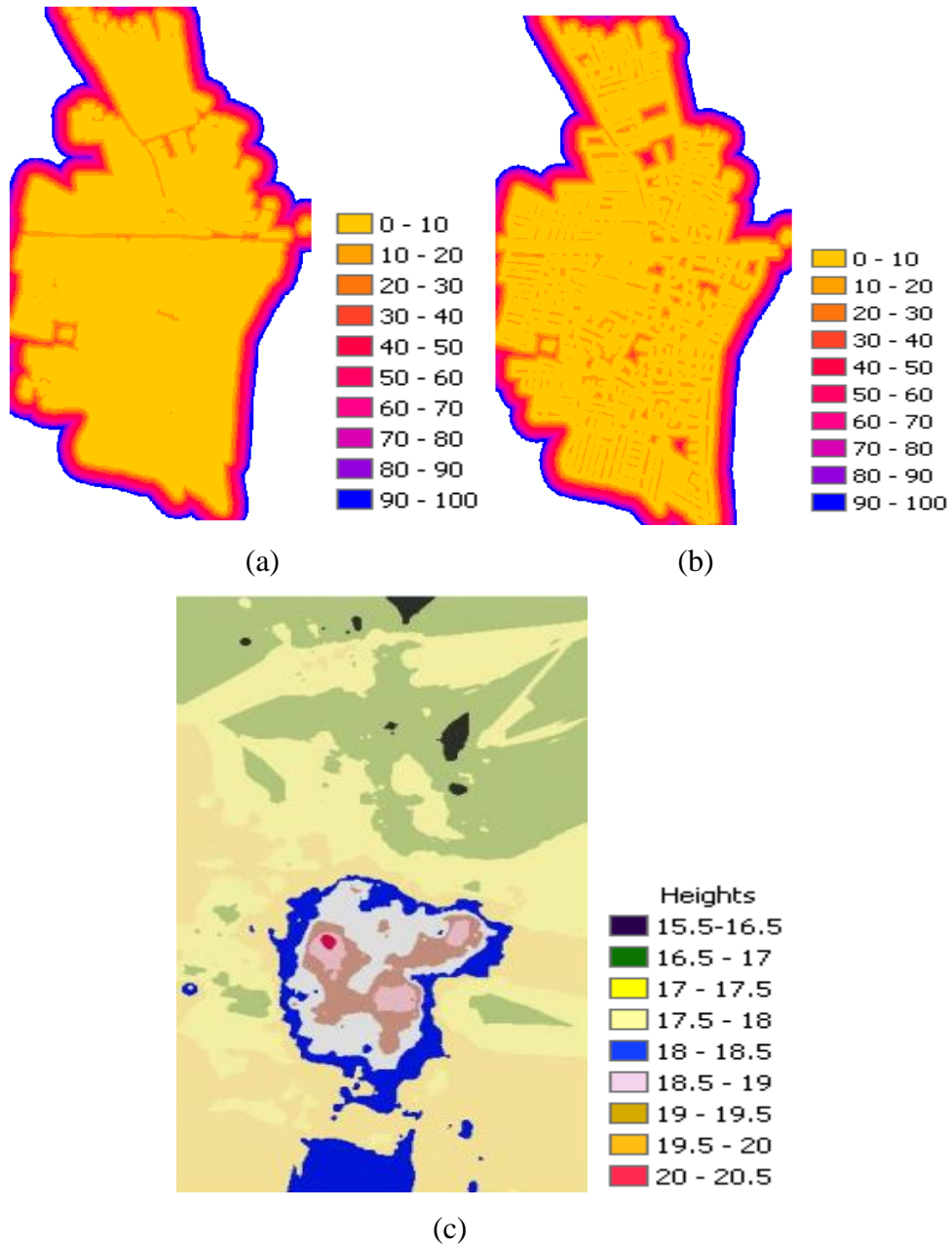


Figure (4.31): (a) Classification of Distances to Buildings (b) Classification of Distances to Streets (c) Classification of Elevations.

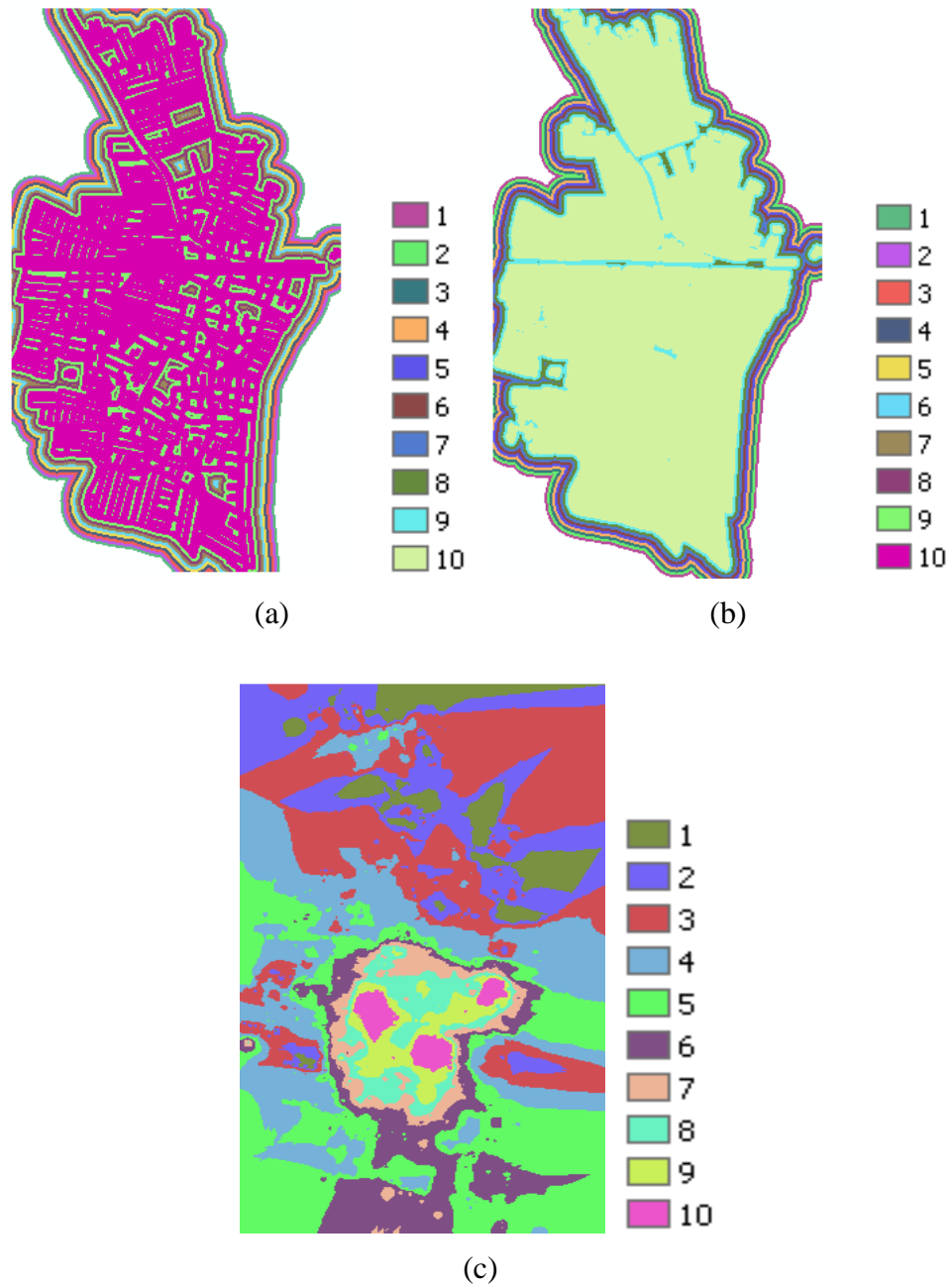


Figure (4.32): (a) The Reclassification of Distances to Buildings Class 10 with Distance 10m (b) The Reclassification of Distances to Streets Class 10 with Distance 10m (c) The Classification of Elevations Class 10 the Highest Elevations.

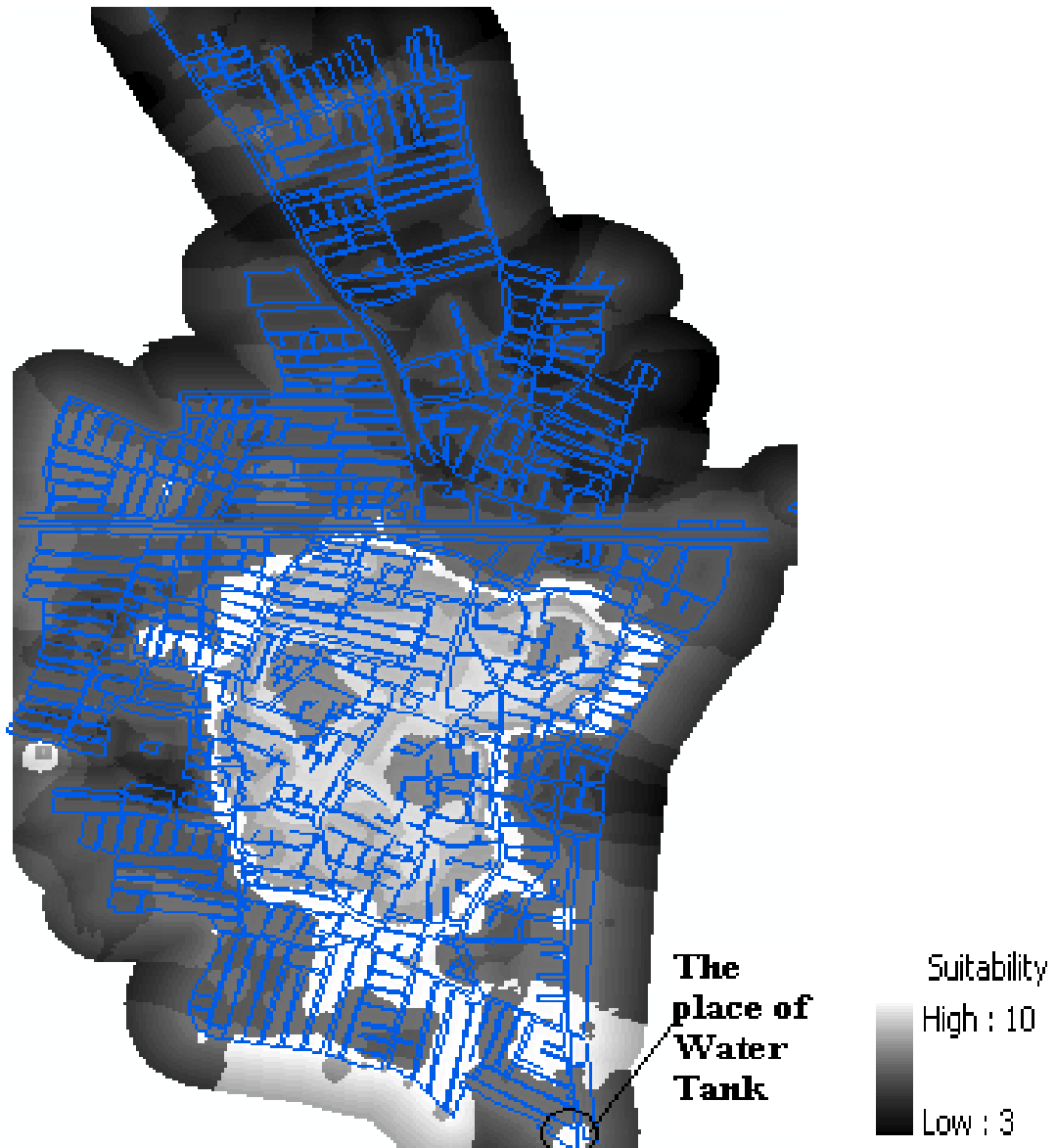


Figure (4.33): The Overlap of the Streets with the Suitability Map and the Most Suitable Location of the Water Tank.

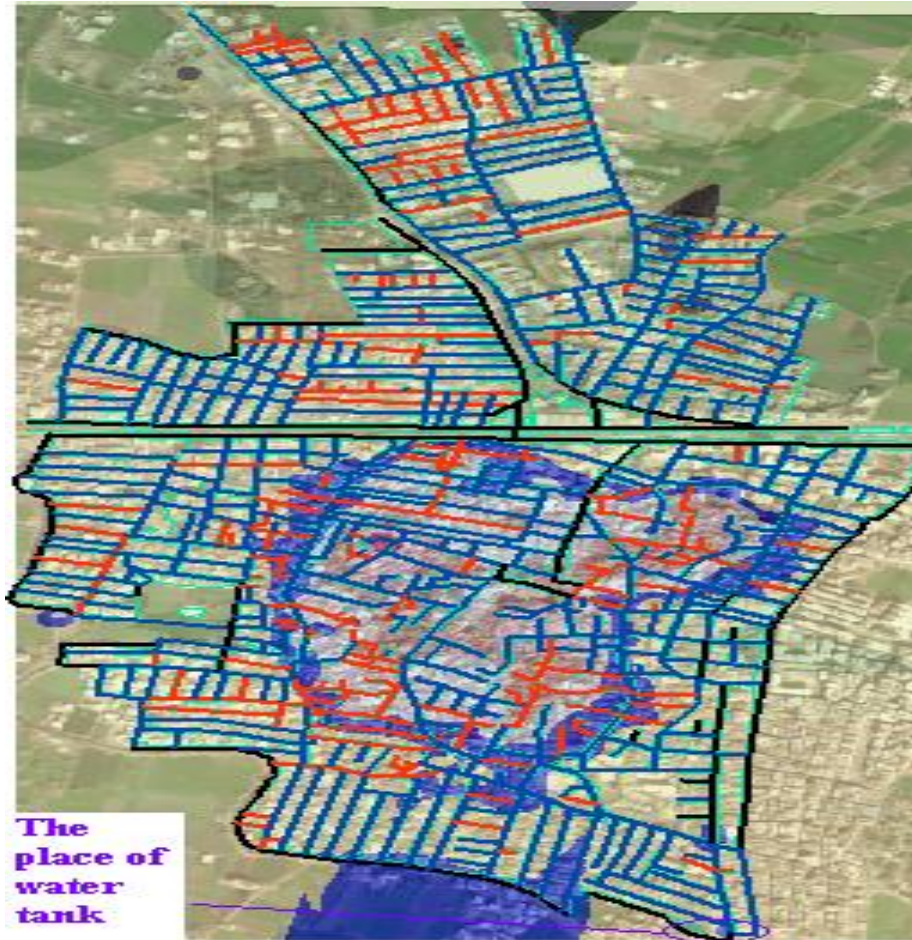


Figure (4.34): The Suitable Location of the Water Tank.

B. Planning of water networks in the study area for this purpose the population of this area which is 102045 pop. Should be known then calculate the population in the next 40 years (the period of time which this network will serve the study area) found according to the equations of the geometrical method as it gives the largest number of population (*Egyptian Code, 2010*).

$$\ln P_n = \ln P_1 + K_g \times (t_n - t_1) \quad (4.6)$$

Where:

P_n is the population in the target year, K_g is constant = 2.5% and $(t_n - t_1)$ is the time of the network that serves the study area so P_n found to be 277000 pop.

C. Determining the population water consumption of the study area. According to the (*Egyptian Code, 2010*), the average daily water consumption Q_{avg} for the study area is 210 liter/capital/day and the maximum daily consumption Q_{max} is $(1.8 \times Q_{avg})$ then the design consumption will be $Q_{design} = 277000 \times 210 \times 1.8 / 1000 \times 24 \times 60 \times 60 = 0.99 \text{ m}^3/\text{sec}$.

Also the population density equals population / area = $277000/1.13 \times 10^6 = 0.25$ capital/m²

D. According to the nature of the study area, the ring system will be used for the water distribution. The area will be divided into pressure zones according to the population density and the primary feeders will be in the outlines of these zones and the distribution mains will be inner of these zones. Using the classification of streets and the population density, the zones are divided as shown in Figure (4.35).

By using the ARC GIS, we find the population of each zone by designing automatic calculators from the formula (*Egyptian Code, 2010*).

$$\text{pop.} = \text{area} \times \text{pop. Density} \quad (4.7)$$

also the Q_{design} for each zone is calculated using equation ($Q_{design} = \text{pop.} \times 210 \times 1.8 / 1000 \times 24 \times 60 \times 60$) as shown in table (4.22).



Figure (4.35): Pressure Zones of the Study Area.

Table (4.22): Data of Water Pressure Zones of the Study Area.

Zone number	Shape	Zone area (m ²)	population	Q_design (m ³ /s)
1	polygon	130558.8	31334	0.097919
2	polygon	216728.5	52015	0.162546
3	polygon	292863.2	70287	0.219647
4	polygon	213963.6	51351	0.160472
5	polygon	121115	29068	0.090836
6	polygon	250259.5	60062	0.187694

E. Determining the diameter of pipes in these zones using the continuity equation as $Q=A \times V$ Equation (4.8) in which Q is the amount of water in pipe, A is the cross-section area of pipe (equal to $\pi/4 \times D^2$ (D is the diameter of the pipe) and V is the velocity of water in pipe. Assume that the velocity =1.0 m/sec < 1.5 (safe) so the diameter of the main pipe from the water tank will be Determined from equation $Q=A \times V$ so $0.99= \pi/4 \times D^2 \times 1.0$, so $D=1.1$ take $D=1000$ mm.

A program was designed using (Microsoft Visual Basic) in ARC GIS environment to find the diameter of the primary feeders pipes. Each pipe load half zone consumption and the half of load it will transfer water to. Except zone 3 and zone 1 both divided to three loads and we start from the opposite direction to the water tank as shown in Figure (4.33). The

user will add only the population number and the program will calculate the Q_{design} and the diameter of the pipe. As an example the diameter of pipe (1) is 250 mm because it doesn't have any load and the diameter of pipes (2,3) serve half of area (6) so its $Q_d = 0.5 \times 0.187 = 0.09$ so $D = 0.338$ take $D = 300$ mm for each pipe and the same for all pipes as shown in Figure (4.36). All pipes were calculated and the results tabulated in Table (4.23)

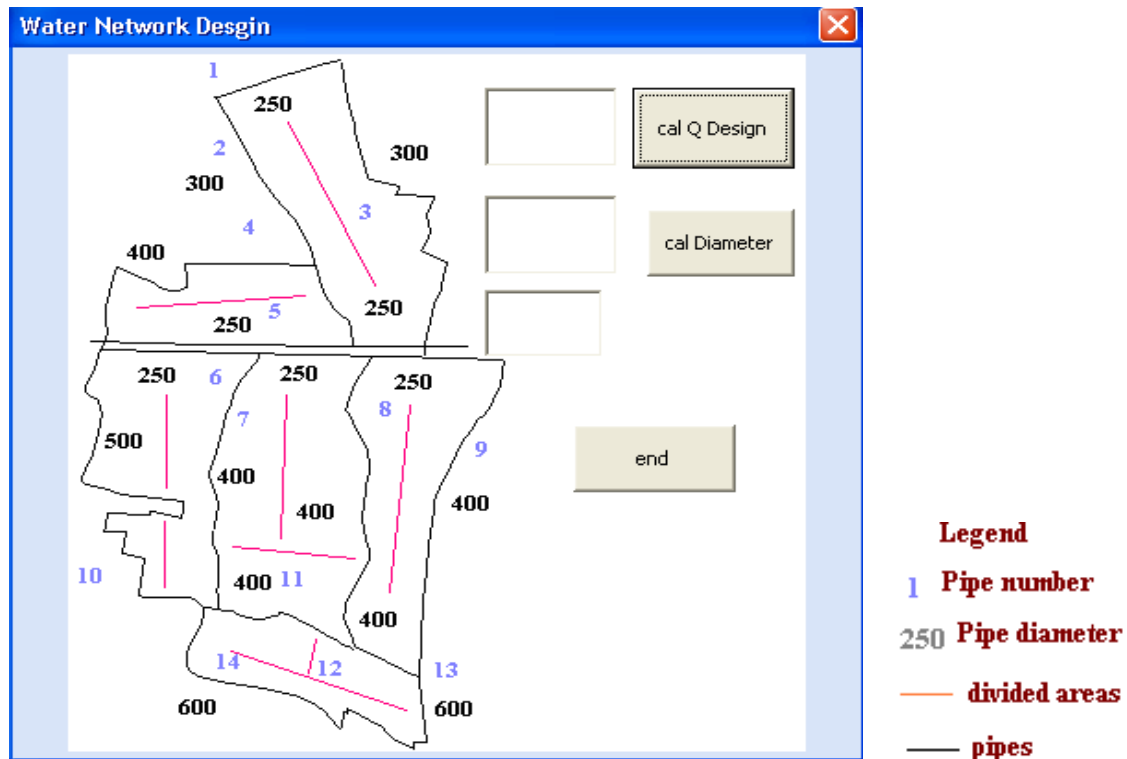


Figure (4.36): Distribution of the Primary Feeder Pipes Viewed in the Designed Program.

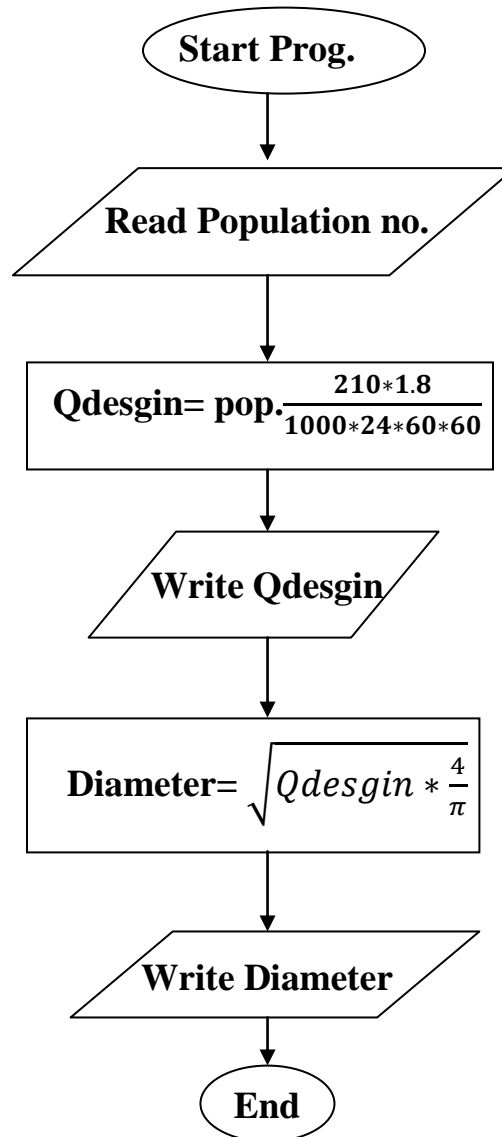


Figure (4.37): Flow Chart of the Designed Program for Water Network Pre-Planning.

Table (4.23): Diameters of the Water Primary Feeder Pipes.

No.	type	load	Diameter mm	Life time	Length mt
1	UPVC	NO load	250	40	356
2	UPVC	0.5 x Q6	300	40	835
3	UPVC	0.5 x Q6	300	40	1105
4	UPVC	0.5 x Q5 + 0.5 x Q6	400	40	879
5	UPVC	NO load	250	40	1017
6	UPVC	NO load	250	40	1084
7	UPVC	0.5 x Q2 + 0.3 x Q3	400	40	793
8	UPVC	0.5 x Q4 + 0.3 x Q3	400	40	913
9	UPVC	0.5 x Q4 + 0.5 x Q6	400	40	987
10	UPVC	0.5 x Q2 + 0.5 x Q5 + Q (250 mm)	500	40	1503
11	UPVC	0.25 x Q1 + 0.3 x Q3	400	40	399
12	UPVC	0.25 Q1	400	40	194
13	Ductile iron	0.5 x Q4 + 0.25 x Q1 + 0.5 x Q6	600	50	230
14	Ductile iron	0.5 x Q1 + 0.25 x Q1 + 0.5 x Q2 + 0.5 x Q5	600	50	999

Then the inner pipes are distribution mains which have diameter of 150 mm.

F. Water network was created using the utility network analysis in ARC GIS and can be controlled easily by the end user who can specify which pipe (edge) can be enabled or disabled if there is any damaged in this pipe also control valves (junctions) and define the water flow direction through defining which valve is source and which valve is sink as shown in Figure (4.38).

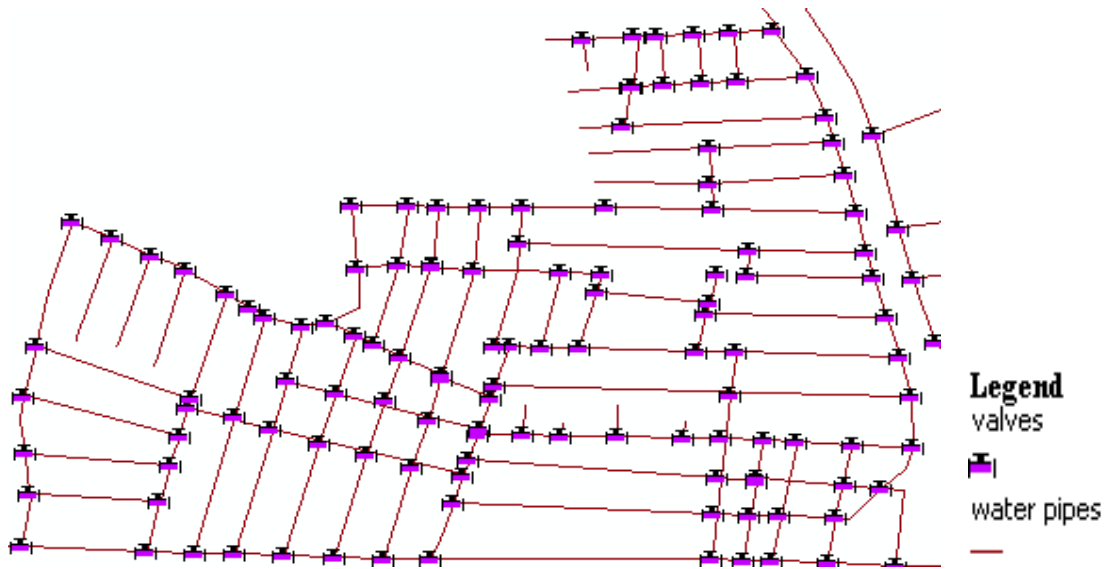


Figure (4.38): Sample of Final Water Network.

4.3.3.2. Pre-planning of the Sewage Networks in the Study Area

For this application the following steps should be followed

A. Determining the population sewage consumption of the study area, According to the (*Egyptian Code, 2010*) as the average daily water consumption (Q_{avg}) for the study area is 210 liter/capital/day and the maximum daily consumption (Q_{max}) is $(0.8 \times 1.5 \times Q_{avg})$ then the design consumption will be $Q_{design} = 277000 \times 210 \times 0.8 \times 1.5 / 1000 \times 24 \times 60 \times 60 = 0.04 \text{ m}^3/\text{sec}$. also the population density equals population / area = $277000 / 1.13 \times 10^6 = 0.25 \text{ capital/m}^2$

B. According to the classification of the levels of the study area and the water flow in the sewage network by gravity, the area is divided to zones according to the population density. The primary pipes will be in the outlines of these zones and the secondary pipes will be inner of these zones. Using the classification of the streets, zones are divided as shown in Figure (4.39). The population of each zone can be determined by designing automatic calculators in ARC GIS using the Equation (4.6) also Q_{design} for each zone can be determined using equation ($Q_{design} = \text{pop.} \times 210 \times 0.8 \times 1.5 / 1000 \times 24 \times 60 \times 60$) as shown in table (4.24).

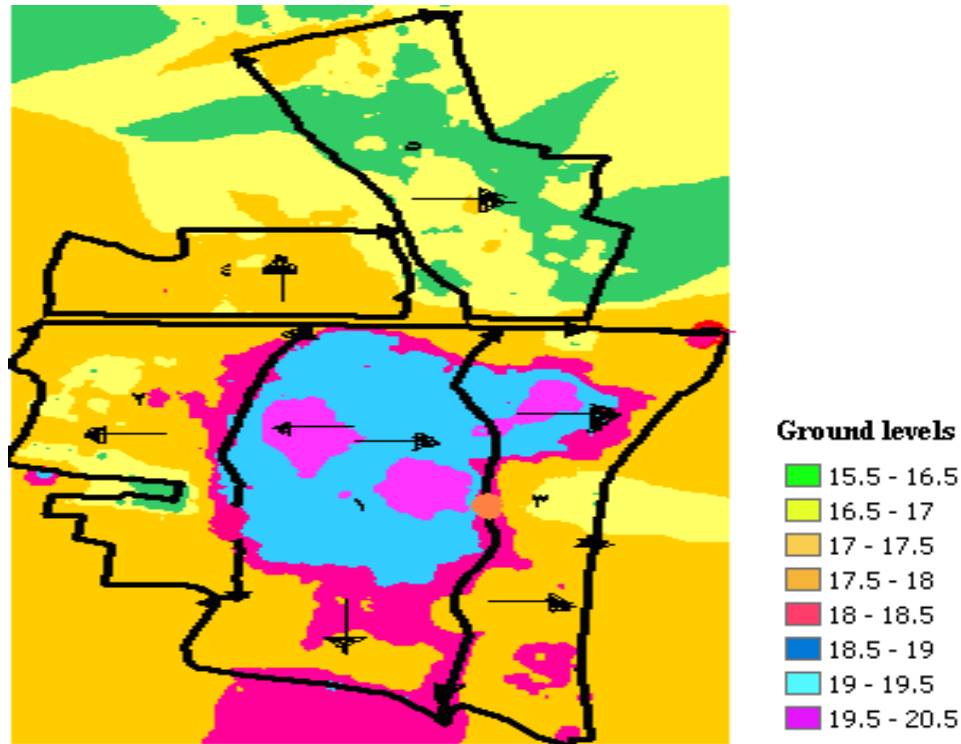


Figure (4.39): Divided Zones with Classified Levels and Arrows give Water Flow Direction on Study Area.

Table (4.24): Data of Sewage Zones of the Study Area.

Zone number	population	Area m ²	Q_Sewage m ³ /sec
1	96163	380946.5	0.200339
2	54182	216728.5	0.112879
3	63184	256440.1	0.131633
4	30279	121115	0.063081
5	62565	250259.5	0.130343

C. Determining the diameter of the pipes at these zones using Manning equation (*Egyptian Code, 2010*) as follows $Q_{sew} = 1/n \times D^{2/3} \times S^{1/2}$ where (n) is constant as a function of type of pipe (take $n=0.025$), (D) is the diameter of pipe and (S) is the slope of pipe ($S=1/1000$). Start from the opposite direction to the pumping station or the beginning of water flow.

For this purpose A program was designed using (Microsoft Visual Basic) in ARCGIS environment to Determine the diameter of the primary sewage pipes. The user will add only the population number and the program will calculate the Q_{sew} and the diameter of the pipe. as each pipe loads all zone sewage consumption and the sewage consumption it will transfer to the direction of pumping station as the diameter of pipe (1) loading $1/3 \times Q_1$ and equals to 400 mm from Manning equation and the diameter of pipes (2) is $0.16 Q_1$ and equals to 400 mm and the same for all pipes as shown in Figure (4.40). All pipes were calculated and the results tabulated in Table (4.25)

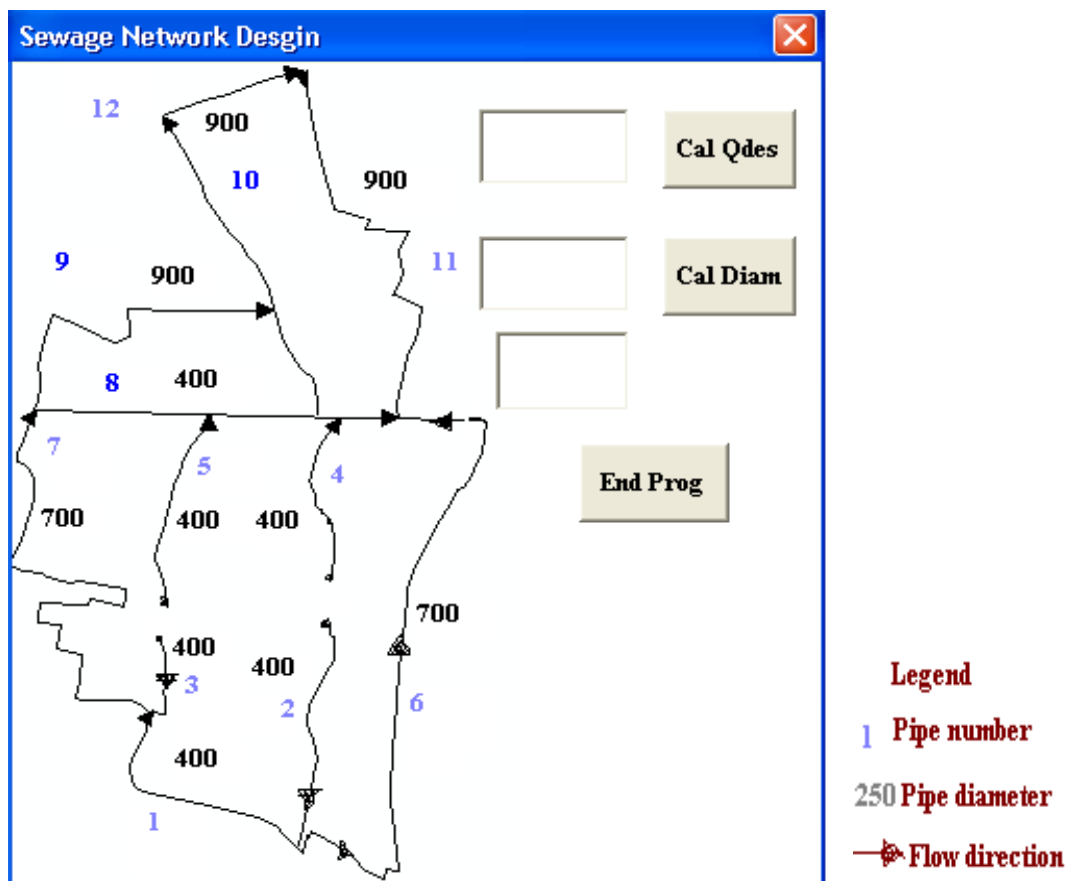


Figure (4.40): Distribution of the Primary Sewage Pipes Viewed in the Designed Program.

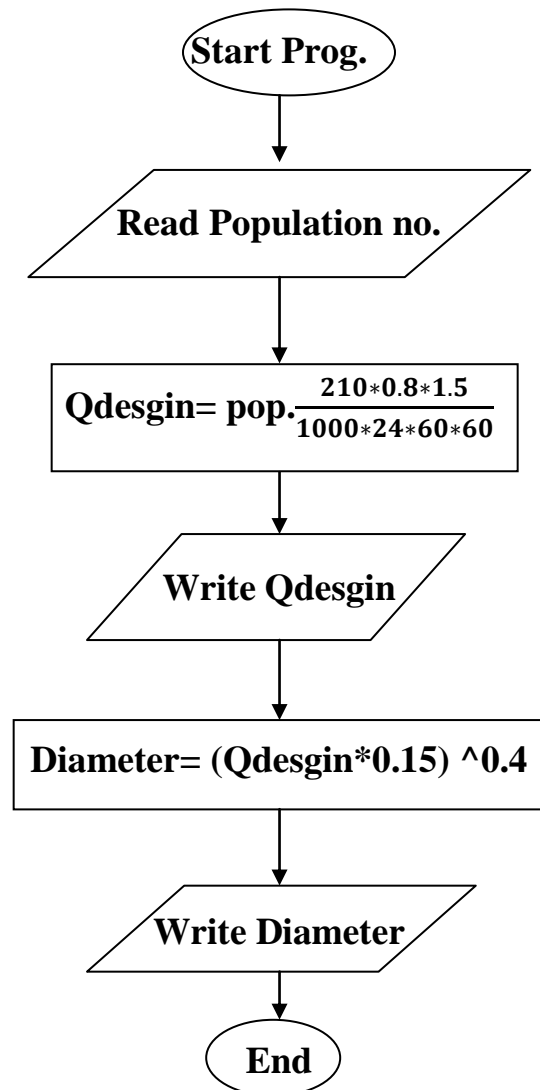


Figure (4.41): Flow Chart of the Designed Program for Sewage Network Pre-Planning.

Table (4.25): Data of the Primary Sewage Pipes.

Pipe no.	type	Load	Diameter mm	life time	Length mt
1	GVC	0.3 x Q1	400	100	965
2	GVC	0.16 x Q1	400	100	652
3	GVC	0.16 x Q1	400	100	275
4	GVC	0.16 x Q1	400	100	435
5	GVC	0.16 x Q1	400	100	505
6	GVC	Q3+ 0.16 x Q1	700	100	1425
7	GVC	Q2+0.3 x Q1+0.16 x Q1	700	100	1503
8	GVC	transfer	400	100	871
9	GVC	Q4+ Q2+0.3 x Q1+0.16 x Q1	900	100	879
10	GVC	Q4+ Q2+0.3 x Q1+0.16 x Q1	900	100	861
11	GVC	Q5+ Q3+ 3 x 0.16 x Q1	900	100	1113
12	GVC	Q4+ Q2+0.3 x Q1+0.16 x Q1	900	100	356

Then the inner pipes are mains of sewage which have diameter of 150 mm.

D. Determining the most suitable location for the pumping station. The rules applied to determine this location are:

1. The location should have the lowest levels in the study area
2. The location should be in a place owned by the country as possible
3. The roads goes to this location must not obstructed by any man-made or nature obstacles
4. The roads goes to this location must have suitable widths to enable the cutting works
5. It should be near as possible to the existing water and electricity networks on the study area
6. The location must not have water or electricity works

Using the spatial analysis tools in ARC GIS, the steps of finding the most suitable location are:

- 1- Decide: Which data set is required as input data. (Elevations, Building and Streets).
- 2- Drive: classifying the available data. (The lowest elevations levels in the study area), Building (classifying Distance to buildings every 10m), Streets with suitable widths (classifying Distance to streets every 10m) as shown in Figure (4.42).
- 3- Reclassify: gives high values for more suitable attribute. such as The elevations (lowest levels in the study area) class 10, Building (Distance to buildings 10m) class10, Streets (Distance to streets 10m) class 10 as shown in Figure (4.43).
- 4- Weight and combination of these values: the lowest elevation in study area has the high weight (75%), Distance to buildings weight (12.5%) and Distance to streets weight (12.5%). The result will be a map of the most suitable locations by which we deciding the most suitable location of the pumping station as shown in Figure (4.44).

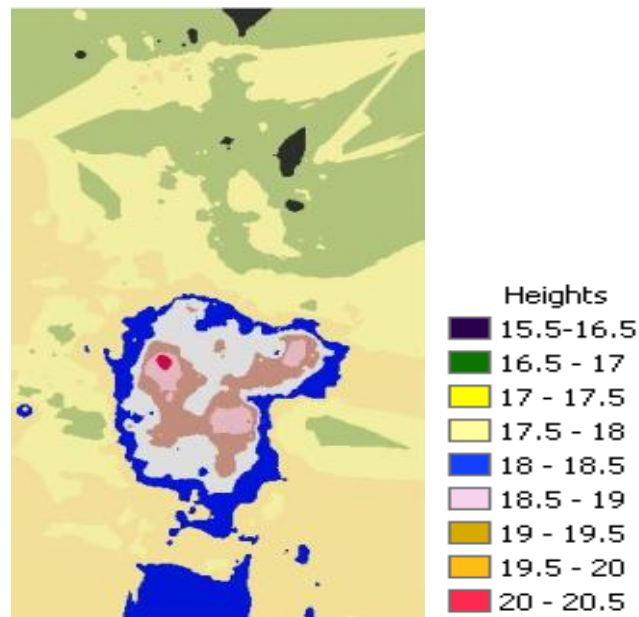
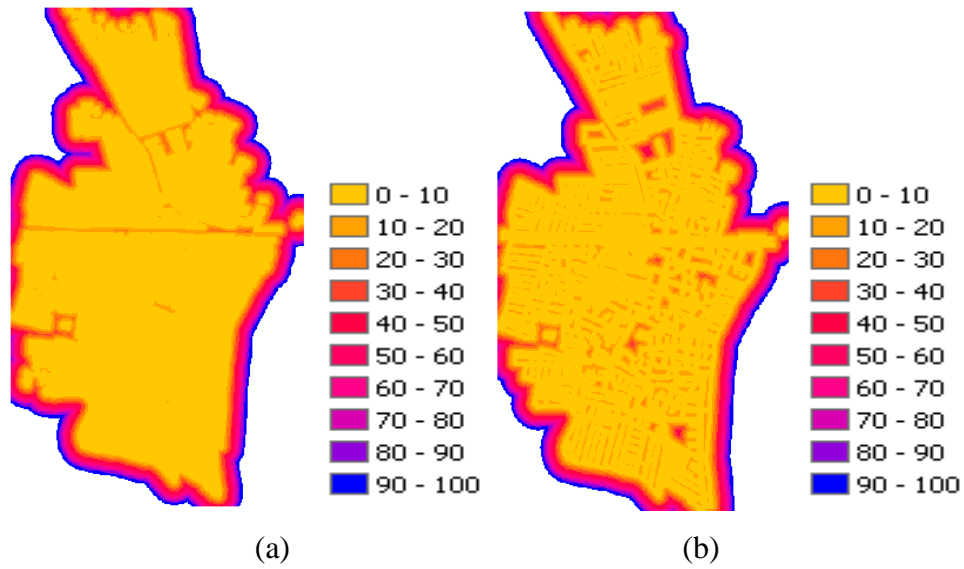


Figure (4.42): (a) Classification of Distances to Buildings (b) Classification of Distances to Streets (c) Classification of Elevations.

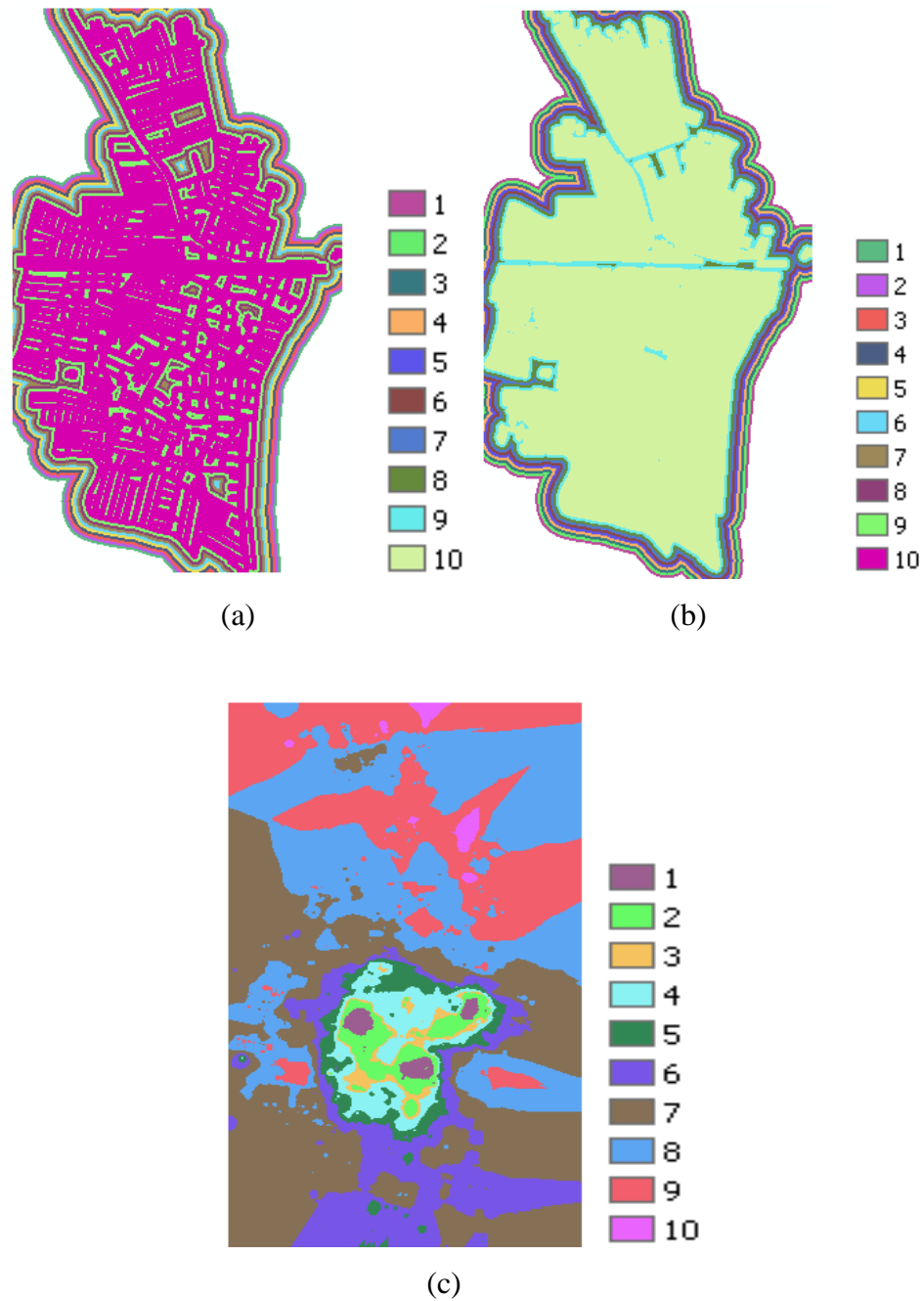


Figure (4.43): (a) Reclassification of the Distances to the Buildings Class 10 with Distance 10m (b) Reclassification of the Distances to the Streets Class 10 with Distance 10m (c) Classification of the Elevations Class 10 the Lowest Elevations.

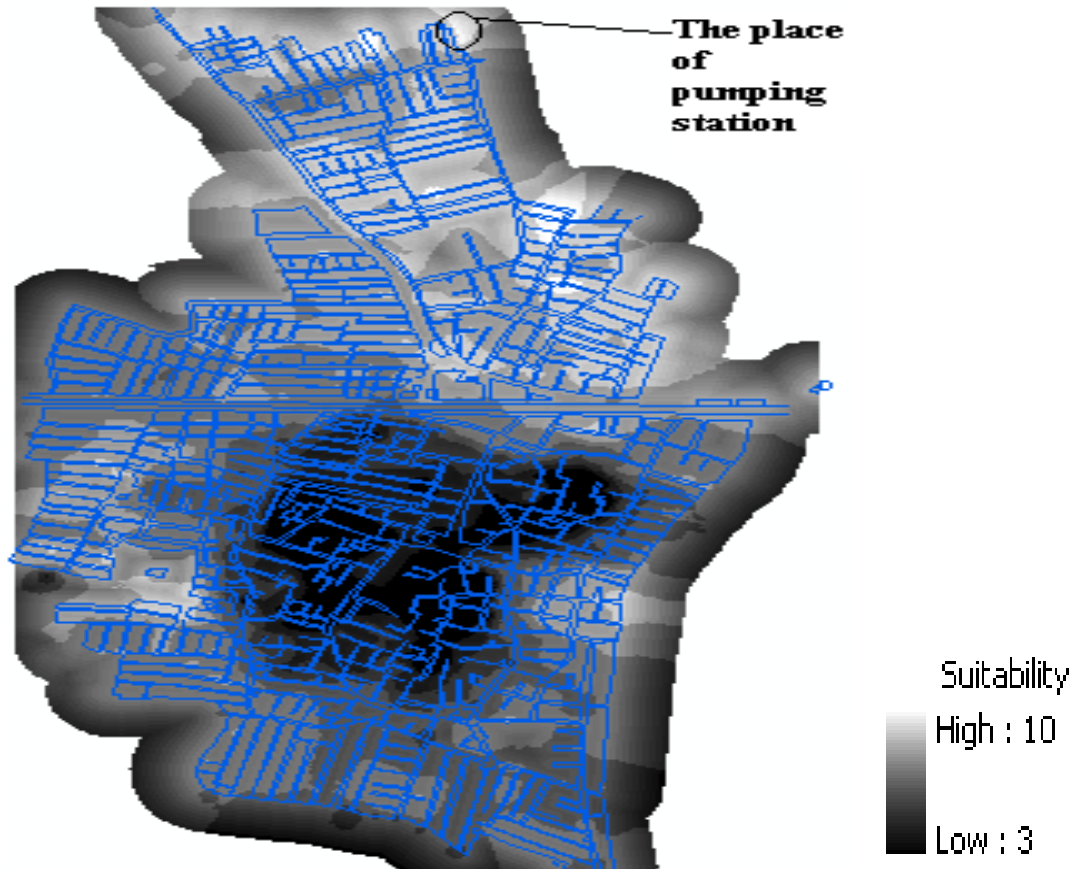


Figure (4.44): Overlap of Streets with the Suitability Map Showing the Most Suitable Location of the Pumping Station.

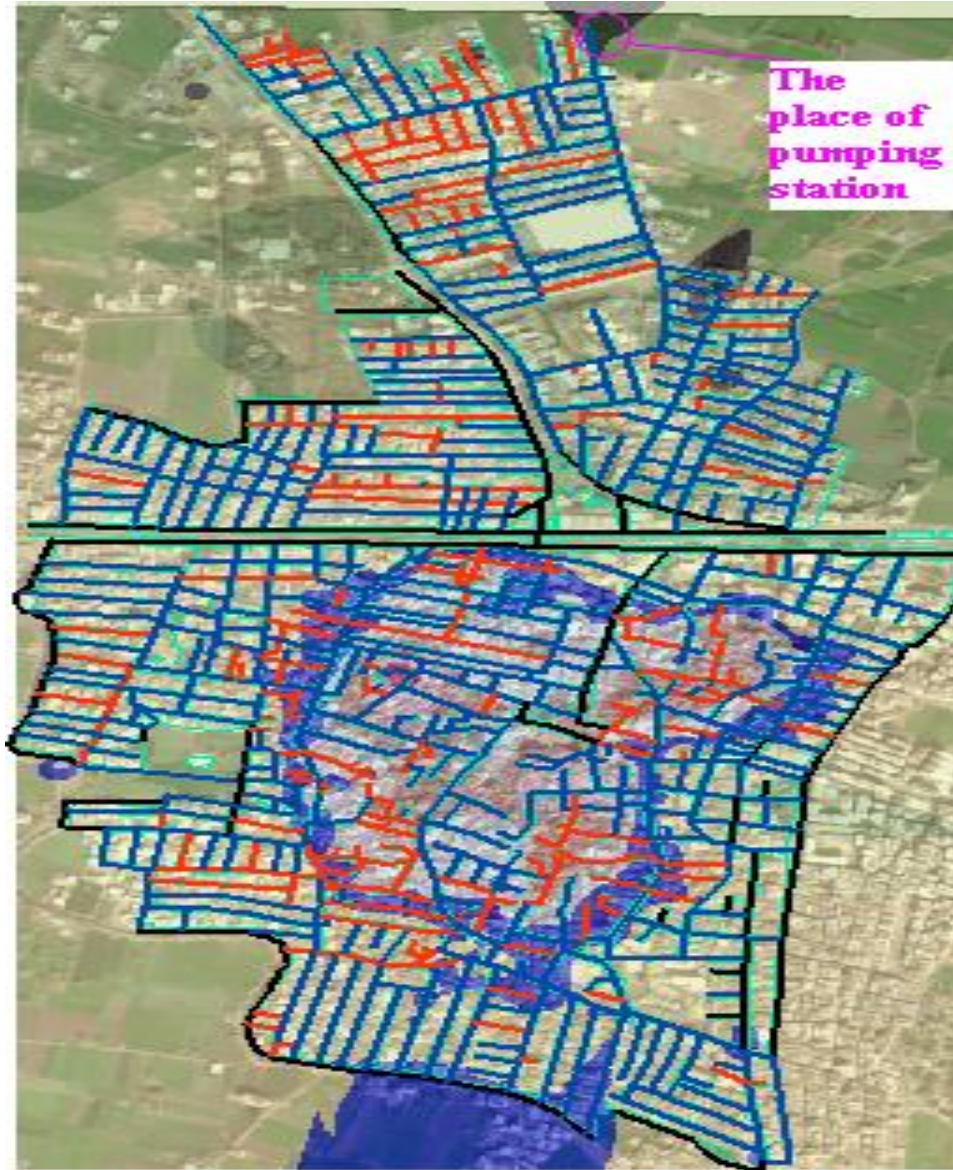


Figure (4.45): The Most Suitable Location of the Pumping Station.

E. Sewage network was created using the utility network analysis and can be controlled easily by the end user who can specify which pipe (edge) can be enabled or disabled if there is any damaged in this pipe also control valves (junctions) and define the water flow direction through defining which valve is source and which valve is sink as shown in Figure (4.46).

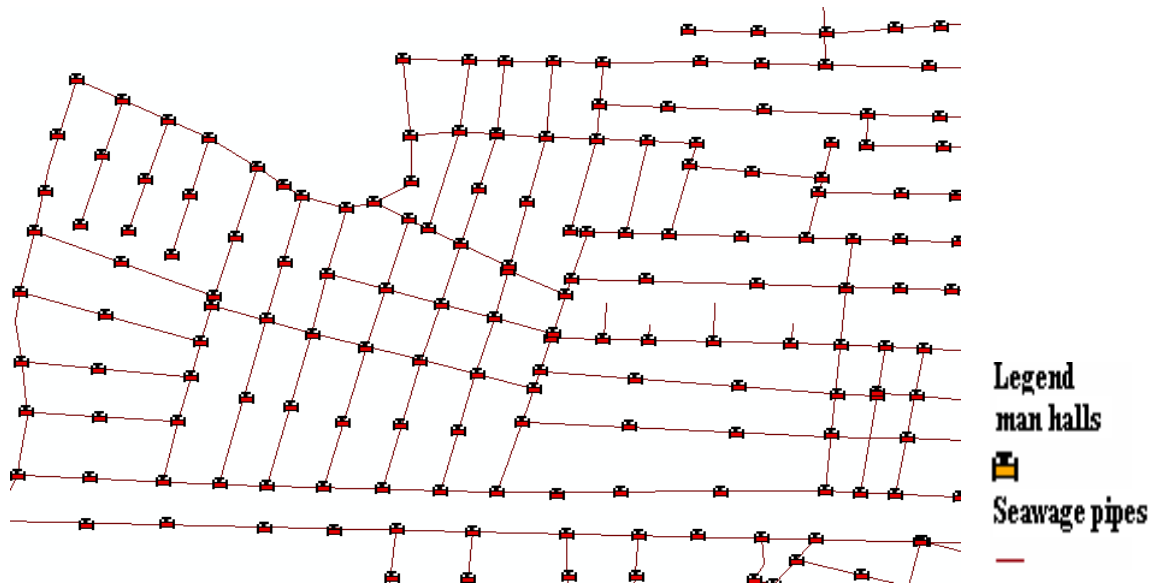
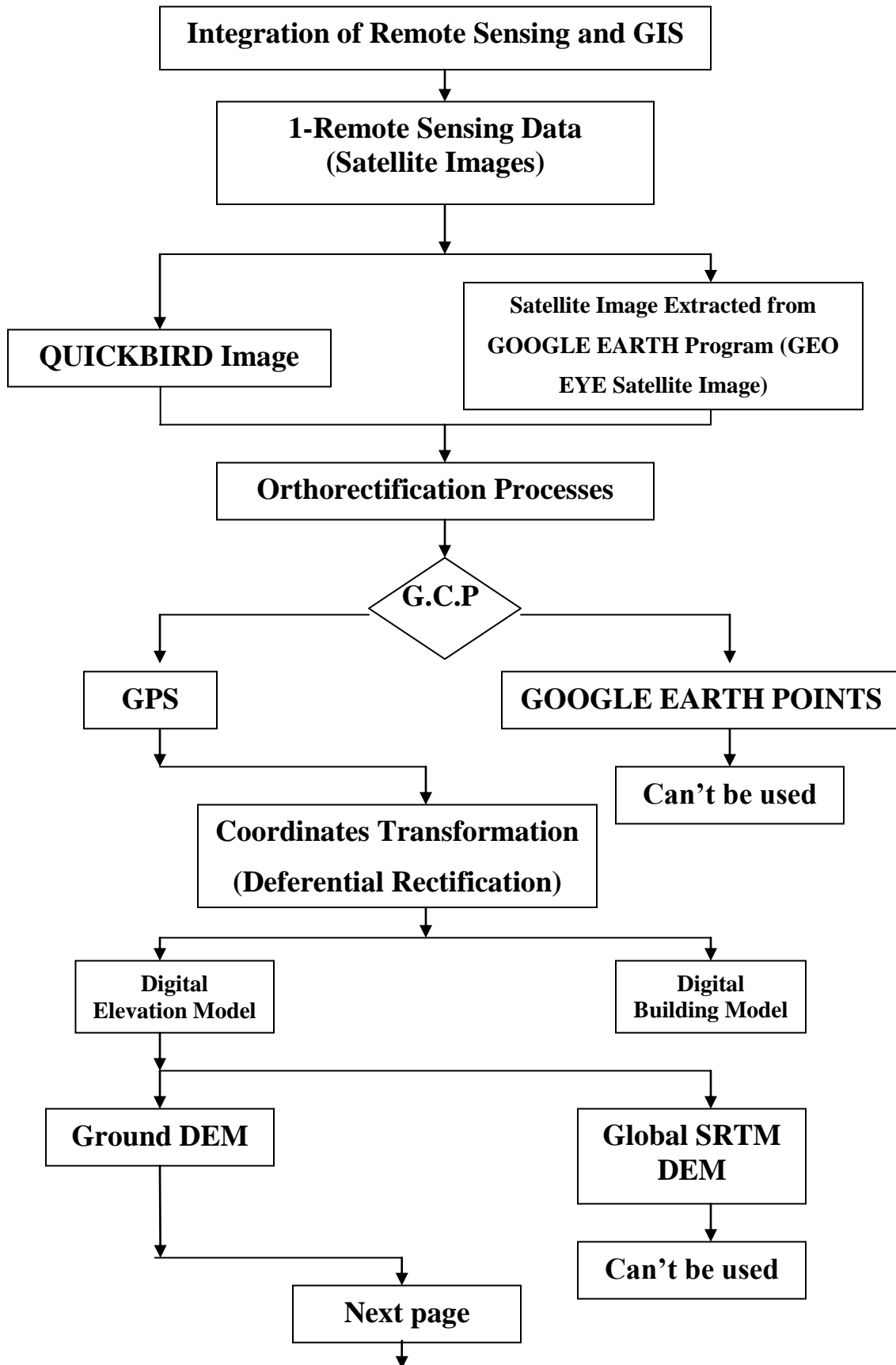


Figure (4.46): Sample of Final Sewage Network.

The following flow chart summarizes the steps of how the integration of Remote Sensing and GIS can be done for infra-structure planning starting from the required data and performed processes as these data, ends with some applications for planning.



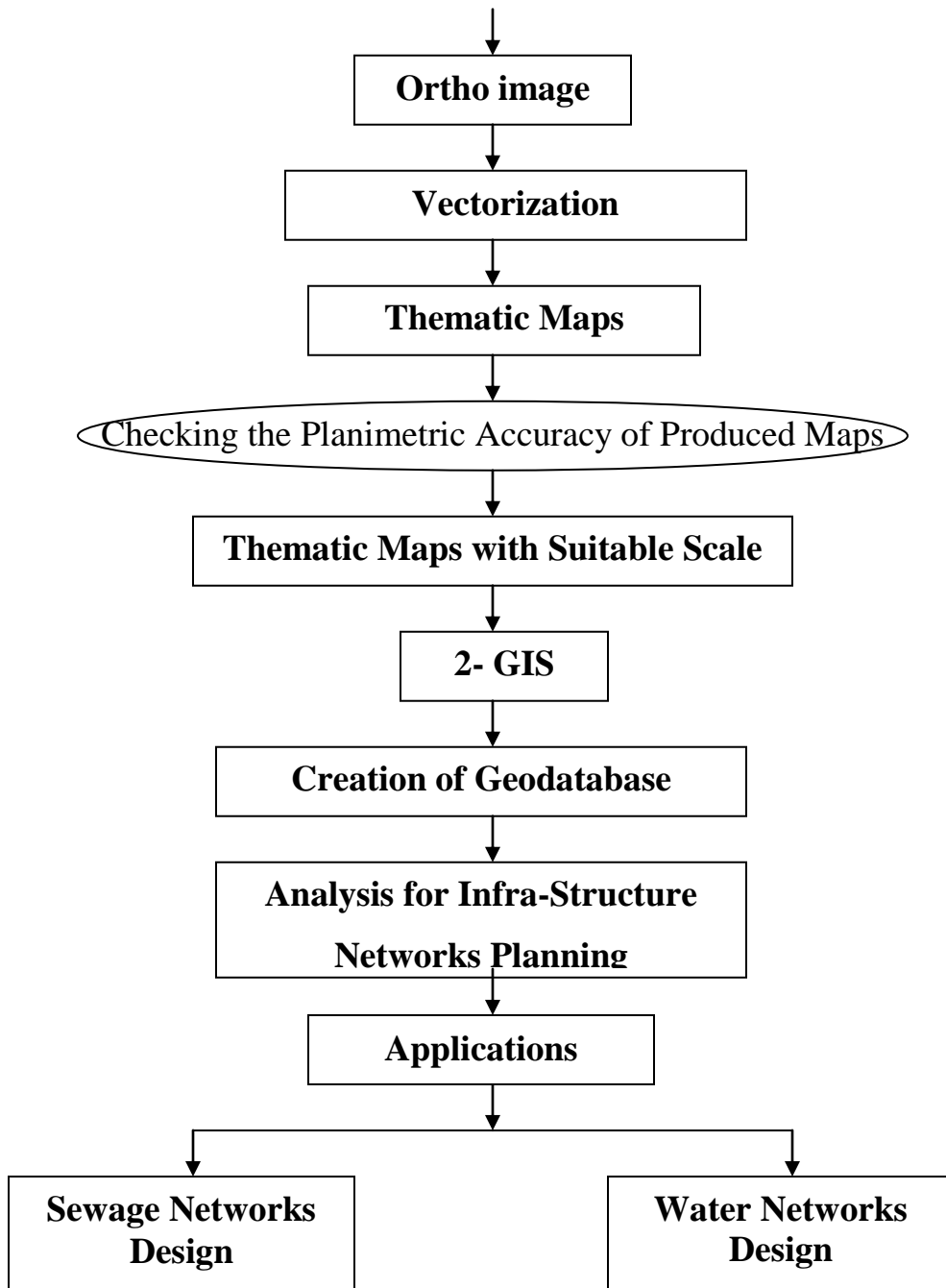


Figure (4.47): Flow Chart of the Integration of Remote Sensing and GIS for Infra-Structure Planning.

Chapter 5

Conclusions and Recommendations

5.1 Conclusions

1. RMS for maps produced from both images (1.05m for QUICKBIRD satellite image and 0.76m for satellite image extracted from Google Earth program (GEO EYE satellite image)) were within the required map accuracy standard for a map scale 1:5,000 according to the three map accuracy standards (NMAS, NSSDA and ASPRS). Also these results within the required map accuracy standard for a map scale 1:2,500 according to both the NMAS and NSSDA standards.
2. Satellite image extracted from Google Earth program (Google Earth program doesn't have the same spatial resolution for all areas) GEO EYE satellite image in this case can be used to produce large scale cadastral maps.
3. Control points extracted from Google Earth program can't be used as GCPs for producing large scale maps because it has different magnitude and direction of shifts in both Easting and Northing directions.
4. Global DEM (SRTM) cant be used even in flat terrain for producing large scale maps because it have large RMS of 1.84m which is more than 0.25m (one half the contour interval of 1:2,500 scale map) when the ground DEM have RMS of 0.16 m less than 0.25m.
5. GIS spatial analysis improves selection of the most suitable location for both water tank and sewage pumping station.
6. Designed programs and automatic calculators improve the calculations for designing purposes of both water and sewage networks.
7. Utility Network analysis tools in ARC GIS improves production of both water and sewage networks.

5.2 Recommendations

Based on the above results, the following recommendations could be suggested:

1. Using the Satellite images extracted from Google Earth program (Google Earth program doesn't have the same spatial resolution for all areas) to produce cadastral maps.
2. Using GIS improve Infra-Structure Planning process for both water and sewage networks.
3. Using GIS spatial analysis for selecting the most suitable location for both water tank and sewage pumping station.
4. Using the designed programs and automatic calculators for designing purposes of both water and sewage networks.
5. Producing water and sewage networks using Utility Network analysis tools in ARC GIS.
6. Finally it is recommended that, the present system for integrating the Remote Sensing and GIS for Infra-Structure Planning should be employed over large cities and villages to insure its economic value.

REFERENCES

Aguilar, M., et al., (2005): “Geometric correction of the Quickbird high resolution panchromatic images”, Departamento de Ingeniería Rural, Universidad de Almería (Spain). Email: maguilar@ual.es. XXII International Cartographic Conference (ICC2005) A Coruña, Spain, 11-16 July 2005.

Ahmed R., et al., (2008): “Planimetric accuracy of orthorectified QuickBird imagery using non-parametric sensor models”, Space Research Institute – Bulgarian Academy of Sciences e-mail: ahmedasi@hotmail.com. Fourth Scientific Conference with International Participation Space, Ecology, Nanotechnology, Safety 4–7 June 2008, Varna, Bulgaria.

Ali E., Maher M., Khaled Z. and Hassan M., (2012):” Assessment of Using Very High Resolution Google Earth Satellite Images for Producing Cadastral Maps” accepted for publication on Civil Engineering Research Magazine, Faculty of Engineering, El-Azhar University, Cairo, Egypt.Vol: 34, No:2, April 2012.

Ali E., Maher M., Khaled Z. and Hassan M., (2012):” Evaluating the Accuracy of the Global DEMs ASTER, SRTM and Elevation Data Derived from Google Earth Program in Urban Areas over Egypt” accepted for publication on Civil Engineering Research Magazine, Faculty of Engineering, El-Azhar University, Cairo, Egypt.Vol: 34, No:2, April 2012.

Albertz, J., and Kreiling, W., (1989): Photogrammetrisches Taschenbuch, Herbert Wichmann Verlag Karlsruhe, 4. Auflage.

Alexandrov, A., et al., (2004): “Application of QUICKBIRD satellite imagery for updating cadastral information”, GIS SOFIA Ltd., 5 Serdika Str., BG-1000 Sofia, Bulgaria, e-mail: photogrammetry@gis-sofia.bg Commission II, WG II/6.

Alkan M., and Marangoz M.A., (2009): “Creating cadastral maps in rural and urban areas of using high resolution satellite imagery”, Department of Geodesy and Photogrammetry, Engineering Faculty Zonguldak Karaelmas University, Zonguldak, Turkey mehmetalkan44@yahoo.com. Applied Geoinformatics for Society and Environment 2009 - Stuttgart University of Applied Sciences.

Alkan, M., et all., (2008): “Integration of high resolution QUICKBIRD images to GOOGLE EARTH”, AZKU, Engineering Faculty, 67100 Zonguldak, Turkey (mehmetalkan44@yahoo.com) Interactive Sessions, WGS II/6, The International Archives of the Photogrammetry, Remote Sensing and Spatial Information Sciences. Vol. XXXVII. Part B2. Beijing 2008.

Anderson J., and Mikhail, E., (1998): "Surveying Theory and Practice", Seven Edition, WCB/McGraw-Hill, Boston.

Arzu, S., and Metin S., (2009): “Digital Elevation Model production from scanned topographic contour maps via thin plate spline interpolation”, Yıldız Technical University Civil Engineering Faculty Geodesy and Photogrammetry Engineering Division Istanbul-Turkey, The Arabian Journal for Science and Engineering, Volume 34, Number 1A.

ASPRS, (1989): “ASPRS interim accuracy standards for large scale maps”. American Society of Photogrammetry and Remote Sensing.

B.Behdinian, (2000):”Generating Orthoimage from IKONOS Data”, Iranian Remote Sensing Center.

Black et al., (1998):”Geographic Information Systems: A New Research Method for Book History”. Book History.

Burrough, P., (1986):”Principles of Geographical Information Systems for Land Resources Assessment. Clarendon, Oxford.

Canada Centre for Remote Sensing Remote Sensing Tutorial:” Fundamentals of Remote Sensing”, [http://www.ccrs.nrcan.gc.ca/resource /tutor/fundam/pdf/fundamentals_e.pdf](http://www.ccrs.nrcan.gc.ca/resource/tutor/fundam/pdf/fundamentals_e.pdf).

Chang, K., (2008):”Introduction to Geographic Information System”, Fourth Edition, New York: Tata McGraw-Hill.

Chen, L., and Teo, T., (2002):”Rigorous Generation Of Digital Orthophotos From EROS A High Resolution Satellite Images”, Center for Space and Remote Sensing Research, National Central University, 320 Chung-Li, Taiwan.

Chrisman, N., (1999):” What Does ‘GIS’ Mean?”, Department of Geography University of Washington. Black well Publishers Ltd.

Chuvieco, E., and Huete, A., (2010):”Fundamentals of Satellite Remote Sensing”, First Edition. Taylor and Francis Group, LLC, United States of America.

Clarke, K., (1995):”Analytical and Computer Cartography”, Edited by K. C. Clarke. 2nd ed. ed, Prentice Hall Series in Geographic Information Science. Upper Saddle River, NJ: Prentice Hall.

Demers, M., (2009):”GIS for Dummies”, Wiley publishing. Inc., Indianapolis, Indiana.

Egyptian Code, (2010) ": "The Egyptian Code for designing and execution of pipe lines for Water and Sewage Networks”, Eleventh Edition.

Elachi, C., and van Zyl J., (2006):”Introduction to the Physics and Techniques of Remote Sensing”, Second Edition. John Wiley & Sons, Inc., Hoboken, New Jersey.

Erdas field guide Fifth Edition, (1999): "Imagine Essentials Training Reference Manual", Atlanta, Georgia, United States of America.

Eurimage products and services WorldView-1, (2009): "WorldView-1 best resolution, accuracy, and agility".

Goodchild, M., (1992): "Geographical information science", International Journal of Geographical Information Systems.

Huxhold, W., (1991): "An Introduction of Urban Geographic Information Systems". New York and Oxford: Oxford University Press.

Koeln, G., et al., (1994): "Geographic information systems". in T.A. Bookhout, ed. Research and Management Techniques for Wildlife and Habitats. Fifth Edition. Bethesda: The Wildlife Society Pages. pp. 540-566.

Indian Remote Sensing Satellite System: http://india.gov.in/sectors/science/indian_remote.php.

Landsat Fact Sheet, (2003): "Landsat: A Global Land-Observing Program Fact Sheet 023-03 (March 2003)", landsat.gsfc.nasa.gov/pdf_archive/USGS_landsat_factsheet.pdf.

Landsat Satellites Historical: www.geoimage.com.au/geoweb/pdfs/flyers/LANDSAT_flyer.pdf.

Li, Z., et al., (2005): "DIGITAL TERRAIN MODELING Principles and Methodology", Boca Raton London New York Washington, D.C., CRC PRESS.

Lillesand, T., and Kiefer, R., (2008): "Remote Sensing and Image Interpretation", Sixth Edition. John Wiley & Sons, Inc., New York.

Litwin P., (2003):” Fundamentals of Relational Database Design”, from the design chapter of Microsoft Access 2 Developer's Handbook, Sybex 1994, by Ken Getz, Paul Litwin and Greg Reddick.

MERCURI, P., et al., (2006):” Evaluation and accuracy assessment of high-resolution IFSAR DEMs in low-relief areas”, Purdue University, Department of Agricultural and Biological Engineering, 225 South University Street, West Lafayette, IN 47907 USA, International Journal of Remote Sensing Vol. 27, No. 13, 10 July 2006.

NMAS; (1947): United States National Map Accuracy Standards. “National Mapping Program Maintained by the U.S. Department of Interior, U.S. Geological survey. Washington D.C. 1941 Revised 1947.

National Mapping Program: Part 2 Specifications, Standards for Digital Elevation Models, U.S. Department of the Interior, U.S. Geological Survey National Mapping Division.

Novak K., (1992):”Rectification of Digital Imagery”, Photogrammetric Engineering & Remote Sensing.

Ochis H., and Russell E., (2000):” Comparison of a piecewise transformation to polynomial-based geometric correction algorithms”, Computer Terrain Mapping, Inc., Boulder, CO.

Oz, E., (2004):”Management Information System”, Fourth Edition. Boston, MA: Course Technology.

Panda., B., (2005):”Remote Sensing principles and applications”, Vinod Vasishtha, Daryaganj, New Delhi.

Projective transformation, (2005): <http://www.fen.bilkent.edu.tr/~franz/ag05/ag-07.pdf>.

- Remote Sensing Engineer manual, (2003):** “Remote Sensing Engineer manual”, Department of the US army corps of Engineers Washington, DC 20314-1000.
- Roberto. C., et al., (2005):** “Orthorectification of High Resolution satellite images with space derived DSM”, a DISTART, University of Bologna.
- Rocchini, D., (2004):**” Misleading Information From Direct Interpretation of Geometrically Incorrect Aerial Photographs”, The Photogrammetric Record.
- Salah., M., (2004):** “Updating Maps Using High-Resolution Satellite Imagery as an Alternative to Traditional Techniques”, Msc. Thesis. Department of Surveying Engineering. Shoubra Faculty of Engineering, Zagazig University.
- Sanderson, R., (2006):**”Introduction to Remote Sensing”, New Mexico State University, http://spacegrant.nmsu.edu/statewide/projects/remote_sensing.pdf.
- Sumathi., S., and Esakkirajand., S., (2007):**” Fundamentals of relational database management system”, First edition. Springer Verlag Berlin Heidelberg.
- Schowengerdt, R., (2007):**”Remote Sensing: Models and Methods for Image Processing”, Third Edition. Elsevier, United States of America.
- Star, J., and John E., (1990):**”Geographic Information Systems: An Introduction”, Englewood Cliffs, NJ: Prentice Hall.
- Temiz, M., and Külür, S., (2008):**” Rectification of Digital Close Range Images: Sensor Models, Geometric Image Transformations and Resampling”, Ondokuz Mayıs University, Geodesy & Photogrammetry Engineering Samsun /TURKEY, Istanbul Technical University, Geodesy & Photogrammetry Engineering Istanbul / TURKEY.

Terborgh, C., (2010):”Introduction to Geographic Information Systems (GIS) - with a focus on localizing the MDGs, http://www.unhabitat.org/downloadsdocs/wuf3Intro_GIS.ppt.

Tiejun, W., (2005):”The Capability of IKONOS Images for 1:10,000 Mapping in China”, International Institute for Geo-information Science and Earth Observation Enschede, The Netherlands.

Transformation Functions for Image Registration, (2003): Image Fusion Systems Research, http://www.imgfsr.com/ifsr_tf.pdf.

Volpe, F., (2004):” Use of QuickBird Satellite Data for Urban Environments”, Urban data management symposium, Chioggia, Italy.

Volpe, F., (2005):” Geometrical processing of QUICKBIRD high resolution satellite data”, Urban data management symposium, Chioggia, Italy. Eurimage S.p.A., Via Edoardo D’Onofrio 212 00155 ROMA - volpe@eurimage.com.

Westin, T., and Forsgren, J., (2002):”Orthorectification of EROS A1 images”, IEEE/ISPRS Joint Workshop on Remote Sensing and Data Fusion over Urban Areas, Rome.

<http://cse.taylor.edu/~btoll/s99/424/res/mtu/Notes/geometry/geo-tran.htm>.

http://en.wikipedia.org/wiki/Digital_elevation_model.

http://en.wikipedia.org/wiki/EgyptSat_1.

<http://en.wikipedia.org/wiki/GeoEye-1>.

http://en.wikipedia.org/wiki/Geographic_information_system.

http://en.wikipedia.org/wiki/Hyperspectral_imaging.

http://en.wikipedia.org/wiki/Landsat_1.

http://en.wikipedia.org/wiki/Multi-spectral_image.

http://en.wikipedia.org/wiki/Network_model.

http://en.wikipedia.org/wiki/Remote_sensing.

<http://encyclopedia2.thefreedictionary.com/database+management+system>.

<http://eoeu.belspo.be/en/satellites/spot.html>.

<http://gislounge.com/methods-for-creating-spatial-databases/>.

<http://landsat.gsfc.nasa.gov/about/mss.html>.

<http://landsat.gsfc.nasa.gov/about/tm.html>.

<http://landsat.gsfc.nasa.gov/about/wrs.html>.

<http://maic.jmu.edu/sic/gis/components.html>.

<http://mathworld.wolfram.com/AffineTransformation.html>.

<http://searchsqlserver.techtarget.com/definition/database>.

<http://www.blurtit.com/q217827.html>.

<http://www.ciesin.columbia.edu/TG/RS/RS-home.html>.

http://www.creaf.uab.es/Miramon/new_note/notes/tablescr.html.

<http://www.crisp.nus.edu.sg/~research/tutorial/spacebrn.html>.

<http://www.crisp.nus.edu.sg/~research/tutorial/spot.htm>.

http://www.cs.jcu.edu.au/Subjects/cp3020/1997/Lecture_Notes/databases/dbms_disadv.html.

http://www.csc.noaa.gov/crs/rs_apps/sensors/spot.html.

<http://www.ctmap.com/assets/pdfprojects/geotin.pdf>.

<http://www.eurimage.com/products/quickbird.html>.

<http://www.eurimage.com/products/wv-1.html>.

<http://www.fas.org/spp/guide/india/earth/irs.html>.

<http://www.gis.usu.edu/Geography-Department/rsgis/RSCC/v6.2/bl.html>.

<http://www.gis.usu.edu/Geography-Department/rsgis/RSCC/v6.2/cc.html>.

<http://www.gis.usu.edu/Geography-Department/rsgis/RSCC/v6.2/nn.html>.

<http://www.gis.usu.edu/Geography-Department/rsgis/RSCC/v6.2/syserr.html>.

<http://www.gras.ku.dk/Products/SatelliteImages/QuickBird.aspx>.

<http://www.itu.edu.tr~turkoglu/documanlar/documanlar/COURSE%202%20ABOUT%20GIS.ppt>.

<http://www.n2yo.com/satellite/?s=31117>.

<http://www.ncgia.ucsb.edu/cctp/units/unit14/14.html>.

http://www.palmbeach.k12.fl.us/maps/gis/slide_4.html.

<http://www.physicalgeography.net/fundamentals/2e.html>.

<http://www.satimagingcorp.com/satellite-sensors/alos.html>.

<http://www.satimagingcorp.com/satellite-sensors/geoeye-1.html>.

<http://www.satimagingcorp.com/satellite-sensors/quickbird.html>.

http://www.satmagazine.com/cgi-bin/display_article.cgi?number=1307290351.

http://www.satmagazine.com/cgi-bin/display_image.cgi?1705129920.

<http://www.spotimage.fr/home/system/welcome.html>.

<http://www.statemaster.com/encyclopedia/QuickBird>.

<http://www.techweb.com/encyclopedia/defineterm.jhtml?term=database&x=&y>.

http://www.terralink.co.nz/products_services/satellite/eros_satellite_images/.

<http://www.uic.edu/classes/sids/cids422gis.ppt>.

<http://www.unixspace.com/context/databases.html>.

http://www.usgsquads.com/prod_satellite_imagery.htm.

<http://www.wamis.org/agm/pubs/agm8/Paper-5.pdf>.

<http://www.wamis.org/agm/pubs/agm8/Paper-5.pdf>.

ملخص البحث

المقدمة:

يعتبر مستوى العمران عامل مهم في قياس تحضر المدن. احد اهم التحديات التي تواجه المخططين لعمل شبكات بنية تحتية لهذه المدن هي الزيادة السكانية التي ينتج عنها مناطق عشوائية. هذه المناطق بنيت بدون تخطيط و تفتقد لخدمات البنية التحتية مثل شبكات الطرق ومياه الشرب والصرف الصحي وشبكات الغاز والكهرباء. المرحلة الرئيسية لعمل شبكات البنية التحتية هو معرفة الوضع الحالى من مصادر البيانات المختلفة. ونظرا للتطور الكبير في تقنية الاستشعار عن بعد و خاصة صور الاقمار الصناعية التي اصبحت ذات قدرات تحليلية كبيرة يمكن من خلالها عمل خرائط ذات مقياس رسم كبير يمكن استخدامها في عمليات التخطيط مثل القمر الصناعي كويك بيرد الذى تصل قدرته التحليلية الى ٦٠ سم. و كذلك احد اسرع و اسهل الوسائل الحالية للحصول على صور الاقمار الصناعية برنامج جوجل ايرث الذى يحتوى على صور اقمار صناعية ذات قدرات تحليلية عالية تصل الان الى ٥٠ سم من القمر الصناعي (GEO EYE). تتم عملية انتاج الخرائط من هذه الصور عن طريق عملية التقويم الرأسى (Orthorectification) للصورتين لتصحيح خطأ فروق الارتفاعات عن طريق نموذج الارتفاع الرقمى (DEM) و ازالة المباني عن طريق نموذج المباني الرقمى (DBM) ثم تحويل هذه الصور الى خرائط عن طريق عملية (Vectorization). ثم عمل قاعدة بيانات حديثة لهذه الخرائط لاستخدامها بواسطة نظم المعلومات الجغرافية في اغراض تخطيط البنية التحتية خاصة شبكات المياه و الصرف الصحى.

الهدف من البحث:

الهدف الرئيسى للبحث هو دراسة التكامل بين الاستشعار عن بعد و نظم المعلومات الجغرافية لعمل خرائط ذات المعلم الواحد للمعالم المطلوبة في التخطيط وكذلك عمل قاعدة بيانات حديثة عن هذه المناطق لاستخدامها في اغراض تخطيط البنية التحتية اسرع و بتكلفة اقل. كذلك دراسة امكانية استخدام المنتجات المتاحة مجانا لبرنامج جوجل ايرث مثل نقاط التحكم بدلا من نقاط GPS او حتى معها و ايضا نموذج الارتفاعات الرقمى العالمى SRTM المتاح مجانا بدلا من نموذج الارتفاعات الرقمى المنتج من المساحة الارضية خاصة في المناطق المستوية و اخيرا امكانية استخدام صور الاقمار الصناعية المتاحة في برنامج جوجل ايرث بدلا من صور الاقمار الصناعية للقمر كويك بيرد.

محتويات الرسالة:

الباب الأول:

اختص هذا الباب بدراسة الاستشعار عن بعد حيث تضمن مقدمة عن الاستشعار عن بعد و كذلك نبذة موجزة عن

تاريخ الاستشعار عن بعد و الأنواع المختلفة من الأقمار الصناعية وكذلك الكاميرات المحمولة عليها والتطبيقات المختلفة لكل منها. و صور الأقمار الصناعية المختلفة وفي نهاية الباب تم عرض عدد من التطبيقات المختلفة للاستشعار عن بعد مع التركيز على إنتاج الخرائط و مقاييس الرسم المختلفة التي يمكن الحصول عليها من الاقمار المختلفة.

الباب الثاني:

اختص هذا الباب بدراسة عملية تقويم صور الأقمار الصناعية حيث تم عرض الاخطاء الهندسية التي تحدث عند التقاط الصور من القمر الصناعي ايضا شرح لخطوات عملية التقويم وكذلك النماذج الرياضية المختلفة لعمل التقويم. و كذلك نماذج الأرض الرقمية بداية من شرح مفهوم نماذج الأرض الرقمية ثم عرض الطرق المختلفة لإنتاج نماذج الأرض الرقمية. ايضا العوامل التي تؤثر جودة عمل نماذج الأرض الرقمية. و اخيرا شرح للطرق المختلفة لعملية تحويل الصور الى خرائط.

الباب الثالث:

اختص هذا الباب بنظم المعلومات الجغرافية بداية بشرح التعريفات المختلفة لنظم المعلومات الجغرافية و كذلك مكونات نظم المعلومات الجغرافية من عنصر بشري و الالات و حزم برامج و بيانات. العمليات المهمة التي يمكن عملها باستخدام نظم المعلومات الجغرافية و طرق تمثيل البيانات المكانية. و اخيرا شرح للطرق المختلفة لتصميم قواعد البيانات.

الباب الرابع:

يختص هذا الباب بالجانب العملي من الرسالة حيث تم استخدام البيانات المتاحة لعمل تكامل بين الاستشعار عن بعد و نظم المعلومات الجغرافية لتخطيط شبكات البنية التحتية. بداية من عمل التقويم الراسي للصور و كذلك دراسة امكانية استخدام المنتجات المتاحة مجاناً لبرنامج جوجل ايرث مثل نقاط التحكم بدلا من نقاط GPS او حتى معها و ايضا نموذج الارتفاعات الرقمية العالمي SRTM المتاح مجاناً بدلا من نموذج الارتفاعات الرقمية المنتج من المساحة الارضية خاصة في المناطق المستوية و اخيرا امكانية استخدام صور الاقمار الصناعية المتاحة في برنامج جوجل ايرث بدلا من صور الاقمار الصناعية للقمر كويك بيرد لعمل خرائط ذات المعلم الواحد للمعالم المطلوبة في التخطيط. وفي كلتا الحالتين تم استخدام نموذج الأرض الرقمية وكذلك نموذج المباني الرقمية. وقد شرحت حسابات هذه التجارب بالتفصيل مرفقة بالجداول والرسومات وكافة الملاحظات. ايضا تقييم الخرائط المنتجة من هذه الصور حسب المقاييس العالمية. اخيرا عمل تخطيط اولى لشبكات المياه و الصرف الصحي باستخدام نظم المعلومات الجغرافية من خلال عمل تحليل مكاني لايجاد افضل مكان لكل من خزان المياه و محطة رفع الصرف الصحي ثم عمل برامج لايجاد اقطار المواسير المختلفة لتسهيل عملية التخطيط و اخيرا اخراج الشبكتين في صورة شبكات مرافق تمكن المستخدم من التحكم في مسارات المياه في المواسير و كذلك فتح و غلق المحابس في حالة حدوث عطل او صيانة في احد المواسير.

الباب الخامس:

يحتوى هذا الباب على ملخص لما تم استخلاصه من نتائج ثم عرض للتوصيات المقترحة بناءً على ما تقدم من دراسات ونتائج.

استنتاجات البحث

من خلال النتائج التي تم الحصول عليها تم التوصل الى بعض الاستنتاجات الخاصة بعمل تكامل بين الاستشعار عن بعد و نظم المعلومات الجغرافية لتخطيط شبكات البنية التحتية. وهذه الاستنتاجات يمكن ايجازها فيمايلي:

1. نتائج البحث دلت على ان (RMS) معدل الخطأ كان افضل في حالة الخرائط المنتجة من صورة القمر الصناعي (GEO EYE) الماخوذة من برنامج جوجل ايرث و تساوى ٠,٧٦ متر من حالة الخرائط المنتجة من صورة القمر الصناعي كويك بيرد و تساوي ١,٠٥ متر و كلتا النتائج تدل على انه يمكن استخدام هذه الصور لانتاج خرائط بمقياس رسم ١:٥٠٠٠٠ حسب المقاييس العالمية الثلاثة و بمقياس رسم ١:٢٥٠٠ حسب اثنين من هذه المقاييس.
2. يمكن استخدام صورة القمر الصناعي (GEO EYE) الماخوذة من برنامج جوجل ايرث المتاحة في منطقة الدراسة في هذه الحالة لانتاج خرائط ذات مقياس رسم كبير.
3. لا يمكن استخدام نقاط التحكم من برنامج جوجل ايرث لانتاج خرائط ذات مقياس رسم كبير حيث انها لها ازاحات مختلفة المقدار و الاتجاهة عن مكانها الصحيح.
4. لا يمكن استخدام نموذج الارتفاعات الرقمية العالمي SRTM المتاح مجاناً في برنامج جوجل ايرث بدلا من نموذج الارتفاعات الرقمية المنتج من المساحة الارضية حتى في المناطق المستوية لانتاج خرائط ذات مقياس رسم كبير.
5. استخدام التحليل المكاني في نظم المعلومات الجغرافية سهلت وحسنت عملية ايجاد افضل مكان لكل من خزان المياه و محطة الرفع الخاصة بالصرف الصحي.
6. تصميم المعادلات و البرامج في البرنامج سهلت عملية ايجاد اقطار المواسير في تخطيط شبكات البنية التحتية (المياه و الصرف الصحي).
7. اخراج الشبكات في صورة شبكات المرافق في برنامج ARC GIS يسهل عملية التحكم في هذه الشبكات.

توصيات البحث

طبقا للنتائج التي تم الوصول اليها فان هناك بعض التوصيات المقترحة يمكن تلخيصها فيما يلي:

١. استخدام صور الاقملر الصناعية الماخوذة من برنامج جوجل ايرث لانتاج خرائط ذات مقياس رسم مختلفة حسب القدرات التحليلية المتاحة لكل منطقة.
٢. استخدام نظم المعلومات الجغرافية قى عملية تخطيط شبكات البنية التحتية (المياه و الصرف الصحى).
٣. استخدام التحليل المكانى فى نظم المعلومات الجغرافية فى عملية ايجاد افضل مكان لكل من خزان المياه و محطة الرفع الخاصة بالصرف الصحى.
٤. استخدام المعادلات و البرامج التى صممت فى برنامج ARC GIS فى عملية ايجاد اقطار المواسير فى تخطيط شبكات البنية التحتية (المياه و الصرف الصحى).
٥. اخراج شبكات المياه والصرف الصحى فى صورة شبكات المرافق فى برنامج ARC GIS
٦. يوصى بتطبيق النظام المقترح لتخطيط شبكات البنية التحتية على مدن و قرى ذات مساحات شاسعة لدراسة مدى جداوه الاقتصادية.

التكامل بين الاستشعار عن بعد و نظم المعلومات الجغرافية لتخطيط البنية التحتية

رسالة

مقدمة إلى كلية الهندسة بشبرا
جامعة بنها

لاستيفاء متطلبات الحصول على
درجة الماجستير في الهندسة المساحية

مقدمة من

م/ حسن محمد حسن حسين
بكالوريوس الهندسة المساحية- كلية الهندسة بشبرا
جامعة بنها

تحت إشراف

أ.د/ على أحمد الصغير
أستاذ المساحة و الجيوديسيا - رئيس قسم الهندسة المساحية
كلية الهندسة بشبرا

أ.م.د/ ماهر محمد امين
أستاذ مساعد المساحة - قسم الهندسة المساحية
كلية الهندسة بشبرا

أ.م.د/ خالد محمد ذكى
أستاذ مساعد المساحة - قسم الهندسة المساحية
كلية الهندسة بشبرا

٢٠١٢